Updated report on
"Standard Configurations for Unsteady Flow Through Vibrating Axial-Flow Turbomachine-Cascades"

Status as of July 1991.

Compiled by

T. H. Fransson[&] and J. M. Verdon[%]

ABSTRACT

As part of the Symposium series "Unsteady Aerodynamics and Aeroelasticity of Turbomachines and Propellers" a set of cascade standard configurations, with emphasize on the unsteady aerodynamics, was established [Bölcs and Fransson, 1986]. These have been used extensively by several authors since the "Fourth Aeroelasticity Symposium" in 1987. As both experimental and numerical procedures presently undergo a rapid development it was at that time recognized that a continuous update of the standard configurations is a necessity.

The present report gives an overview of unsteady experimental and theoretical flow models (as regards to vibrating blades in cascades) that have appeared in the open literature between the 1987 and 1991 Symposia on Aeroelasticity, together with a brief description of the major findings presented by the authors. The application domain presented for the different prediction models is pointed out, and it is concluded that the largest number of publications has appeared in the domain of development of non-linear computations. Viscous phenomena have started to be included, in different ways, in prediction models, both for actuator disk and flat plates, as well as for time-linearized and fully time-dependent methods. Many authors validate thoroughly their models against any analytical results available, as well as against existing experimental data. Unfortunately it must today be concluded that, although some well documented experiments have been presented in the last years, a large need for detailed viscous flow data through vibrating cascades exist.

The "Standard Configurations" have been updated in the sense that three cascade geometries have been reduced in importance, whereas one geometry has been extended to include experimental data at high incidence angles. The flat plate standard configuration has been extended to include two supersonic geometries that have been proven useful for comparisons in the past. Finally, a new analytical inviscid high subsonic/transonic compressor cascade geometry is proposed as "Standard Configuration 10", with the aim of detailed studies of shock wave influences on the unsteady load on vibrating blades.

Figure illustrating aeroelasticity in axial-flow turbomachines

_____
[&] Royal Institute of Technology, Stockholm, Sweden.
[%] United Technologies Research Center, East Hartford, Connecticut, USA.

CONTENTS

---

[1] The sub-sections are here numbered according to the number of the standard configurations in order to keep with the numbers in the original report.

NOMENCLATURE

Symbol	Explanation	Dimension
A	Amplitude (A=h in pure sinusoidal bending)	-
	(A=α in pure sinusoidal pitching)	rad
A	Fourier coefficient	-
C(x)	Camber distribution (eq. 3.10.2)	-
c	Blade chord	m
$\tilde{c}_f$	Real amplitude of unsteady force coefficient	-
$\tilde{c}_f\,(t)$	Unsteady perturbation force coefficient vector per unit amplitude, positive in positive coordinate direction	-
$\tilde{c}_h$	Real amplitude of unsteady force coefficient	-
$\tilde{c}_h\,(t)$	Unsteady force coefficient in direction of bending vibration, in traveling wave mode $\tilde{c}_h\,(t) = \sum_i \tilde{c}_{p,i}\,\Delta\,(x/l_i)$	-
$\tilde{c}_l$	Real amplitude of unsteady lift coefficient	-
$\tilde{c}_l\,(t)$	Unsteady perturbation lift (= force normal to chord) coefficient vector per unit amplitude, positive in positive y-direction	-
$\tilde{c}_m$	Real amplitude of unsteady moment coefficient	-
$\tilde{c}_m\,(t)$	Unsteady perturbation moment coefficient vector per unit amplitude, positive in clockwise direction	-
$\tilde{c}_p\,(x)$	Real amplitude of unsteady pressure coefficient	-
$\tilde{c}_p\,(x,t)$	Unsteady perturbation pressure coefficient in traveling wave mode $\tilde{c}_p\,(x,t) = \dfrac{1}{h}\cdot\dfrac{\tilde{p}\,(x,t)}{\overline{p}_{w1}-\overline{p}_1}=\tilde{c}_p\,(x)\cdot e^{i\,(\omega t+\Phi_p)}$	-
☐	Steady-state pressure coefficient $\overline{c}_p\,(x)=\dfrac{\overline{p}\,(x)}{\overline{p}_{w1}-\overline{p}_1}$	
$\hat{c}_p\,(x)$	Quasi-steady perturbation pressure coefficient $\hat{c}_p\,(x)=\dfrac{1}{h}\cdot\dfrac{\overline{p}_{\text{modified pitch}}\,(x)\,\overline{p}_{\text{nominal pitch}}\,(x)}{\overline{p}_{w1}-\overline{p}_1}$	-
$\tilde{c}_w$	Aerodynamic work coefficient per cycle of blade vibration	-
d	Maximum blade thickness ratio	-
e	Distance between blades and measuring station	m
$\vec{e}_f$	Unit vector in direction of force coefficient	-
$\vec{e}_h$	Unit vector in vibration direction	-
$\vec{e}_n$	Unit vector normal to blade surface	-
$\vec{e}_n$	Unit vector tangent to blade surface	-
$\vec{e}_x$	Unit vector in chord direction	-
$\vec{e}_y$	Unit vector normal-to-chord	-
f	Blade vibration frequency	Hz
f	Function	
h	Channel height of test facility	m
h	Dimensionless (with chord) bending vibration amplitude	-

Symbol	Explanation	Dimension
H_C	Height of camber-line at midchord (eq. 3.10.2)	-
H_T	Maximum (full) blade thickness, normal to chord (eq. 3.10.1)	-
$H_\pm$	Blade thickness on upper / lower surfaces (Fig. 3.10.1)	
i	Complex notation = $(-1)^{0.5}$	
i	Incidence angle, from mean camberline at leading edge	o
Im	Imaginary part of complex value	
k	Reduced frequency, $k = (c\cdot\omega)/(2\cdot v_{ref})$	-
M	Mach Number	-
p	Pressure	mbar
R	Radius of camber line (eq. 3.10.2)	-
$\vec{R}$	Dimensionless (with chord) vector from mean pivot axis to an arbitrary point on the mean blade surface	-
Re	Real part of complex value	
Re	Reynolds number = $(v_{ref}\cdot c)/\nu$	-
t	Time	sec
t	Blade pitch	m
T	Dimensionless time = t/T_0	-
T_0	Period of a cycle	-
T(x)	Blade (full) thickness distribution	-
v	Velocity	m/sec
v_{ref}	Reference velocity $v_{ref}=v_1$ for compressor cascade $v_{ref}=v_2$ for turbine cascade	m/sec
w	Relative flow velocity	m/sec
x	Dimensionless (with chord) coordinate along chord	-
X	Dimensionless (with chord) blade surface coordinate (eq. 3.10.3)	-
x_α	Dimensionless (with chord) chordwise position of torsional axis	-
y	Dimensionless (with chord) blade coordinate normal to chord	-
Y	Dimensionless (with chord) blade surface coordinate (eq. 3.10.3)	-
y_α	Dimensionless normal-to-chord position of torsional axis	-
z	Dimensionless (with chord) span wise coordinate	-
α	Real amplitude of blade vibration pitching amplitude	rad
$\tilde{\alpha}\,(t)$	Complex amplitude of blade pitching oscillation	rad
β	Flow angle, measured from axial, positive in direction of rotation	deg
γ	Chordal stagger angle, from axial	deg
$\Delta\tilde{c}_p\,(x)$	Real amplitude of unsteady perturbation pressure difference	-
$\Delta\tilde{c}_p\,(x,t)$	Unsteady perturbation pressure difference coefficient in traveling wave mode	-
$\_(x/l)_i$	Normalized blade surface element projected normal to the direction	

	of vibration	-
δ	Blade bending vibration direction $= \tan^{-1}(h_y/h_x)$ deg	
ρ	Density	kg/m^3
θ	Angle of mean camber line (eq. 3.10.3)	rad
$\theta_\alpha^{(m)}$	Phase lead of pitching motion towards heaving motion of blade (m)	deg
ν	Kinematic viscosity	m/sec
Ξ	Aerodynamic damping coefficient $\Xi_h = \mathrm{Im}\,\tilde{c}_h$) for pure bending	-
σ	Interblade phase angle. σ is positive when blade "n+1" leads blade "n"	deg
τ	Dimensionless, with chord, pitch	-
ϕ	Phase angle. Positive when disturbance leads blade "n"	deg
φ	Phase angle in Fourier series	deg
ω	Circular frequency of the blades	rad/s

Subscript

aero	Aerodynamic damping
c	Stagnation value in absolute frame of reference
G	Center of gravity
global	Global values (=time-averaged + unsteady perturbation)
global	Global values along the whole blade (in contrast to local below)
h	Bending motion
i	Pressure transducer "i"
ic	Influence coefficient
LE	Leading edge
loc	Local values on the blade surface
mech	Mechanical damping
p	Pressure
ps	Blade pressure surface
ref	Reference value
s	Isentropic
ss	Blade suction surface
TE	Trailing edge
twm	Traveling wave mode
w	Stagnation values in relative frame of reference
1	Upstream flow conditions
2	Downstream flow conditions
1B	First bending mode
- _	Values at "infinity" upstream
_	Values at "infinity" downstream
α	Pitching motion
α	Position of pitch axis

Superscript

~	Time dependent perturbation values
-	Time-averaged values
c	Complex value (used only in ambiguous contexts)
ls	Lower surface of profile
m	Blade number
m, n	Influence of blade "m" on blade "n"
ps	Pressure surface
ss	Suction surface
us	Upper surface of profile

Note:
A question as regards the definition of dimensionless pressures have been brought up during some discussions between different researchers working with the standard configurations. It must be remembered that all the standard configurations use the time-averaged dynamic pressure $(\bar{p}_{w1} - \bar{p}_1)$ as a means to obtain non-dimensional pressure coefficients, both for the steady-state and time-dependent cases. However, as historically theoretical models rather use the incompressible dynamic pressure, $(\bar{\rho}_{-\infty}\bar{v}_{-\infty}^2 / 2)$, at the upstream infinity for this purpose, some of the authors have instead used the latter value as dynamic pressure. In general it can be stated the differences between the two definitions are negligible for standard configurations 1 and 2 (incompressible flow). All participants have, as far as the present authors are aware, employed the compressible dynamic pressure for the standard configurations 3-7. For standard configurations 8 and 9 it seems as if everyone has used the incompressible definition, whereas for the 10th standard configuration mixed responses have been received. As far as possible, it has been tried to note the various definitions in the text.

It is recommended to use the compressible definition for all standard configurations in the future.

1. INTRODUCTION AND OBJECTIVES

Vibration-related fatigue failures have been, and remain, a major concern for turbomachine manufacturers and operators worldwide. If such a failure appears, it has major consequences, normally in significant shut-down time of the machine and sometimes in the loss of human life, and can become extremely expensive. It is not probable that blade vibration problems will disappear in the next few years while, although the quality of design methods increases, manufacturers constantly push the aerodynamics and materials used for blades into higher performances. Modern turbomachine blades are thus constantly at the high end of possibilities of the materials employed.

The two most important blade vibration problems are the forced vibration, which is a flow interaction between the rotor and the stator, and the blade flutter, which is a self-excited vibration. The correct prediction of the unsteady forces from both these phenomena is essential to an acceptable design of fans and compressors, as well as turbines.

Evidence of a tremendous improvement in predicting the unsteady aerodynamic behavior of the high-speed flow through vibrating turbomachine-cascades, together with an increase in the number of well documented experimental data, can be found in the literature during recent years. Furthermore, two excellent review manuals concerning the important aeroelastic effects in axial-flow turbomachines have recently been published [Platzer and Carta; Editors, 1987, 1988].

The agreement between theoretical and experimental results in the domain of turbomachine blade aeroelasticity ranges from extremely good to extremely bad, depending on such factors as geometry and flow conditions, but also on experimental procedure and numerical method. Generally it can be concluded that the low subsonic attached flow can be reasonably well measured and predicted (whereas the transonic flow conditions on realistic profile types show discrepancies between theory and experiments) and that virtually no data or prediction models are available for separated flow conditions. A large need exists thus for both well documented experimental test cases and for appropriate prediction models.

Within the framework of the symposia "Aeroelasticity in Turbomachines" [1976, 1980, 1984, 1987, 1989, 1991] a workshop, with the aim to define the state-of-the-art of prediction models and experimental test rigs for unstalled two-dimensional cascade flow, was performed with the conclusion that several successes could be found but that also some significant differences, both between theories and experiments and between different prediction models, had to be documented [Bölcs and Fransson, 1986].

At the outset of the present workshop (1980) no well-documented comparisons existed between different theoretical models and experimental data. A wide scope of different "standard configurations" was thus established, and different aeroelastic sample cases within each standard configuration were defined, with the obvious objective to better define and eventually reduce/extend the aeroelastic sample cases in a later phase of the project as possibilities and limitations of prediction models and experimental data became clearer.

At the 1987 Aeroelasticity symposium a task force[2] was thus created with the objectives to:
- follow up the literature on new experimental and theoretical procedures
- redefine the standard configurations to evolve together with the present need of aeroelastic information in transonic and high incidence flow regimes
- reduce, where possible, the number of aeroelastic sample cases for unstalled flow
- seek explanations for agreements and disagreements between prediction and experiment
- present an updated version of standard configurations at the 1991 aeroelasticity meeting.

The present note constitutes a documentation in this context. First, an attempt to give a brief, certainly non-exhaustive, overview about new experimental and numerical results on unsteady flow through vibrating axial-flow turbomachine cascades that has appeared in the open literature during the years 1987-1991 is made. The purpose of this is to guide researchers through the large amount of literature in connection with validation of experimental, theoretical and numerical procedures for the field of interest discussed here and to indicate some of the conclusions the respective authors have found important. We apologize to anyone who's contributions have not been mentioned.

Secondly, some of the standard configurations, as defined in the 1986 report [Bölcs and Fransson, 1986], have been reduced in importance[3]. Of the remaining configurations the number of aeroelastic cases has been modified, whereas one more configuration has been added in order for the sample cases to better reflect the fields in which basic research is needed today. Furthermore, some authors have recently asked for more information on time-dependent stalled and partially stalled flow. To this end the fifth standard configuration has been extended with a few such aeroelastic sample cases. It

---

[2]   S. Fleeter, E. Széchényi, J. M. Verdon, T. H. Fransson.

[3]   This corresponds to those with small participation or presently small industrial interest. (Standard configurations 2, 3 and 6 have been reduced in importance.)

is foreseen that the standard configurations also in the future will be extended to stalled flow conditions as soon as detailed data on separated flow becomes available. It is hoped that this will happen in the near future.

Finally, as one of the objective of the present study was to solicit comparison of results during the 1991 Symposium on Aeroelasticity, some results which have been published on the standard configurations in the years 1987-1991 have also been included in the present note.

It is hoped that as time goes on researchers will find it useful to compare more and more of their results on specific sets of test cases, as only through such a broad comparison will it be possible to assess possibilities and limits of different experiments and predictions. Through this the different results (experimental, numerical, analytical) can also be used towards the ultimate goals of understanding the physical phenomena involved in aeroelasticity in axial-flow turbomachines and design blades with optimal unsteady forces. To facilitate the comparisons for everyone interested, it is recommended that new results should be sent to the first author of the present report to be incorporated in the data base. This will help to judge if (and why) fundamental differences appear between experiments and predictions.

The authors express their gratitude to everyone who participates in the study, and apologizes for any errors that may have slipped into the data that are represented in the appendices.

2.   OVERVIEW OF UNSTEADY INTERNAL FLOW INVESTIGATIONS DURING 1987-1991.

In the years 1987-1991 a large amount of information on unsteady flow through vibrating axial-flow turbomachine blade rows has appeared in the open literature.

As mentioned above the AGARD "Manuals on Aeroelasticity in Axial-Flow Turbomachines" [Platzer and Carta, Editors, 1987 (Vol. 1), 1988 (Vol. 2)] provide an excellent overview of the state-of-the-art in the field, both as regards to experimental techniques and as to prediction models.

The fourth, fifth and sixth "Symposium on Unsteady Aerodynamics and Aeroelasticity of Turbomachines and Propellers" were held in Aachen, Germany on September 6-10, 1987 [Gallus and Servaty, 1988], Beijing, China, on September 18-21, 1989 [Pan et al, 1989] and Notre Dame, USA [Atassi, 1992], respectively, and an AGARD Propulsion and Energetics Panel meeting on "Unsteady Aerodynamic Phenomena in Turbomachines" took place in Luxembourg on August 28-30, 1989 [AGARD, 1989].

A symposium on "Transonic Unsteady Aerodynamics and Aeroelasticity" [Bland, 1987] was held at NASA Langley Research Center on May 20-22, 1987. Most of the presentations are concerned with aeroelastic effects in external flow, but some also treat cascade effects.

Bendiksen [1990] reviews the areas of unsteady cascade flow, structural modeling and flutter prediction models, from the theoretical point of view, and gives examples of important parameters from a large literature base (126 references). He states that with the decreasing computing costs the way to perform complete aeroelastic (i.e. interactively coupled structural and fluid) predictions on parallel super computers will be changed to incorporate novel approaches in the future.

The literature survey below gives indications about publications concerning experimental and theoretical investigations on flow through cascades with vibrating blades, as well as experimental studies of the viscous flow around isolated airfoils vibrating in wind tunnels. These latter experimental studies on isolated airfoils are included as data on viscous phenomena in cascades are still today fairly rare and the isolated airfoil experiments may be of use for understanding and predicting unsteady viscous flow in cascades. Computational efforts on isolated airfoils are however not included. On the other hand, numerical computations on nozzle flows with oscillating shock waves are mentioned as non-linear effects can relatively well be studied in such geometries, and comparisons with linearized asymptotic theories are possible. Purely structural aspects of the aeroelasticity, although extremely important, have not been included as the emphasis of the working group has, from the start, been put on relations with the unsteady flow. It should finally be noted that the study treats axial flow turbomachines and that, thus, aeroelastic effects on centrifugal impellers and helicopter rotors are not included.

2.1   Experimental Studies

Several experimental investigations have been presented in the open literature since the Aachen Symposium in 1987 [Gallus and Servaty, Editors, 1988]. A small attempt is here made to give an overview of these, with the reservation that other experiments, not reported here, certainly have been performed. The objective is only to give a comprehensive view of the experiments and the main findings put forward by the authors, and not to discuss the results in detail. The publications the present authors have come across in this field are presented, for a quick reference, in Table 2.1, together with the main cascade and aerodynamic characteristics.

Rotating blades:

Kurkov and Mehmed [1991] present unsteady displacements, as a function of frequency, during flutter of an unducted, composite, fan model under transonic flow conditions. They show the stability limits of a counter rotating rotor and indicate that high incidence was found to be destabilizing. Mehmed and Murthy [1991] show the aeroelastic response of the blades for two mistuned propfan rotors, for a wide range of off-axis flow angles, blade pitch angles and rotational speeds. They indicate that an inherent random mistuning gave a large, intuitively unpredictable, variation in the aeroelastic response. The intentional alternate mistuning was beneficial for the aeroelastic response.

A parametric investigation about the flutter characteristics on a sub-velocity scaled propfan rotor was performed by Crawley and Ducharme [1989]. They find that the unsteady aerodynamic forces significantly modify the frequencies at speed for this kind of blades, even well below the flutter speed. It is concluded that the dominating flutter mechanism is the modal coalescence in a single blade and not the highly aerodynamically coupled single mode cascade flutter of turbofans.

Song et al [1989] summaries experiments on a series of rotors in a single and double-stage transonic compressor facility. Factors influencing stall flutter, such as blade clearance, airfoil geometry, mistuning and inlet distortions, are studied. It is concluded that the aeroelastic stability of the rotor can be improved by changing the radial clearance or the inlet distortion.

Chen [1989] discusses a case of non-synchronous vibrations of shrouded blades in a steam turbine under field operation. He concludes that the vibration occurred only in a narrow region characterized by constant moisture lines and that the aeroelastic phenomena is caused by interaction with the condensation, and possibly with the shock and boundary layer.

Non-rotating cascades:

A review of the latest years work performed on linear compressor cascade flutter at ONERA has been given by Széchényi and Cafarelli [1989]. They conclude that the pressure surface has essentially no influence on the instabilities for subsonic flow and that an increase of incidence decreases the stability margin of the cascade. For supersonic flow conditions their experience indicate that the shock waves are important sources for pressure fluctuations when the blades oscillate.

Buffum and Fleeter [1991, 1990, 1989a,b,c, 1988] (see also Buffum [1990]) have continued their investigation of the high subsonic and low transonic flow on a linear cascade consisting of nine uncambered biconvex airfoils (8% thickness) oscillating in torsion at realistic reduced frequencies. One of the objectives of these investigations was the experimental validation of the superposition technique (of "single blade oscillation" to obtain results for the "traveling wave mode" [Hanamura et al, 1980; Crawley, 1984)) for compressor blades undergoing torsional vibrations in attached flow. The results indicate, in most subsonic sample cases shown, relative good trend wise correlation with an analytical flat plate model. They also show that reflections from the nozzle liners in their linear cascade facility may influence the experimental results for certain interblade phase angles [Buffum and Fleeter, 1991]. This can eventually explain some differences found between the traveling wave mode and influence coefficient results.

The above mentioned superposition (or "influence coefficient") principle has also been validated experimentally, in detail, for annular turbine cascades oscillating in bending mode (at reduced frequencies realistic for last stages of modern steam turbine and industrial gas turbine blades) by Schläfli [1989; see also Bölcs et al, 1989a]. These results show an extremely good agreement for three different types of cascades, over a large Mach number range of subsonic, transonic and supersonic outlet flow conditions and over 20 interblade phase angles. The results were obtained for cascades and flow conditions for which the acoustic resonances (based on linear flow theory) in the up- and downstream flow are fairly close to each other and no attempt was made to investigate the influence of the acoustic resonance. The results indicate that, in most cases in an annular set-up, it is sufficient to consider 2 blades on each side of the reference blade in order to capture most of the time-dependent aerodynamic cascade coupling effects in annular test facilities. However, the authors state that it is probably necessary to have more blades in the cascade in order to avoid reflections from the wind tunnel walls.

Kovats [1991] presents experimental transonic flow data, obtained with the "influence coefficient technique" in a turbine test facility with three blades in the cascade, with the middle blade vibrating. Several cascades are investigated and the author has put all the data into a data base for design purposes. Interpolations from this data base are made to obtain influence coefficients for blade shapes and flow conditions similar to the empirical results in the data base. The author states that predictions by "FINSUP" [Whitehead, 1990] approximate the empirical data obtained.

Hanamura and Yamaguchi [1988] used the "influence coefficient technique" to determine the unsteady moments on linear turbine cascades oscillating in torsion at transonic outlet flow conditions. They state

that measurements on two blades upstream and four blades downstream of the oscillating blades should be enough to capture the main unsteady aerodynamic coupling effects.

In a similar way, Schläfli [1989] (see also Bölcs et al [1989b]) indicate that, for sub- and supersonic outlet flow conditions on three annular turbine cascades studied in bending mode, the influence of a blade on itself is an "eigen-damping", but that an instability may arise because of the aerodynamic coupling effects between, essentially, the reference blade and its immediate suction surface neighbor. For transonic outlet flow velocities they observe a clear destabilizing effect of the normal shock wave on the blade itself. It is furthermore observed that the largest time-dependent coupling effects appear in the part of the blade passage which is overlapped, a statement which is also made by Ezzat et al [1989a,b] and Fransson [1990] on another type of transonic turbine geometry. The last author also indicates that the driving forces for an overlapped steam turbine cascade at realistic reduced frequencies and transonic flow conditions can partly be explained by quasi-steady <u>cascade</u> effects involving the correlation between shock movements and the immediate vibrating neighbor blades.

Kobayashi [1989, 1988] has presented unsteady aerodynamic results on vibrating turbine and compressor cascades under transonic flow conditions, over a large range of reduced frequencies in torsion. These studies are performed in an annular non-rotating test facility, operating in freon. The compressor cascade (non-symmetric DCA-profiles) results indicate that the region of unstalled flutter changes significantly when the flow in the blade passage becomes transonic and that shock movements due to blade oscillations generate markedly large time-dependent forces which stimulated and damped the blade oscillation for low and high reduced frequencies, respectively. The results on the turbine cascade investigated [Kobayashi, 1988] indicate also that the shock wave motion can either damp or excite the blade vibration, depending on the interblade phase angle of the cascade vibration.

Watanabe and Kaji [1989, 1988] have investigated, with the vortex lattice method, the unsteady aerodynamic response, at low flow speeds, to tip clearance changes on a straight cascade in a linear test facility. These results indicate that the effect of a variation of tip clearance is largest for unloaded blades, and that the tip clearance induced unsteady aerodynamic forces are considerably suppressed by the steady-state blade loading. The aerodynamic damping force was most strongly influenced when the interblade phase angle was 180 degrees. Quantitatively good agreement with experimental results is found for the aerodynamic damping coefficient at tip clearances larger than 1.7%, whereas

the theory did not agree with data for lower tip clearances. The authors' state furthermore that, from the theoretical results obtained, the influence of the tip clearance on the unsteady aerodynamic forces is similar for low and high reduced frequencies.

Kaminer et al [1989] show experimentally obtained unsteady aerodynamic forces from a subsonic shear flow interacting with three vibrating compressor blades in a linear cascade. It is concluded that the shear flow can decrease the unsteady aerodynamic forces on the cascade.

A new cascade wind tunnel, for subsonic flow, has recently been taken into operation at the DFVLR in Göttingen, Germany [Kiessling and Hennings, 1991]. It can accommodate 11 compressor blades with a span of 200mm and a chord of 150mm. The blades being tested presently consists of NACA 65 series airfoils, and both "self-started" and controlled vibration modes can be obtained.

Giordano and Fleeter [1990] presents a study, conducted on a water table, of oscillating airfoil shock phenomena for supersonic axial flow at high reduced frequencies. They indicate that the phase of the bow shock motion is dependent on the interblade phase angle and the amplitude of the oscillation, and that the magnitude of shock motion is a strong function of the reduced frequency.

Detailed studies of some effects, like unsteady flow separation and dynamic stall has not up to now, to the authors' knowledge, been reported for cascade flow. Recently, such results have however been presented on single airfoils in nozzles.

First author	Flow type	Number and type of airfoil	Thickness (d/c, %)	Camber (deg)	Chord (mm)	Span (mm)	Stagger (deg)	Solidity (-)	Reynolds No. (-)	Torsion/ Bending	Red. freq. (k,-)	Type of facility	Blades vibrated	Working fluid
Kurkov 1991	Trans	Propfan	Different over span	Different over span	Twisted	Diff	Diff	Diff		Mainly B		Unduc. fan	Flutter	Air
Mehmed 1991	Trans	8	Different over span	Different over span	Twisted					Bending				
Crawley 1989	Sub	Propfan 2-12	Different over span	Different over span	Twisted		Variable	Variable		Torsion Coupled	0.14	Rotating	All	Air
Song 1989	M_1, $M_2<1$ Sub	Propfan Compressor	Different	Different	31 at	77				Torsion	(at 80%) 0.05 (B)	Rotating	All	Air
Chen 1989	Trans	(1+2 stages) Steam	over span	over span	tip					Bending 2nd	0.16 (T)	Rotating		Steam
Buffum-88	Sub, trans	turbine 9	7.6	0.	76.2	97.8	53	1.3		bending Torsion	0.22, 0.39	Linear Linear	9,1	Air
-89a,b,c -90,-91 Kobayashi	M_1, $M_2<1$ Sub, trans	Compressor 16	12.4	60.1	72	25	45.1	1.24		Torsion	0.32, 0.46 0.04-0.55	Annular	16	Freon
-88,-89 Kobayashi	$M_1<1$, $M_2<>1$ Sub, trans	Turbine 16	4	6	72	25	58	1.24		Torsion	0.03-0.46	Annular	16	Freon
-89 Watanabe	$M_1>1$, $M_2<1$ Low sub	Compressor 1, 8	10	0	60	180	-, 45	-, 1.0		Bending	0.10,0.13	Linear	1	Air
-88, -89 Hanamura	M_1, $M_2<<1$ Sub, trans	Flat plate 11		10	50	80	60	1.25		Torsion	0.30 0.1-0.8?	Linear	1	Freon
-88 Hanamura	$M_1<1$, $M_2<>1$ Sub, trans	Turbine 11			55.6	80	54	1.39		Torsion	0.1-0.7?	Linear	1	Freon
-88 Ezzat	$M_1<1$, $M_2<>1$ Sub, trans	Turbine 20	5.1	6.5	78	40	65	1.38	_1.2×10^6	Bending	0.06-0.13	Annular	20	Air
-89a,b Fransson-90 Schläfli-89	$M_1<1$, $M_2<>1$ Sub, trans	Turbine 20	10	49.2	78.5	40	49	1.39	$7\text{-}13 \times 10^5$	Bending	0.14-0.21	Annular	20,1	Air
Bölcs -89a,b	$M_1<1$, $M_2<>1$	Turbine												

Table 2.1:   Continued (1 of 2).

First author	Flow type	Number and type of airfoil	Thickness (d/c, %)	Camber (deg)	Chord (mm)	Span (mm)	Stagger (deg)	Solidity (-)	Reynolds No. (-)	Torsion/ Bending	Red. freq. (k,-)	Type of facility	Blades vibrated	Working fluid
Schläfli-89	Sub, trans	20	17	45	74.4	40	56.6	1.35	$\_7 \times 10^5$	Bending	0.08-0.13	Annular	20,1	Air
Bölcs -89a,b Schläfli-89	$M_1<1, M_2<>1$ Sub, trans	Turbine 20	5.2	14	52.8	40	73.4	0.93		Bending	0.08-0.17	Annular	20,1	Air
Bölcs -89a,b Széchényi -89	$M_1<1, M_2<>1$ Sub, trans, Super	Turbine 7-9	Different		80-100	120	Different	Different		Torsion Bending	$\_0.3$ at M=1	Linear	1	Air
Kovats -91	Sub, trans	Compressor 3	Variable	Var	Var		Var	Var		B, T, coupled	0.23-1.86	Linear	1	Air
Kaminer -89	Subsonic	Turbine 5					30, 45	0.75-1.25			0.03-0.1	Linear	3	Air
Kiessling -91	Sub	Compressor 11	6	10	150	200	45			Bending		Linear	9	Air
Yamamoto -89	(incompr) Sub, trans	Compressor 1	10, 12	0	75	75	-	-		Torsion Torsion	$\_0.6$	Nozzle	0	Air
Carr-89,-90 -91	$M_1<1, M_2<>1$ Sub	Single blade 1	12	0	75	250	-	-		Torsion	Max 0.15 at M=0.5	Nozzle	1	Air
Chandrasekhara -89,-90,-91 De Ruyck	$M_1, M_2<1$ Sub	Single blade 1					-	-	$0.3 \cdot 10^6$	Torsion	0.3	Nozzle	1	Air
He-91a	Sub	Single blade 1					-	-		Torsion	0-0.69	Nozzle	1	Air
Currier-91		Single blade 1					-	-		Torsion		Nozzle	1	Air
Giordano -90	Super $M_1<>1, M_2>1$	Single blade 1, 5	7.6	0	254	-				Torsion	0-2.75	Water	All	Water
First author	Flow type	Number and type of airfoil	Thickness (d/c, %)	Camber (deg)	Chord (mm)	Span (mm)	Stagger (deg)	Solidity (-)	Reynolds No. (-)	Torsion/ Bending	Red. freq. (k,-)	Type of facility	Blades vibrating	Working fluid

Table 2.1:   *Experimental unsteady aerodynamic investigations on vibrating blades 1987-1991.*

<u>Isolated airfoils:</u>

An investigation towards the understanding of self-oscillating flow around an isolated fixed airfoil in nozzles has been performed by Yamamoto and Tanida [1989]. Their measurements of the shock wave, wake motions and unsteady pressure field indicate that the pressure disturbances induced by the oscillation of the boundary layer separation (close to the trailing edge of the blade) propagate upstream in the main flow and force the shock to oscillate.

Carr et al [1989; 1990] (see also Carr and Chandrasekhara [1989], Chandrasekhara and Carr [1989], Chandrasekhara and Brydges [1990] and Chandrasekhara and Platzer [1991]) present results on a dynamically stalled isolated airfoil in subsonic compressible flow. They indicate that the dynamic stall vortex occurs at significantly lower angles of attack as the Mach number increases. On the other hand, an increase in reduced frequency helps in retaining the dynamic stall vortex on the airfoil surface to higher angles of attack. Furthermore, an increase in the blade oscillation amplitude delays deep stall to higher angles of attack. From real-time interferograms obtained, Carr et al [1991] concludes that the dynamic stall develops as a region of strong gradients enclosing a region of low energy while still supporting the dynamically modified outer flow associated with the increase of lift that is typical of dynamic stall.

Low speed unsteady flow, at high incidence, over a two-dimensional NACA-65 airfoil oscillating in torsion at 2° amplitude and at reduced frequencies up to 0.69 is reported by He and Denton [1991a]. They show detailed measurements of unsteady surface pressure and skin friction coefficients and indicate that the aerodynamic moment coefficient changes from stable to unstable close to the dynamic stall phenomena. De Ruyck et al [1989] present experimental data on velocity profiles and Reynolds stresses, for both leading edge and trailing edge separations, on an isolated airfoil in low speed flow at a reduced frequency of 0.3 and a Reynolds number of 300'000. Leading edge stall is found to be triggered by the bursting of the leading edge bubble soon after the static stall limit is exceeded. The authors did not observe any interaction with the trailing edge separation during this phenomenon.

An overview of several earlier published dynamic stall data on isolated airfoils is given by Currier and Fung [1991]. Based on the experimental results they conclude that the onset of dynamic stall depends whether the flow is sub- or supercritical. The accompanying analysis supports that stall onset is the consequence of the bursting of the separation bubble and that this bursting is promoted by the upstream biased pressure gradient which shifts the bubble to a

more laminar environment when the outer flow becomes locally supersonic.

2.2.   Theoretical studies

The "theoretical" articles presented between the Aachen and Notre Dame Symposia and reviewed here can be separated into four main parts, in which:
- actuator disk models
- linearized methods, both as regards to the airfoil (flat plate) and the time-dependency,
- models linearized in time but non-linear in space
- fully non-linear models

are either developed or used as tools for studies of certain phenomena. Most of the studies have treated inviscid flow, but viscous cascade investigations are coming into use.

As regards to general theoretical studies of time-dependent cascade flow, Verdon [1989a] has given a detailed analytic description of the unsteady response far up- and downstream of an isolated two-dimensional cascade. The far-field solution given can be implemented into numerical time-linearized analyses developed to predict the aerodynamic response of the blading to prescribed small-amplitude unsteady excitations (blade motions, incident entropic, vortical and acoustic gusts). In a similar context, Giles [1989] develops non-reflecting boundary conditions, for the Euler equations, that are exact (within the assumption of linear theory) for unsteady one-dimensional and steady two-dimensional, and approximate for unsteady two-dimensional, flows. He concludes that the non-reflecting steady-state boundary conditions increase the accuracy of the calculation for flows with shocks extending out of the computational domain. However, no large improvements in accuracy (over the one-dimensional non-reflecting boundary conditions) could be found in the unsteady sample application with the new improved boundary condition treatment.

Quiniou [1989] has given a brief overview of the different computational methods employed at SNECMA for prediction of flutter.

<u>Actuator disk and flat plates:</u>

Chiang and Fleeter [1989a,b] developed a first order mathematical model to demonstrate the enhanced torsion mode stability associated with alternate blade circumferential aerodynamic detuning in an incompressible flow field, based on the aerodynamic influence coefficient technique. Good agreement with flat plate analytical results and experimental data (among others "Standard Configuration 1") is shown for blades vibrating in the traveling wave mode [Chiang and Fleeter, 1989b]. The model is thereafter applied to a 10% alternate circumferential spacing

detuning and it is concluded that aerodynamic detuning is a viable passive control mechanism for the torsion mode flutter [Chiang and Fleeter, 1989a]. This complements previous results by Topp and Fleeter [1986] for aerodynamic detuning in supersonic flow.

The enhancement of aeroelastic detuning on the stability in unstalled supersonic flow, with subsonic leading edge locus, was studied by Fleeter and Hoyniak [1989]. They investigated the effects of different combinations of two aerodynamic detunings as well as blade structural detuning. The authors conclude that, from an application based on Verdon's "Cascade B" [Verdon, 1973] flow geometry, aeroelastic (i.e. combined structural and aerodynamical) detuning appears to be a viable passive control mechanism for supersonic unstalled flutter. Similar conclusions are put forward, for supersonic throughflow cascades, by Spara and Fleeter [1989; 1990]. They state, however, that for certain cascade geometries the purely aerodynamic detuning resulted in decreased stability.

Kielb and Ramsey [1988] apply a combination of three unsteady flat plate cascade theories[4] together with a structural model consisting of a two degree of freedom oscillator suspended by bending and torsional springs to predict the flutter of an advanced supersonic axial flow fan. They conclude that supersonic axial fan and compressor blades are susceptible to a strong torsional mode flutter at low reduced velocities and that the worst pitching axis location is slightly upstream of mid-chord. A pure weak plunging instability was found at low supersonic velocities, but was considered of little practical interest. It was concluded that the stability is strongly dependent on solidity and weakly dependent on stagger angle.

The unsteady supersonic flow computer code used in this investigation is presented by Ramsey and Kielb [1987]. Ramsey [1991, 1989] gives an engineering extension of this model to include non-linear effects of thickness and camber. His results indicate that the inclusion of thickness, with or without camber, may increase or decrease the aeroelastic stability, depending on the airfoil geometry and operating conditions, and may change the critical interblade phase angle.

A modification of this aerodynamic model to include non-rigid blade vibrations is introduced by Jacquet-Richardet [1990] and Jacquet-Richardet and Henry [1990], and combined with a finite element structural model derived from Lagrange's equations. The importance of considering non-rigid blade vibrations for the third and higher modes is shown in examples.

Iminari and Kaji [1989] reports a study on the influence of three-dimensional loading and twist, as well as three-dimensional vibration modes, on the unsteady characteristics of vibrating blades in incompressible flow. Their results indicate a significant difference towards two-dimensional strip theory predictions at lower reduced frequencies, especially for highly loaded and staggered cascades, and that the treatment of the three-dimensional vibrating modes can be critical in determining the flutter boundary. However, the differences towards the two-dimensional theory decrease, in their study, for higher reduced frequencies.

The double linearization theory in two-dimensional sub- and supersonic flow has been applied to nonrigid blade vibrations, for lightly loaded cascades, by Namba and Toshimitsu [1990], Namba and Li [1990] and Toshimitsu et al [1990, 1989]. The results indicate that the unsteady work for section deformation is largely influenced by steady-state loading and that chordwise displacement for translational oscillations may be either stabilizing or exciting, depending on the phase difference between the chordwise and normal-to-chord oscillation. Furthermore, the effect of chordwise displacement is opposite for subsonic and supersonic cascades. Results from the theory covering three-dimensional subsonic flow through annular cascade blades are presented by Namba et al [1989; 1988] and compared to strip theory calculations. The authors conclude that three-dimensional effects are important for high Mach numbers and when the steady loading increases from hub to tip. They state that the strip theory approximation fails to predict instability for some flow configurations.

A three-dimensional lifting surface theory for annular cascades with swept blades, without thickness and steady loading, is presented by Kodama and Namba [1990; 1991] for subsonic and transonic flow, respectively. They find that the magnitude of total aerodynamic work due to blade vibrations is reduced at large sweep angles. Chi [1991] uses a similar theory to study the unsteady aerodynamic pressure loads on oscillating blades of a ducted subsonic fan. Also this model treats blades without thickness and steady-state loading. The author concludes that three-dimensional effects on swept blades are important, both for low and high aspect ratios, in the latter case as, generally, the radial variation of the vibration mode shape is large enough to trigger significant span wise unsteady flow interactions.

Butenko et al [1989] discuss the unsteady two-dimensional and three-dimensional linearized flow around lightly loaded vibrating turbomachine blades, in which a set of integral equations are solved. Both subsonic, transonic and supersonic flow is discussed.

---

[4]   Lane [1957] for supersonic flow, Adamczyk and Goldstein [1978] for transonic and Rao and Jones [1976] for subsonic conditions.

Incompressible two-dimensional, unstalled and stalled, flow in a cascade of thin curved high solidity plates is studied by Saren [1989]. He uses an asymptotic Kernel function theory, together with an oscillating stall zone model, to arrive at a qualitative analysis of the change of stall flutter limit with aerodynamic loading. Duan and Zhou [1989] present the initial phase of a small perturbation stall flutter theory for incompressible flow, based on an isolated airfoil stall model by Perumal and Sisto [1974].

Chen et al [1989] uses Whitehead's [1962] incompressible flat plate theory together with a structural model to study the flutter boundaries of several parameters, such as blade mistuning, coupling of disk-blade and location of the elastic axis. It is concluded that mistuning has a stabilizing effect and that coupling of blade and disk can decrease the stability. Yue et al [1989] use a two-dimensional unsteady aerodynamic model to get the aerodynamic influences for the finite element structural dynamics analysis presented. They conclude that coupling effects of modes decrease the stability of the blade and that the interblade phase angle has a large effect on the aeroelastic response.

″ First author	Type of model	Viscous / Inviscid	2-D / 3-D	Application										Special study
				Flow	Type of airfoil	Thickness Camber	Stagger Interbl. phase	Re (-)	Torsion/ Bending	Reduc. freq. (k,-)	Structural model	Nonrigid blade vibrat.		
Verdon -89a	Time-linear Potential	Inviscid	2D	Sub Trans	Compr			-	Torsion Bending		No	No		Boundary conditions
Giles-89	Non-linear Euler	Inviscid	2D					-			No	No		Boundary conditions
Liu -89	Variational principles	Inviscid FE	2D	Trans			-			No	No	Basic theory		
Chiang -89a,b		Inviscid	2D	Incom	Flat plate			-						Aerodynamic detuning
Hoyniak -89		Inviscid	2D	Super	Flat plate			-						Aerodynamic detuning
Spara -89,-90		Inviscid	2D	Super	Flat plate			-						Aerodynamic detuning
Ramsey-87 Kielb-88		Inviscid	2D	Sub Trans Super	Flat plate	No No	Yes Yes	-	Coupled		Yes	No		Red. freq., pitching axis
Ramsey-89 -91		Inviscid	2D	Sub Trans Super	Thick- ness	Small Small	Yes Yes	-	Coupled		Yes	No		Thickness effects
Ramsey-87 Kielb-88		Inviscid	2D	Sub Trans Super	Flat plate	No No	Yes Yes	-	Coupled		Yes	No		Red. freq., pitching axis
Jacquet -90, -90		Inviscid	2D	Super	Flat plate	No No	Yes Yes	-	Coupled		Yes	Yes		Structural model
Iminari-89		Inviscid	3D	Incom	Flat plate	No No	Yes Yes	-			No	No		3D vibrating modes important
Namba-90 -89, -88	Double linearization	Inviscid	2D 3D	Sub Super	Flat plate	No No	Yes Yes	-			No	No		3D effects important at high M
Toshimitsu -89,-90	Double linearization	Inviscid	3D	Sub Super	Flat plate	No No	Yes Yes	-			No	No		
First author	Type of model	Viscous / Inviscid	2-D / 3-D	Application										Special study
				Flow	Type of airfoil	Thickness Camber	Stagger Interbl. phase	Re (-)	Torsion/ Bending	Reduc. freq. (k,-)	Structural model	Nonrigid blade vibrat.		

Table 2.2: Continued (1 of 7)

| First author | Type of model | Viscous / Inviscid | 2-D / 3-D | Flow | Type of airfoil | Application | | Re (-) | Torsion/ Bending | Reduc. freq. (k,-) | Structural model | Nonrigid blade vibrat. | Special study |
						Thickness Camber	Stagger Interbl. phase						
Kodama-90 -91	Lifting surface	Inviscid	3D	Sub Trans	Flat plate	No No	Yes Yes	-			No	No	Sweep
Chi-91	Lifting surface	Inviscid	3D	Sub	Flat plate	No No	Yes Yes	-			No	No	3D effects on swept blades imp.
Butenko -89		Inviscid	2D 3D	Sub Trans Super	Flat plate	No No	Yes Yes	-			No	No	
Saren-89		Unstalled Stalled	2D	Incom	Flat plate	No No	Yes Yes	-			No	No	
Duan-89		Stalled	2D	Incom	Flat plate	No No	Yes Yes	-			No	No	
Chen-89	Whitehead -62	Inviscid	2D	Incom	Flat plate	No No	Yes Yes	-			Yes	No	Coupling blade/disk Mistuning
Jun-89	Whitehead -62	Inviscid	2D	Incom?	Flat plate	No No	Yes Yes	-			Yes Fin. elem.	No	Coupled modes decrease stability
Fujimoto -89	Singularity	Stalled	2D	Incom?	Flat plate	No No	Yes Yes	-	Torsion		Yes??	No	Mistuning beneficial
Yamane -89	Smith -72	Inviscid	2D	Sub	Flat plate	No No	Yes Yes	-			Yes??	No	Anisotropy of composites
Schroeder -89	Small perturbation	Viscous	2D	Incom	Flat plate	No No	Yes Yes	-	Torsion		Yes??	No	Viscous effects decrease stability
Yang -89	Actuator disk	Stall	2D	Sub?	Flat plate	No No	Yes Yes	-			Yes??	No	Non-constant interblade phase
Yang -89	Actuator disk	Stall	Strip theory	Sub?	Flat plate	No No	Yes Yes	-			Yes??	No	Inlet distortion increase stability
Sisto -89,-90 Abdel-Rahim -91	Vortex method	Stall	2D	Incom	Flat plate	No No	Yes Yes	-			Yes??	No	Freq. entrainment Stall propagation otherwise indep. of blade freq.
							Application						Special study
First author	Type of model	Viscous / Inviscid	2-D / 3-D	Flow	Type of airfoil	Thickness Camber	Stagger Interbl. phase	Re (-)	Torsion/ Bending	Reduc. freq. (k,-)	Structural model	Nonrigid blade vibrat.	

Table 2.2: Continued (2 of 7)

| ″ First author | Type of model | Viscous / Inviscid | 2-D / 3-D | Application | | | | | | | | | Special study |
				Flow	Type of airfoil	Thickness Camber	Stagger Interbl. phase	Re (-)	Torsion/ Bending	Reduc. freq. (k,-)	Structural model	Nonrigid blade vibrat.	
Koller -89	Asymptotic expansion	Inviscid	2D	M_1	Flat pla. +DCA			-			No	No	Agreement with Verdon-86
Chen -89	Time-lin potential	Inviscid	2D					-			No	No	Porous wall influence
Liu Time-lin -89	Stall potential	2D (Sisto-74)	M_1	Single airfoil			-			Yes	No		
Whithead -90	Time-lin potential	Inviscid FE	2D quasi-3D	Sub Trans Super	Compr Turbine	Yes Yes	Yes Yes	-	Torsion Bending Coupled		No	No	Comparison with different results (STCF 10)
Klose -89	Whitehead -85	Inviscid FE	2D quasi-3D	Sub Trans Super	Compr	Yes Yes	Yes Yes	-	Torsion Bending Coupled		Yes	No	Mode coupling: small titanium bl., large composite
Verdon-90 -87b, -89b Usab-90	Time-lin potential	Inviscid FD	2D	Sub Trans	Compr	Yes Yes	Yes Yes	-	Torsion Bending Coupled		No	No	Overview of different resulty (STCF 10)
Smith-91	Verdon-84	Inviscid FD	2D	Sub Trans	Compr	Yes Yes	Yes Yes	-	Torsion Bending Coupled		Yes	No	Non-conservative estimate if d/c, i, camber neglected
Smith-90	Verdon-84	Inviscid FD	3D struct. Strip aero	Sub Trans	Compr	Yes Yes	Yes Yes	-	Torsion Bending Coupled		Yes	No	Friction dampers stabilizing
Stecco-88 -89a,b	Time-lin Potential	Inviscid	2D	Sub	Turbine	Low Low	Yes Yes	-	Torsion Bending		No	No	Comp. flat plate +exp (Ezzat-89)
Yang-89	Time-lin Potential	Inviscid FE	3D	Sub	Turbine	Yes Yes	Yes Yes	-	Torsion Bending		No	No	Good agr. with Namba-88 at low load, bad at high
First author	Type of model	Viscous / Inviscid	2-D / 3-D	Application									Special study
				Flow	Type of airfoil	Thickness Camber	Stagger Interbl. phase	Re (-)	Torsion/ Bending	Reduc. freq. (k,-)	Structural model	Nonrigid blade vibrat.	

Table 2.2: Continued (3 of 7)

″ First author	Type of model	Viscous / Inviscid	2-D / 3-D	Application								Structural model	Nonrigid blade vibrat.	Special study
				Flow	Type of airfoil	Thickness Camber	Stagger Interbl. phase	Re (-)	Torsion/ Bending	Reduc. freq. (k,-)				
Hall-89	Time-lin Euler Shock fitting	Inviscid FD	2D	Sub Trans	Comp Nozzle	Low Low	Yes Yes	-	Torsion		No	No	Good agr. with Atassi-78
Allmares -87, -89	Non-linear Euler Upwind	Inviscid Inv / Visc	2D	Sub Trans	Nozzle	- -	- -	-	-		No	No	Trends of self-exciting flow in diffusor predicted
Bassi-89	Non-linear Euler TVD	Inviscid	2D	Trans	Nozzle	- -	- -	-	-		No	No	Non-linearities important in high-frequency flows
Bölcs-89c	Non-linear Euler Upwind	Inviscid	2D	Sub Trans	Nozzle	- -	- -	-	-		No	No	Time-averaged shock position _ unsteady mean
Li-90	Non-linear Euler Upwind	Inviscid	2D	Sub Trans	Compr	Low No	No 180°	-	Torsion		No	No	Agreement with analytical model at d/c=2%, not at 5%
Yamamoto -89	Non-linear N-S	Viscous	2D	Sub Trans	Single blade in nozzle	Low No	No -	1×10^6	None		No	No	Self-exciting flow in diffusor
Wu-88	Non-linear N-S	Viscous (Baldwin-Lomax +k-ε)	2D	Sub	Single blade	Low No	No -	$2-9 \times 10^6$	Torsion		No	No	Differences in Reynold stresses between the two turbulence mod.
Carr-89	Non-linear N-S	Viscous	2D	Sub	Single blade	Low No	No -	$0.6-4 \times 10^6$	Torsion	0-0.05	No	No	Dynamic stall
First author	Type of model	Viscous / Inviscid	2-D / 3-D	Application								Structural model	Nonrigid blade vibrat.	Special study
				Flow	Type of airfoil	Thickness Camber	Stagger Interbl. phase	Re (-)	Torsion/ Bending	Reduc. freq. (k,-)				

Table 2.2: Continued (4 of 7)

| First author | Type of model | Viscous / Inviscid | 2-D / 3-D | Flow | Type of airfoil | Application | | Re (-) | Torsion/ Bending | Reduc. freq. (k,-) | Structural model | Nonrigid blade vibrat. | Special study |
						Thickness Camber	Stagger Interbl. phase						
Krainer-88	Non-linear	Viscous / inviscid interact.	2D	Incom	Single blade	Low No	No -	1×10^6	Ramp-type pitch		No	No	
Jang-89	Non-linear N-S	Viscous / inviscid interact.	2D	Incom	Single blade	Low No	No -	10^5-> $3\cdot10^6$	Pitch		No	No	Agreement at low red.freq but differences at high
Lee-91	Non-linear potential	Inviscid	2D	Incom	Comp Single blade	Low Low	Yes Yes	-	Pitch		No	No	Agreement with exact analytical model
Bakhle-89 -90,-91	Non-linear potential	Inviscid	2D	Sub	Comp	Low? Low?	Yes Yes	-	Pitch?		Yes	No	Agreement with Smith-72
Ku-90	Non-linear potential	Inviscid	3D	Sub Trans	Propfan	Low? Low?	Yes 0°	-	Pitch		No	No	Comparison with panel model and exp. data
Kau-89 Gallus-89	Non-linear Euler	Inviscid	2D	Sub Trans	Compr Turbine	Yes Yes	Yes Yes	-	Bending Torsion		No	No	Comparison with Smith-72 and STCF4
Gerolymos -90a,b -88a,b,c	Non-linear Euler	Inviscid	3D	Super	Compr	Low Low	Yes Yes	-	Pitch		No	No	Strip theory valid in super-sonic flow (Comp. STCF7)
He-89 -91a,b	Non-linear Euler	Inviscid / viscous interact.	2D quasi 3D	Sub Trans	Compr Turbine	Yes Yes	Yes Yes	-	Bending Torsion		No	No	Viscous solution different from invi-scid close to shock (Comp. STCF4)
						Application							Special study
First author	Type of model	Viscous / Inviscid	2-D / 3-D	Flow	Type of airfoil	Thickness Camber	Stagger Interbl. phase	Re (-)	Torsion/ Bending	Reduc. freq. (k,-)	Structural model	Nonrigid blade vibrat.	

Table 2.2: *Continued (5 of 7)*

First author	Type of model	Viscous / Inviscid	2-D / 3-D	Flow	Type of airfoil	Application Thickness Camber	Stagger Interbl. phase	Re (-)	Torsion/ Bending	Reduc. freq. (k,-)	Structural model	Nonrigid blade vibrat.	Special study
Huff-89a,b -91	Non-linear Euler + N-S Upwind	Inviscid Viscous	2D	Sub Super	Compr Turbine	Yes Yes	Yes Yes	-	Bending Torsion		No	No	Comparison with Smith-72, Buffum -87,-89 and STCF1. Nonlinearities
Reddy-91	Non-linear Euler Upwind	Inviscid	2D	Sub Super	Propfan Flat pl. Compr	Yes Yes	Yes Yes	-	Bending Torsion		No	No	Coupled aero- and structures. Comp. STCF5
Carstens -91	Non-linear Euler Upwind	Inviscid	2D	Sub Trans	Turbine	Yes Yes	Yes Yes	-	Bending Torsion		No	No	Comparison with STCF4
Arkadyev -89	Non-linear Euler TVD	Inviscid	2D?	Sub? Trans	Turbine?	Yes? Yes?	Yes? Yes?	-	Bending? Torsion?		No	No	Tip section of fan stage
Giles -91	Non-linear Upwind?	Inviscid / viscous interact	2D	Sub Trans	Compr Turbine	Yes Yes	Yes Yes	-	Bending Torsion		No	No	Basic validations (Smith-72 + Stokes' layer)
Kobaya- kawa-91	Non-linear NS	Viscous	2D	Trans	Compr Turbine	Yes Yes	No 0°	-	Bending Torsion		No	No	Basic validations (Smith-72 + Stokes' layer)
						Application							Special study
First author	Type of model	Viscous / Inviscid	2-D / 3-D	Flow	Type of airfoil	Thickness Camber	Stagger Interbl. phase	Re (-)	Torsion/ Bending	Reduc. freq. (k,-)	Structural model	Nonrigid blade vibrat.	

Table 2.2: *Continued (6 of 7)*

First author	Type of model	Viscous / Inviscid	2-D / 3-D	Flow	Type of airfoil	Thickness Camber	Stagger Interbl. phase	Re (-)	Torsion/ Bending	Reduc. freq. (k,-)	Structural model	Nonrigid blade vibrat.	Special study
							Application						
Sidén-91a -91b,c, -90	Non-linear N-S	Viscous (Baldwin- Lomax)	2D quasi 3D	Sub Trans Super	Compr Turbine	Yes Yes	Yes Yes		Bending Torsion		No	No	STCF5 Fan stage
-89a,b Bloemhof -88	Influence coefficients	FE -	3D	-	-							Yes	Viscous effects important Frequency mistuning
Afolabi -88		-		-	-								Which blades to instrument
First author	Type of model	Viscous / Inviscid	2-D / 3-D	Flow	Type of airfoil	Thickness Camber	Stagger Interbl. phase	Re (-)	Torsion/ Bending	Reduc. freq. (k,-)	Structural model	Nonrigid blade vibrat.	Special study

Table 2.2:   *Theoretical unsteady aerodynamic investigations on vibrating blades 1988-1991.*

Fujimoto et al [1989] use a singularity method to study mistuning effects on fully stalled blades oscillating in torsion. They conclude that the mistuning is beneficial both for unstalled and for stalled flow and that mistuning is more beneficial for turbines than for compressors.

Yamane and Friedmann [1989] study aeroelastic tailoring, with anisotropy of composites, of a structural model coupled with strips of Smith's [1972] linearized flat plate theory. The sample case of a propfan blade show that the natural frequencies of the blade can be changed from 100% to 35% by changing the fiber direction.

Schroeder and Fleeter [1989] have performed a viscous small perturbation analysis of the incompressible flow around a single flat plate oscillating in torsion. Their preliminary results indicate that viscous effects in general decrease the relative stability of the airfoil.

A deforming actuator disk method is used by Yang et al [1989] to predict stall flutter under non-constant interblade phase angles. They indicate good agreement with measured stall flutter limits in a compressor.

The interaction of distortion on stall flutter limits is studied computationally by Yang and Feng [1989]. They employ an actuator disk method and the strip theory applied to an experimental sample case of stall flutter in a single stage axial-flow compressor. The authors state that the strip theory assumption is of limited usefulness in predicting three-dimensional stall flutter, and that an inlet distortion at the hub or tip can increase the stability of the rotor.

Sisto et al [1989] present a numerical simulation for propagating stall in a linear cascade of vibrating blades using the vortex method in incompressible flow. The method is first validated against unstalled analytical data. The mean incidence was thereafter increased. It was confirmed that the spectra of lift and drag responses to the imposed blade motion contain frequencies related to the oscillation frequency as well as non-synchronous frequencies associated with the inherent propagating stall frequency of the cascade. It is shown that an entrainment of the stall and blade vibration frequencies appears over an appreciable interval of the blade frequency [Sisto et al, 1990]. Outside the entrainment region the stall propagation is independent of the blade natural frequency. The computational results show also that there is no entrainment in the pure bending mode [Abdel-Rahim et al, 1991].

Time-linearized studies, on profiles with thickness:

Liu [1989] discusses a family of variational principles for two-dimensional unsteady transonic flow. He states that the theory can serve as a base for a finite element analysis.

The two-dimensional flow (M_1) of a perfect gas is analyzed with matched asymptotic expansions, for low frequencies, by Koller and Kluwick [1989]. Results presented for a flat plate cascade and a double circular arc cascade agree satisfactorily with numerical results by Verdon [1986].

Chen et al [1989] study the possibilities to passively suppress blade flutter by using porous wall casings. Their numerical studies, based on the linearized potential flow equations, show that the porous walls can have both a beneficial and a detrimental effect on the flutter.

Liu et al [1989] present the initial stages of a small perturbation potential flow model, in which they consider completely separated flow with the Helmholtz model by Perumal and Sisto [1974] for an isolated plate airfoil extended to the case of a propeller. The energy method is coupled to the aerodynamic calculation to determine the aeroelastic stability.

Whitehead [1990] presents the complete theory, together with some applications, of his linear unsteady cascade finite element potential flow model, called "FINSUP". Results are compared to, for incompressible flow, a flat plate analysis [Smith, 1972] and a singularity theory [Atassi and Akai, 1980], with excellent agreements. At compressible Mach numbers the agreement with NACA 0006 results by Verdon [1989b] ("Standard Configuration 10") is generally satisfactory, apart from in the regions of acoustic resonances. In supersonic flow, major differences as regards to Verdon's "Cascade A" [Verdon and McCune, 1975] are found for the unsteady blade surface pressure coefficient (as the shocks are smeared out by "FINSUP"), although the overall lift and moment coefficients agree well. Comparison for a normal shock configuration with the theory by Goldstein et al [1977] does not agree very well, as concluded earlier on "Standard Configuration 8" [Bölcs and Fransson, 1986, pp. 171-175]. However, Whitehead points out that configurations with normal shocks are very severe test cases.

Klose and Heinig [1989] combine Whitehead's "FINSUP" program with an eigenvalue and an energy method to solve the equations for the motion of the blades and study the flutter characteristics of a typical section of a two degree-of-freedom cascade with different mass ratios. It is concluded that mode coupling is small for a titanium wide chord fan blade but relevant for some eigenmodes of a composite (carbon-fiber-reinforced-plastic) propfan.

Verdon [1987b; 1989b; 1990] reviews the theory behind his linearized two-dimensional potential cascade flow model and reports on the importance of the unsteady, concentrated, load from an oscillating shock wave in transonic flow. This unsteady load can be well identified with the local pressure-displacement function defined. He also gives an overview of results (on NACA 0006 airfoils, see "Standard Configuration 10") computed with the model and points out important changes of the local unsteady pressure and the global aerodynamic damping for different vibrations (torsional, chordwise and edgewise bending) when such parameters as incidence, blade shape, reduced frequency and Mach number are systematically varied.

New mesh developments on the finite difference unsteady potential flow solver by Verdon and Caspar [1982, 1984] are reported by Usab and Verdon [1990]. They discuss higher resolutions in the leading edge and shock regions with the new meshes and indicate that the linearized unsteady solution is sensitive to the numerical modeling of shock effects. It is concluded that it is important to fit the shocks both in the steady-state and unsteady solutions for an accurate capture of the unsteady moments and forces on the blades. Results are shown on "Standard Configuration 10".

The unsteady aerodynamic potential flow model by Verdon and Caspar [1984], combined with a two degree-of-freedom structural model to determine the aeroelastic stability of a two-dimensional subsonic compressor cascade, is used by Smith and Kadambi [1991]. Their results indicate that neglecting either the airfoil thickness, camber or incidence can result in non-conservative estimates of flutter behavior. Smith [1990] shows also a quasi three-dimensional aeroelastic model, in which a three-dimensional finite element modal calculation is used with several strips of the above mentioned two-dimensional aerodynamic analysis. The model is applied to a high-energy turbine blade and the author states that the second mode (first edgewise bending) was found to be unstable in the absence of mechanical damping. A modal damping ratio of 1%, used to simulate the blade-to-blade friction dampers, stabilized the blade for all interblade phase angles.

Stecco and Marchi [1989, 1988] and Stecco et al [1989] present a linear potential model for subsonic flow conditions. The authors compare their results with the analysis by Smith [1972] and by experimental data by Ezzat et al [1989a,b]. Good trend wise agreement is shown.

A three-dimensional small perturbation potential subsonic flow finite element model, with uniform mean blade loading along the span is presented by Yang et al [1989]. They indicate similar results as for a double linearization theory [Namba and Toshimitsu, 1988] for small angles of attack, camber and blade

thickness, but considerable differences are found for highly loaded cascades.

Hall and Crawley [1989], and Hall [1991], present two-dimensional cascade calculations using a linearized Euler model with explicit shock and wave fitting. The method allows for blade loading, blade geometry, shock motion and wave motion. It also accounts for vorticity and entropy generation at the shocks. Results presented show good agreement with an earlier semi-analytical technique by Atassi and Akai [1978] for cascades oscillating in torsion in low subsonic flow and with a time-marching Euler solver [Giles, 1987] for incoming vortical and entropic gusts. Transonic results are presented for a nozzle flow with harmonically oscillating inlet density. The authors conclude that further work on the shock-fitting algorithm is necessary for oblique shocks.

Non-linear (in time and space) models:

In the last few years some fully non-linear methods for calculating the unsteady flow through vibrating cascades have appeared in the open literature. Some of these treat, at the present stage, the nozzle flow with emphasize on the sharp shock capture, and some are based on usual shock capturing techniques as employed for steady-state calculations.

Allmares and Giles present unsteady transonic flow results, in a nozzle, with an upwind Euler model [1987] and a coupled inviscid/viscous [1989] solver. Experimental trends of the self-exciting flow in a diffuser are predicted, but some differences are shown in the magnitude.

Bassi et al [1989] present a two-dimensional finite volume "Total Variation Diminishing" method to calculate the unsteady inviscid transonic flow through nozzles. The authors conclude that their model indicates that non-linearities can play an essential role in some transonic high-frequency oscillating flows. Similarly, Bölcs et al [1989c] present a fully non-linear inviscid model for the calculation of large amplitude shock fluctuations in a nozzle. The emphasize is put on the sharp capture of the unsteady shock waves ("flux vector splitting") and results are presented for one-dimensional and two-dimensional steady-state and time-dependent flow, with the oscillations introduced by a fluctuating back pressure. The model is applied to normal and slightly oblique shock waves and indicate good agreement with an analytical small perturbation theory [Liou and Adamson, 1977]. The results indicate that large shock oscillations can appear for small changes in downstream pressure if the area change in the nozzle is small, and that the aerodynamic shock waves under some circumstances can be pushed into the subsonic flow region. Furthermore, the time-averaged position of the unsteady shock is in principle not identical with its

steady-state location. Results with a similar numerical model, compared to the same small perturbation analytical theory, but applied to the case of thin unstaggered blades vibrating in out-of-phase pitch motion in low transonic flow is presented by Li et al [1990]. They indicate good agreement between the numerical and analytical models for 2% thick blades at low reduced frequency but some differences with blades of 5% thickness. It is suggested that retaining higher-order terms in the asymptotic theory should improve the agreement. Preliminary calculations of staggered blades suggests also the usefulness of the numerical model for such cascades.

Yamamoto and Tanida [1989] complements their measurements of self-excited flow oscillations on a fixed airfoil with the development of a Navier-Stokes solver for the flow around a single airfoil in a channel. The simulated flow oscillation is similar to the experiment, although it has larger amplitude, and the oscillation frequency is well predicted.

Wu [1988] presents a fully non-linear two-dimensional Navier-Stokes method, with k-ε and Baldwin-Lomax turbulence models, for an oscillating airfoil with application, among others, to the dynamic stall phenomena. The author indicates qualitative agreement between the two turbulence models and experimental data for the aerodynamic loads, whereas the Reynolds shear stress profiles show dramatic differences between the two models.

A fully unsteady two-dimensional Reynolds-averaged compressible Navier-Stokes model, written in the finite difference form, is described by Carr et al [1989]. The model shows good agreement with experimental lift and pitching moment magnitudes once a prior knowledge of the state of the flow turbulence is given as an input. Krainer [1988] presents preliminary results on a viscous-inviscid coupled model for a ramp-type motion of an isolated airfoil in incompressible flow. Both these projects are further developed by Jang et al [1990] who show comparison with steady-state and time-dependent experimental data for a single airfoil at Reynolds numbers 10^5 and $3\bullet10^6$. The authors indicate a good agreement in the unsteady velocity profiles between the two methods for reduced frequencies up to k=0.015 at the higher Reynolds number, but significant differences with increasing reduced frequency.

A time-dependent incompressible potential flow method to calculate the vortex shedding and blade-vortex interaction for cascades, vibrating or multi-blade-row, or single airfoils is described by Lee et al [1991|. Good agreement with the exact solution of the Theodorsen function is shown for the unsteady lift coefficient.

Bakhle et al [1989, 1990] report on the development of a fully non-linear potential flow solver for the unsteady flow through vibrating two-dimensional cascades, coupled with a two-degree-of-freedom structural model. The model is validated against unsteady flat plate analytical results at subsonic flow [Smith, 1972] with trend wise agreement for the sample cases shown. Calculations for the traveling wave, single blade and indicial response excitation modes are performed by Bakhle et al [1991]. As the sample case blade vibration amplitude is small, the problem is linear and all three methods give identical results. The flat plate examples shown do not capture the acoustic resonances and the agreement with the theory by Smith [1972] is fair to good for the different vibration modes, with the largest deviations in moment coefficient due to plunging, for inlet Mach numbers ranging from 0.2 to 0.8. The authors conclude that the flutter reduced frequency is seen to increase with Mach number, as well as with the airfoil thickness.

A fully time-dependent three-dimensional potential flow solver, valid at zero degree interblade phase angles, coupled with a linear structural model to simulate the aeroelastic behavior of propfans is presented by Ku and Williams [1990]. It is demonstrated that, for subsonic flow, the results obtained agree well with those of a panel method and reasonably well with experimental data. For supercritical flow the full potential flow solver predicts better agreement with the data in the neighborhood of the shock.

A non-linear Euler model in conservation law form is presented by Kau and Gallus [1989] and Gallus and Kau [1989]. Comparisons with the analytical flat plate solution by Smith [1972] and experimental cascade data on a compressor and turbine ("Standard Configuration 4") are shown for subsonic flow conditions. A frequency, Mach number and interblade phase angle study is shown for the flat plate cascade.

Gerolymos [1990b, 1988a,b,c] presented a fully three-dimensional non-linear unsteady inviscid numerical model, for supersonic inlet flow, by the explicit integration of the Euler equations in finite difference form. Results are presented on a fan rotor in transonic flow, with good steady-state agreement with data measured in a rotating full-scale machine. Preliminary results, for the cases investigated, indicate that the strip theory assumption is valid for unsteady supersonic flow. An implicit method by the same author [Gerolymos, 1990a] reduce significantly the required computing time for unsteady flow calculations, while giving satisfactory agreement with the explicit model although some parasite entropy generation was noticed with the implicit scheme.

Results from the above mentioned explicit model (for supersonic inlet flow) was compared with two-dimensional analytical predictions and two sets of experimental data by Gerolymos et al [1990b], together with an evaluation of differences between

reflecting and non-reflecting boundary conditions. The use of a non-reflecting (in a one-dimensional flow) and a capacity condition gave almost similar results as regards to the unsteady moment coefficient of a vibrating flat plate cascade for all interblade phase angles. These results compared also very well with analytical results from Adamczyk and Goldstein [1978] in the subresonant region of interblade phase angles. However, in the region were the unsteady waves decay (i.e. superresonant domain for supersonic flows) some differences between the analysis and the computation could be found. The author points out that this corresponds to previous subsonic (numerical) results by Fransson and Pandolfi [1986], who also found less good agreement in regions of attenuating waves. No evidence of acoustic resonances could however be found with the numerical model. A fairly good agreement can be found for two sets of experimental data ("Standard Configuration 7" and an ONERA cascade), and the author states that the discrepancies found may appear because of viscous effects and, secondary, non-rigid blade oscillations.

Several investigations using the concept of "single blade excitation" towards "traveling wave mode" [Hanamura et al, 1980; Crawley, 1984] have appeared also among theoretical studies. Numerical Euler calculations by Gerolymos [1988a] indicate that the superposition principle of influence coefficients gives results identical to the full rotor vibrating in the traveling wave mode if 3-4 blades are considered on each side of the reference blade.

Another time-marching Euler model for two-dimensional and quasi three-dimensional flow is shown by He [1989]. This method is based on a finite volume scheme with a two-step Runge-Kutta integration in time. Results show good agreement with linearized flat plate models and with high subsonic turbine experimental data ("Standard Configuration 4"). Furthermore, strong nonlinear behavior of the shock movement is shown for an oscillating biconvex cascade under transonic flow conditions. This inviscid quasi three-dimensional model has been coupled with an integral boundary layer solution by He and Denton [1991b] to obtain solutions on vibrating cascaded blades. Steady laminar and turbulent correlations are adopted in a quasi-steady way for the time-dependent solution. Presented results show good agreement with experimental unsteady (fixed wall) turbulent boundary layer data. The model has been applied to calculate the unsteady flow around an isolated airfoil, a transonic duct flow, a bi-convex cascade and a fan tip section [He and Denton, 1991c]. The authors conclude that the viscous and inviscid numerical solutions are quit different in the neighborhood of a shock wave. An experimentally determined phase shift in a leading edge separation bubble could also be predicted with the viscous model.

A fully non-linear finite difference numerical analysis, based on the Euler and full Navier-Stokes equations, for unsteady inviscid and viscous two-dimensional supersonic [Huff and Reddy, 1989] and subsonic [Huff, 1989] flow through vibrating cascades is developed at NASA Lewis Research Center. The authors indicate good agreement, for the inviscid version of the code, in the moment coefficients with supersonic axial flow flat plate results by Ramsey and Kielb [1987], as well as good trend wise agreement for the unsteady pressure difference coefficient. They conclude that blade thickness, for the sample case computed, has a large positive influence on the stability of the cascade. This has to be compared to the above results by Ramsey [1989] who indicate positive or negative effects on the stability in dependence of cascade geometry and flow conditions.

The viscous version of the code was run against two sets of experimental data in the low ("Standard Configuration 1") and high (biconvex airfoils by Shaw et al [1985], Buffum et al [1987]) subsonic flow domains, and against a flat plate analysis [Smith, 1972]. The agreement, at low subsonic flow, is good for the two aeroelastic sample cases showed[5]. The flat plate calculations show good agreement at non-zero interblade phase angles but major discrepancies close to the acoustic resonance. In such a case calculations with reflective and non-reflective inlet and outlet boundary conditions give major differences between the numerical and analytical results (compare results by Gerolymos and Fransson/Pandolfi above). Finally, the predictions for the biconvex airfoil is in fair agreement with the data.

A flux-difference inviscid version of the model, based on an H-grid, has been presented by Huff et al [1991]. The authors indicate a good agreement with the flat plate theory by Smith [1972], except for certain cases in the super-resonant flowfield (see above), and trend wise agreement with experimental data by Buffum and Fleeter [1989a,b]. From a study concerning the nonlinear behavior in an oscillating cascade, by varying the vibration amplitude, they conclude that the responses may become nonlinear for amplitudes greater than one degree. Nonlinearities are more dominant near the shocks. Reddy et al [1991] present a coupling of this unsteady aerodynamic model with a structural model and compare with similar test cases as above. Furthermore, they present a flutter calculation on a propfan as an application, in which a good agreement with a full potential solver by Bakhle et al [1990] is shown.

Carstens [1991a] show an inviscid nonlinear transonic flow solver, based on the flux vector splitting technique. Results are presented for the "Fourth Standard Configuration". Excellent agreement is

---

[5]   This corresponds to conclusions by other researchers [Bölcs and Fransson, 1986, pp. 57-80].

demonstrated for subsonic outlet flow conditions, whereas the measured unsteady influence of the shock waves is not predicted by the theory, neither in amplitude nor in phase.

Inviscid computations with a "Total Variation Diminishing" two-dimensional model is presented by Arkadyev et al [1989]. They show results in the transonic flow region on a tip section of a fan stage.

Giles and Haimes [1991] present unsteady validations of the hybrid numerical viscous/inviscid model "UNSFLO" against flat plate theories, both for wake interactions, nozzle flow and oscillating blades. A very good correlation against results from "LINSUB" [Smith, 1972] is shown for the inviscid model. The unsteady component of the vorticity in the viscous model is validated against the "Stokes' layer" with excellent agreement.

A Navier-Stokes model, based on the Baldwin-Lomax turbulence model, for unsteady viscous transonic flow is shown by Kobayakawa and Ogushi [1989]. The model is applied towards a two-dimensional unstaggered NACA0012 cascade oscillating at 0° interblade phase angle.

Sidén et al [1989a,b, 1990, 1991a,b,c] present a model for the solution of two-dimensional and quasi three-dimensional viscous flow through cascades with vibrating blades. They employ the Baldwin-Lomax turbulence model to close the equations and implement the model on a finite element non-structured mesh in the outer, non-moving, region and a structured moving mesh attached to the airfoils. Results are presented on some test cases (among others on "Standard Configuration 5") and a flutter prediction on a fan is performed [Sidén and Albråten, 1991b]. The authors conclude that viscous effects are important in the leading edge region of the fifth standard configuration, but that their viscous model gives a fairly large over-prediction in this region, at least for moderate inlet flow angles.

2.3:   Conclusions

Significant progress has been made towards prediction of unsteady flow phenomena through vibrating blade rows during the period 1987-1991. In many cases numerical possibilities have advanced so that new detailed experimental results are urgently needed as validation of, for example, viscous flow models. More details about this is given in the main conclusions in section 4 below.

3.   STANDARD CONFIGURATIONS

3.0   General.

3.0.1   Previous standard configurations.

The collection of two-dimensional standard configurations, for attached flow, compiled by Bölcs and Fransson [1986] consisted of 9 different cascade-geometries, with the objective to validate both experimental data and prediction models. To this end, two different sets of data were put forward for each class of test cases. During the project it was established that most of the data selected for purely subsonic flow gave a reasonable agreement with some prediction models, which validated both the experiments and the theories. The largest computational efforts thus went into standard configurations 1 (low subsonic flow compressor cascade), 4 (cambered transonic turbine cascade), 8 (flat plate) and 9 (double circular arc profiles with low camber), with some additional work put into configurations 5 (high subsonic compressor profile) and 7 (supersonic compressor). It was concluded from the project that certain geometries and flow conditions could be accurately predicted, whereas discrepancies existed for other sample cases.

Some inconsistency has been found in the definition of the pressure coefficients (steady-state and time-dependent). These are, in the present work, defined with the compressible dynamic pressure, $(p_{w1}-p_1)$, as non-dimensionalized value. However, some researchers have used the incompressible value, $(\rho_- v_-{}^2/2)$, instead. It has been tried to, as accurately as possibly, mention these inconsistencies in the text for the various standard configurations, but it is important to keep this eventual difference in mind for some comparisons.

3.0.2   Modifications of standard configurations

As the predictions on the configurations 2, 3 and 6 (see Bölcs and Fransson [1986]) were considerably smaller than on other cascade configurations, it is proposed that efforts for comparisons with low subsonic compressor blades and cambered transonic turbine blades should be reduced to configurations 1 and 4 (Figs. 3.1.1 and 3.4.1). Configuration 5 (Fig. 3.5.1) is today of larger interest than in the beginning of the project because of its systematic parameter-study from attached to stalled flow, although data are only available for one blade vibrating (here the question of superposition of influence coefficients in stalled flow may arise). Configuration 7, which treats supersonic inlet flow conditions for a compressor (Fig. 3.7.1), is also of present interest, especially as some major discrepancies between the data and the predictions exist. It is probable that some of these can

be explained by viscous effects and by short comings in the numerical methods but that some can certainly also be found in the data. However, as no other complete data base has been found for supersonic flows to date, this configuration should be kept presently.

Flat plate cascades, double circular arc profiles and other analytically defined geometries are still today of large interest and are necessary in order to compare prediction models with each other and to draw physical conclusions from the results. Furthermore, modern compressor blades in the high subsonic and supersonic flow domains are often derivatives of such profiles, and there seems to be a renewed interest in cascades with supersonic leading edge locus. The flat plate and double circular arc geometries (configurations 8 and 9) are thus kept in a redefined way (Figs. 3.8.1 and 3.9.1). Finally, a supplementary configuration is proposed, based on a modified NACA four digit series airfoil (Fig. 3.10.1)[6].

It is important to note that the configurations are presently still limited to two-dimensional flow conditions, with mostly attached flow. Although numerical results today are available for solving the Navier-Stokes equations with different (steady-state) turbulence model assumptions there are hardly no separated experimental cascade data available (see however the extension of "Standard Configuration 5" below). Furthermore, three-dimensional unsteady cascade effects are today not taken into full account experimentally. However, it is reasonable to expect that some data for separated and three-dimensional flow will appear in the not too distant future. These will then, if possible, be incorporated in the present data base. All present sample cases are, furthermore, considered to be of uncoupled modes, although the coupling effects are of large importance for the stability of the blading. It is presently assumed that the coupled modes are obtained by superimposing the heaving and pitching motions.

The number of aeroelastic sample cases in the report are still out of necessity large. This can not be otherwise as the standard configurations should cover all velocity domains from low subsonic to supersonic velocities and both compressor and turbine geometries, and as the interblade phase angle is a parameter of major importance in turbomachine applications. Furthermore, it is well known that the overall time-dependent blade lift and moment

---

[6] Please note, however, tthat all he original information and experimental results for the other standard configurations still exist in the workshop data-base.

coefficients may give reasonable agreement between different prediction models and with experimental data, although the unsteady blade surface pressure coefficient results may represent quite different trends and to a certain extent may indicate different physical interpretations. It is thus today even more important than at the outset of the workshop to represent, for different interblade phase angles and for different cascade and flow configurations, the pressure and suction surface time-dependent pressure coefficients separately.

For the benefit of those who may eventually be interested in comparing different results not included in the appendices, some publications treating results on the different standard configurations are given in each section below.

Please also note that all airfoil coordinates as well as experimental data and numerical results presented, either in the first [Bölcs and Fransson, 1986] or the present standard configuration report, exist on computer files and can be obtained upon request. The plots of all the data obtained from different researchers are given in Appendix A4, and the corresponding data are listed in Appendix A3.

3.1   First standard configuration (compressor cascade in low subsonic flow).

The first standard configuration, included by the courtesy of Dr. Frank Carta at the United Technologies Research Center [Carta 1982a,b; 1984], and its 15 recommended aeroelastic sample cases, gives an overview of different steady-state and time-dependent flow conditions at low Mach numbers (see Fig. 3.1.1, Tables 3.1.1-2). Most prediction models give good agreement with the data, but some minor differences between the different models became apparent.

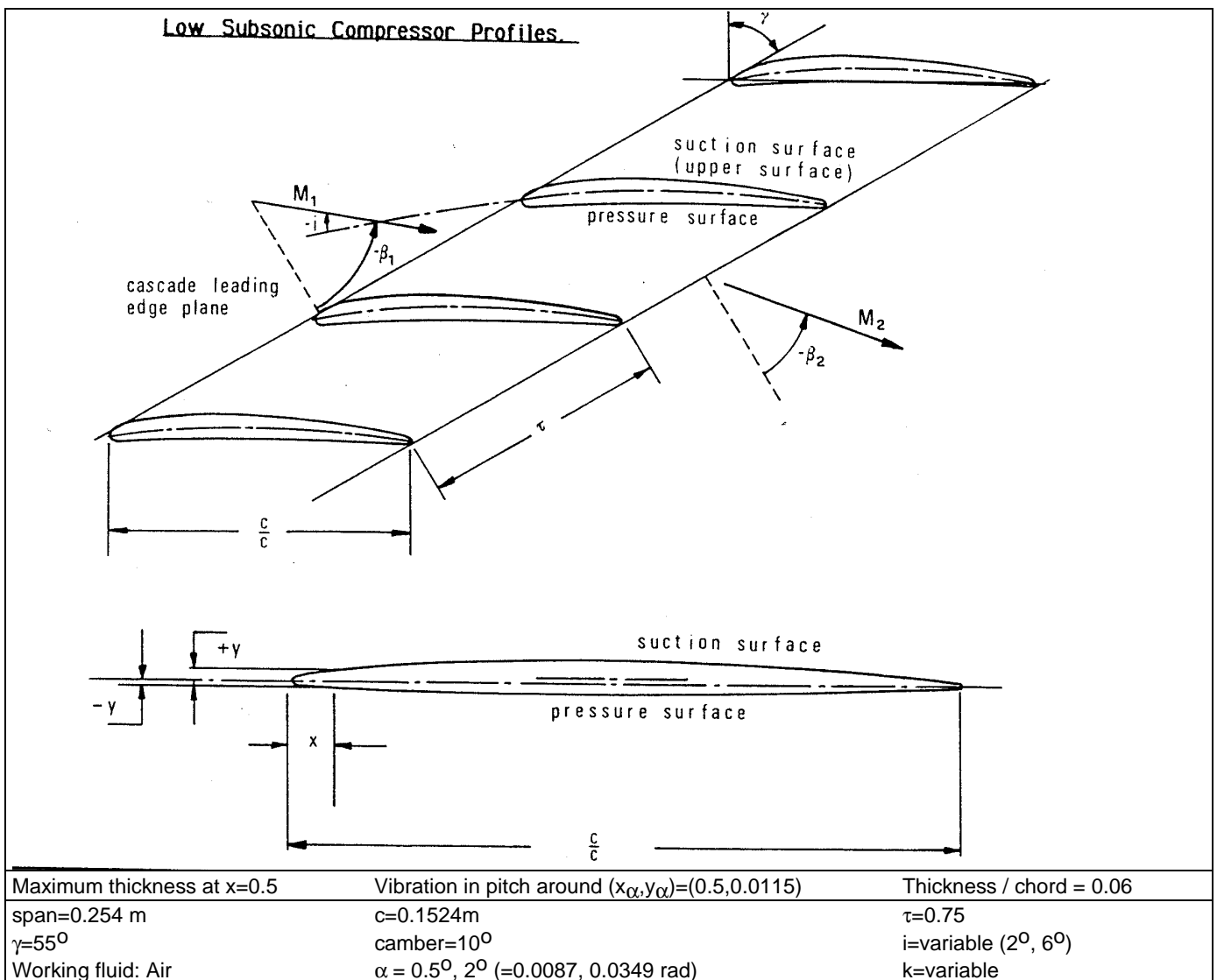| Maximum thickness at x=0.5	Vibration in pitch around $(x_\alpha, y_\alpha) = (0.5, 0.0115)$	Thickness / chord = 0.06
span=0.254 m	c=0.1524m	τ=0.75
γ=55°	camber=10°	i=variable (2°, 6°)
Working fluid: Air	α = 0.5^o, 2° (=0.0087, 0.0349 rad)	k=variable

Fig. 3.1.1:   First standard configuration: Cascade geometry [Bölcs and Fransson, 1986, p. 58]

All results (experimental as well as predictions) presented on this standard configuration have been (as the flow velocity is very low) non-dimensionalized with the incompressible dynamic pressure, $(\rho_- \bullet v_-^2/2)$.

The most important conclusion from this standard configuration is that the detailed blade surface pressures, and thus the flutter limits, can be fairly accurately predicted for low incidence flows on this type of cascades. The reader is referred to section 7.1

in the original report on the standard configurations [Bölcs and Fransson, 1986] for details.

It is however of importance to note that although the results obtained are positive, the agreement between the data and the predictions, or between the different predictions, is not as good as would be wished from a theoretical point of view. It should especially be mentioned that, in several cases, a flat plate model gives as good agreement, or better, with the data as some prediction models that consider the blade thickness.

Point	Suction surface		Pressure surface	
No.	x/c	y/c	x/c	y/c
1	0.0008	0.0020	0.0012	-0.0019
2	0.0046	0.0053	0.0054	-0.0042
3	0.0070	0.0064	0.0080	-0.0050
4	0.0120	0.0083	0.0130	-0.0061
5	0.0244	0.0116	0.0256	-0.0077
6	0.0494	0.0164	0.0507	-0.0098
7	0.0743	0.0204	0.0757	-0.0115
8	0.0993	0.0237	0.1007	-0.0129
9	0.1494	0.0290	0.1506	-0.0150
10	0.1994	0.0331	0.2006	-0.0165
11	0.2495	0.0364	0.2505	-0.0177
12	0.2996	0.0387	0.3004	-0.0185
13	0.3998	0.0411	0.4002	-0.0188
14	0.5000	0.0406	0.5000	-0.0176
15	0.6002	0.0370	0.5998	-0.0146
16	0.7003	0.0306	0.6997	-0.0104
17	0.8003	0.0223	0.7997	-0.0069
18	0.8503	0.0176	0.8497	-0.0053
19	0.9003	0.0127	0.8997	-0.0040
20	0.9502	0.0078	0.9497	-0.0032
21	0.9975	0.0030	0.9973	-0.0025
Chord:	c=0.1524 m (=6 inches)			
L.E. radius/c=0.0024;		L.E. radius center at x/c=0.0024, y/c=0.0002		
T.E. radius/c=0.0028;		T.E. radius center at x/c=0.9972, y/c=0.0003		

Table 3.1.1: *First standard configuration: Dimensionless airfoil coordinates [Bölcs and Fransson, 1986, p. 59]*

Aeroelastic test case	Time averaged				Time dependent parameters				
	M_1 (-)	i (°)	p_1/p_{w1} (-)	p_1/p_{w1} (-)	β_1 (°)	k (°)	α (-)	σ (°)	f (Hz)
1	0.18	2	0.9774	0.9818	-62.0	0.122	0.5	-45	15.5
2	"	"	"	"	"	"	"	+45	"
3	0.17	6	0.9790	0.9852	-62.5	0.122	0.5	-45	15.5
4	"	"	"	"	"	"	2.0	+45	"
5	"	"	"	"	"	"	"	-45	"
6	"	"	"	"	"	"	"	180	"
7	"	"	"	"	"	"	"	-135	"
8	"	"	"	"	"	"	"	-90	"
9	"	"	"	"	"	"	"	0	"
10	"	"	"	"	"	"	"	+90	"
11	"	"	"	"	"	"	"	+135	"
12	"	"	"	"	"	0.072	"	-90	9.2
13	"	"	"	"	"	0.151	"	"	19.2
14	"	"	"	"	"	0.301	"	"	38.4
15	"	"	"	"	"	0.603	"	"	76.8

Table 3.1.2: *First standard configuration: Experimental values for 15 recommended aeroelastic sample cases [Bölcs and Fransson, 1986, p. 60]*

The aeroelastic sample cases originally defined have proven their value and are thus presently kept in the data-base. It is however important to point out that some uncertainties as regards to the exact value of the inlet flow angle still exist. It has been found by different researchers that a better agreement with the steady-state blade surface pressure distribution is obtained if the inlet flow angle is modified about 2°

[Bölcs and Fransson, 1986, p. 61], or if a stream-tube variation is introduced.

Results on this standard configuration have been presented by Chiang and Fleeter [1989b] and Huff [1989]. These authors have, as other researchers, found a good agreement with the experimental data.

3.2   Second standard configuration

No modifications have been made to this standard configuration. All results, and a discussion thereof, are found in the 1986 report [Bölcs and Fransson, 1986]. A listing of all the results are found in appendix A3.

As with the first standard configuration, the incompressible dynamic pressure is employed as a non-dimensionalized value for the pressure coefficients.

3.3   Third standard configuration

No modifications have been made to this standard configuration. All results, and a discussion thereof, are found in the 1986 report [Bölcs and Fransson, 1986]. A listing of all the results are found in appendix A3.

The compressible dynamic pressure, $(p_{w1}-p_1)$, is employed as non-dimensionalized value for the pressure coefficients.

3.4   Fourth standard configuration (cambered turbine cascade in transonic flow).

The fourth standard configuration, with results obtained at the Swiss Federal Institute of Technology [Bölcs et al, 1985], is shown in Fig. 3.4.1, with the profile coordinates and aeroelastic sample cases given in Tables 3.4.1-2. Please note that the blade coordinates are given with more significant decimals than earlier as it was pointed out that the coordinates showed some oscillatory behavior. The Reynolds number was not given earlier and are included now as a basis for viscous calculations. Furthermore, experimental data exist for many more steady-state and time-dependent operating conditions (see for example Schläfli [1989]). These can be obtained upon request.

It is important to point out that the time-averaged dynamic pressure $(\overline{p}_{w1} - \overline{p}_1)$ is used as the quantity with which the pressure coefficients are made dimensionless. This should be remembered when predictions are performed. As far as the present authors are aware of all predictions have also been presented with this dynamic pressure.

The results obtained so far show a good general agreement between the data and prediction models for shock-free flows, both as regards to the time-dependent blade surface pressures as the unsteady forces. At transonic and supersonic outlet flow conditions major discrepancies are found, as presented by Bölcs and Fransson [1986]. It should however be pointed out that a re-evaluation of the original data has indicated that the experimental

uncertainty for the inlet flow angle may be larger than originally thought, which may explain some differences in the experimental and computed steady-state pressure distributions, especially in the leading edge region. Most authors have thus introduced a stream-tube contraction (towards 10%) into the calculations in order to compensate for leakage flow and boundary layer growth in the test facility. A better agreement with the steady-state blade surface pressure distributions is then generally obtained.

The reader is referred to section 7.4 in Bölcs and Fransson [1986] for more details about the cascade geometry and previous results.

Since the first results presented [Bölcs and Fransson, 1986], further predictions have been performed on the cascade by Whitehead [1987], Servaty et al [1987], Gallus an Kau [1989], Kau and Gallus [1989], He [1989] and Carstens [1991a] with the general results that the predictions and experiments agree well, both for steady-state and time-dependent flow, for subsonic flow conditions whereas the predictions do not give results similar to the experiment in the neighborhood of the shock waves. It can probably be concluded that the experiments are good, but some aspects of the data can not be explained with present prediction models. Further numerical developments and experiments in transonic flow seem thus necessary for the future.

It has been pointed out [Carstens, 1991a] that the position of the time-averaged shock wave at the supersonic outlet flow velocity cases can be quite accurately predicted if a sufficiently fine mesh structure is used. The predicted shock strength did however not correspond to the measured one.

Aeroelastic test case	Time averaged					Time dependent parameters			
	M_1 (-)	β_1 (°)	Re_1 (-)	$M_{2,is}$ (-)	β_2 (°)	σ (°)	k (°)	$h^{(0)}$ (-)	δ (°)
1	0.19	-45	5.6x10⁵	0.58	-71	-90	0.168	0.0038	60
2	0.26	"	6.6x10⁵	0.76	"	"	0.128	"	"
3	0.28	"	8.2x10⁵	0.90	"	"	0.107	"	"
4	0.29	"	8.5x10⁵	1.02	"	"	0.095	0.0033	"
5	"	"	"	1.19	"	"	0.082	0.0038	"
6	0.28	"	8.2x10⁵	0.90	"	180	0.107	0.0033	"
7	"	"	"	"	"	+90	"	"	"
8	"	"	"	"	"	0	"	"	"

Table 3.4.2: *Fourth standard configuration: Experimental values for 8 recommended aeroelastic sample cases [Bölcs and Fransson, 1986, p. 103]*

High Subsonic/Transonic Turbine Profiles.

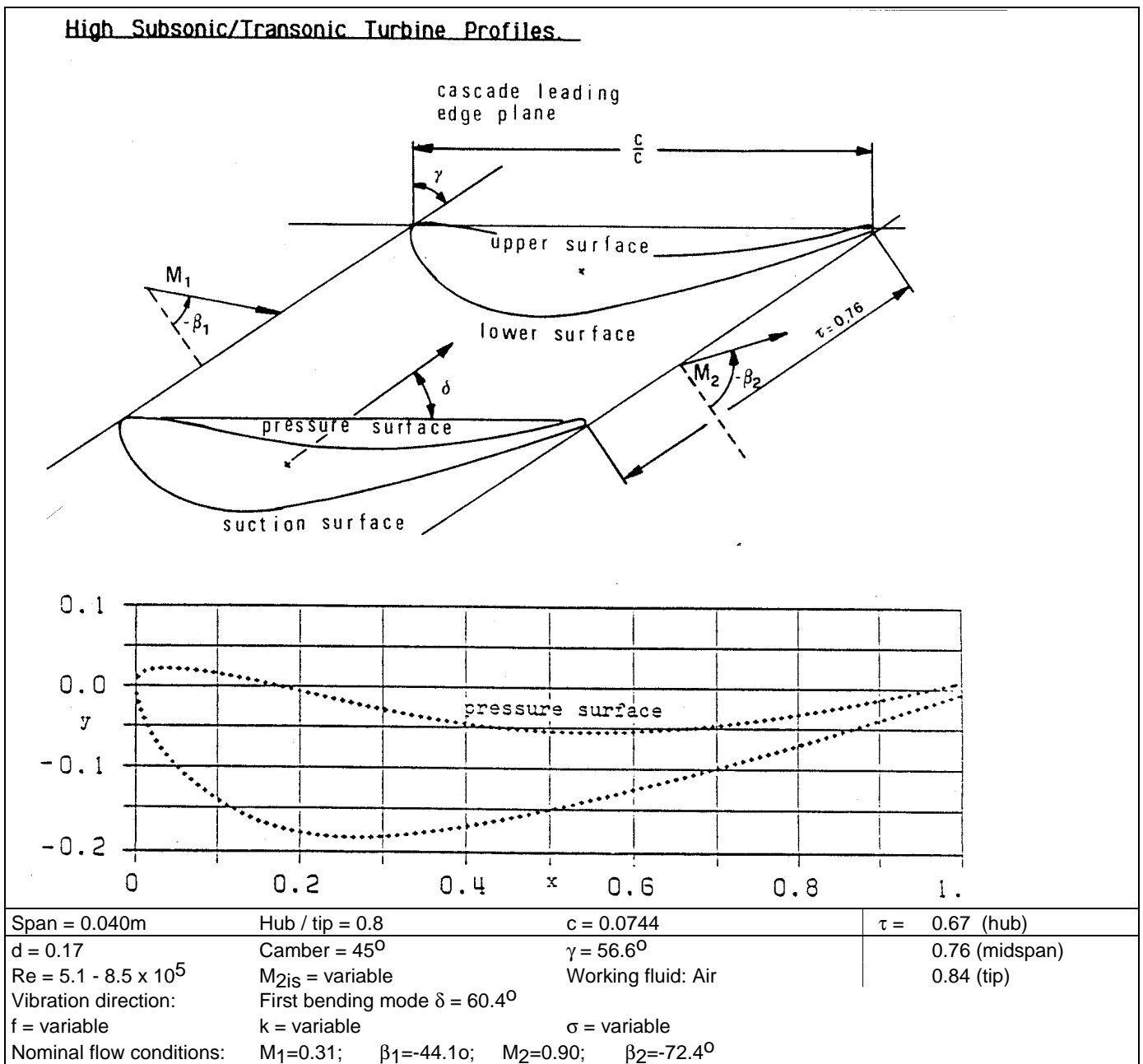| Span = 0.040m	Hub / tip = 0.8	c = 0.0744	τ = 0.67 (hub)
d = 0.17	Camber = 45°	γ = 56.6°	0.76 (midspan)
Re = 5.1 - 8.5 x 10⁵	M_{2is} = variable	Working fluid: Air	0.84 (tip)
Vibration direction:	First bending mode δ = 60.4°		
f = variable	k = variable	σ = variable	
Nominal flow conditions:	M_1=0.31; β_1=-44.1o; M_2=0.90; β_2=-72.4°		

Fig. 3.4.1:   *Fourth standard configuration: Cascade geometry [Bölcs and Fransson, 1986, pp. 99-100].*

Point	x/c	y/c	Point	x/c	y/c	Point	x/c	y/c
1	1e+0	-7.163157e-3	2	9.898891e-1	-1.062851e-2	3	9.797677e-1	-1.407275e-2
4	9.696463e-1	-1.748528e-2	5	9.595144e-1	-2.088725e-2	6	9.493719e-1	-2.426810e-2
7	9.392188e-1	-2.762781e-2	8	9.290657e-1	-3.096639e-2	9	9.189020e-1	-3.427327e-2
10	9.087384e-1	-3.756959e-2	11	8.985641e-1	-4.084478e-2	12	8.883794e-1	-4.409884e-2
13	8.781946e-1	-4.732121e-2	14	8.679992e-1	-5.053301e-2	15	8.577933e-1	-5.372367e-2
16	8.475874e-1	-5.688265e-2	17	8.373709e-1	-6.003106e-2	18	8.271439e-1	-6.315833e-2
19	8.169168e-1	-6.625392e-2	20	8.066792e-1	-6.933893e-2	21	7.964416e-1	-7.240282e-2
22	7.861934e-1	-7.543501e-2	23	7.759453e-1	-7.845664e-2	24	7.656865e-1	-8.145714e-2
25	7.554172e-1	-8.442594e-2	26	7.451479e-1	-8.738512e-2	27	7.348680e-1	-9.031072e-2
28	7.245776e-1	-9.322669e-2	29	7.142872e-1	-9.611097e-2	30	7.039967e-1	-9.898469e-2
31	6.936852e-1	-1.018267e-1	32	6.833842e-1	-1.046476e-1	33	6.730620e-1	-1.074579e-1
34	6.627505e-1	-1.102365e-1	35	6.524178e-1	-1.129940e-1	36	6.420851e-1	-1.157409e-1
37	6.317524e-1	-1.184562e-1	38	6.214091e-1	-1.211503e-1	39	6.110553e-1	-1.238233e-1
40	6.007015e-1	-1.264857e-1	41	5.903476e-1	-1.291164e-1	42	5.799833e-1	-1.317260e-1
43	5.696083e-1	-1.343144e-1	44	5.592333e-1	-1.368818e-1	45	5.488584e-1	-1.394280e-1
46	5.384729e-1	-1.419530e-1	47	5.280768e-1	-1.444570e-1	48	5.176807e-1	-1.469398e-1
49	5.072740e-1	-1.493803e-1	50	4.968568e-1	-1.517997e-1	51	4.864396e-1	-1.541769e-1
52	4.760118e-1	-1.565223e-1	53	4.655735e-1	-1.588255e-1	54	4.551246e-1	-1.610865e-1
55	4.446651e-1	-1.632946e-1	56	4.342056e-1	-1.654393e-1	57	4.237144e-1	-1.675418e-1
58	4.132233e-1	-1.695703e-1	59	4.027215e-1	-1.715354e-1	60	3.921987e-1	-1.734265e-1
61	3.816652e-1	-1.752437e-1	62	3.711107e-1	-1.769553e-1	63	3.605455e-1	-1.785718e-1
64	3.499698e-1	-1.800826e-1	65	3.393730e-1	-1.814666e-1	66	3.287551e-1	-1.827344e-1
67	3.181265e-1	-1.838543e-1	68	3.074769e-1	-1.848157e-1	69	2.968272e-1	-1.855976e-1
70	2.861459e-1	-1.861892e-1	71	2.754646e-1	-1.865590e-1	72	2.647832e-1	-1.866858e-1
73	2.540913e-1	-1.865484e-1	74	2.434100e-1	-1.861470e-1	75	2.327497e-1	-1.854497e-1
76	2.221107e-1	-1.844143e-1	77	2.115138e-1	-1.830302e-1	78	2.009698e-1	-1.812870e-1
79	1.904892e-1	-1.791634e-1	80	1.801037e-1	-1.766489e-1	81	1.698238e-1	-1.737118e-1
82	1.596813e-1	-1.703627e-1	83	1.496761e-1	-1.666015e-1	84	1.398189e-1	-1.624705e-1
85	1.301095e-1	-1.579803e-1	86	1.205092e-1	-1.531626e-1	87	1.112085e-1	-1.480174e-1
88	1.020274e-1	-1.425447e-1	89	9.305765e-2	-1.367338e-1	90	8.429916e-2	-1.306061e-1
91	7.578366e-2	-1.241508e-1	92	6.751117e-2	-1.173680e-1	93	5.953450e-2	-1.102576e-1
94	5.188534e-2	-1.027987e-1	95	4.459540e-2	-9.499107e-2	96	3.769637e-2	-8.682422e-2
97	3.120939e-2	-7.832986e-2	98	2.516613e-2	-6.951854e-2	99	1.959831e-2	-6.039027e-2
100	1.453761e-2	-5.097674e-2	101	1.005800e-2	-4.127795e-2	102	6.201730e-3	-3.130447e-2
103	3.085017e-3	-2.108799e-2	104	8.452102e-4	-1.063908e-2	105	0e+0	0e+0
106	2.842019e-3	1.017421e-2	107	1.037495e-2	1.759093e-2	108	2.052804e-2	2.071821e-2
109	3.116712e-2	2.169020e-2	110	4.184847e-2	2.172190e-2	111	5.252982e-2	2.118308e-2
112	6.317946e-2	2.032730e-2	113	7.380798e-2	1.918627e-2	114	8.440481e-2	1.778111e-2
115	9.496994e-2	1.615408e-2	116	1.055033e-1	1.434744e-2	117	1.160156e-1	1.242459e-2
118	1.265174e-1	1.040665e-2	119	1.369980e-1	8.304191e-3	120	1.474575e-1	6.117209e-3
121	1.578958e-1	3.845706e-3	122	1.683341e-1	1.500248e-3	123	1.787514e-1	-8.769056e-4
124	1.891686e-1	-3.285755e-3	125	1.995752e-1	-5.705169e-3	126	2.099819e-1	-8.135149e-3
127	2.203885e-1	-1.056512e-2	128	2.308058e-1	-1.299510e-2	129	2.412124e-1	-1.542508e-2
130	2.516296e-1	-1.782337e-2	131	2.620468e-1	-2.020052e-2	132	2.724746e-1	-2.254598e-2
133	2.829130e-1	-2.484918e-2	134	2.933619e-1	-2.712068e-2	135	3.038214e-1	-2.932879e-2
136	3.142914e-1	-3.148408e-2	137	3.247720e-1	-3.357597e-2	138	3.352632e-1	-3.559391e-2
139	3.457755e-1	-3.752733e-2	140	3.563089e-1	-3.938679e-2	141	3.668423e-1	-4.115117e-2
142	3.774075e-1	-4.282046e-2	143	3.879726e-1	-4.439467e-2	144	3.985589e-1	-4.586322e-2
145	4.091663e-1	-4.723669e-2	146	4.197736e-1	-4.849394e-2	147	4.304022e-1	-4.964553e-2
148	4.410412e-1	-5.069148e-2	149	4.516909e-1	-5.163178e-2	150	4.623511e-1	-5.245586e-2
151	4.730113e-1	-5.318485e-2	152	4.836821e-1	-5.380820e-2	153	4.943529e-1	-5.431532e-2
154	5.050342e-1	-5.473793e-2	155	5.157261e-1	-5.504432e-2	156	5.264075e-1	-5.526618e-2
157	5.370994e-1	-5.539296e-2	158	5.477807e-1	-5.542466e-2	159	5.584727e-1	-5.537183e-2
160	5.691646e-1	-5.523449e-2	161	5.798459e-1	-5.501262e-2	162	5.905378e-1	-5.470623e-2
163	6.012192e-1	-5.431532e-2	164	6.118899e-1	-5.383989e-2	165	6.225713e-1	-5.327994e-2
166	6.332315e-1	-5.263547e-2	167	6.439023e-1	-5.190647e-2	168	6.545625e-1	-5.110352e-2
169	6.652122e-1	-5.021605e-2	170	6.758512e-1	-4.925463e-2	171	6.864903e-1	-4.821924e-2
172	6.971294e-1	-4.709934e-2	173	7.077474e-1	-4.591604e-2	174	7.183653e-1	-4.465879e-2
175	7.289727e-1	-4.332759e-2	176	7.395695e-1	-4.194356e-2	177	7.501558e-1	-4.048557e-2
178	7.607315e-1	-3.896419e-2	179	7.713072e-1	-3.740055e-2	180	7.818723e-1	-3.577352e-2
181	7.924269e-1	-3.409367e-2	182	8.029709e-1	-3.236098e-2	183	8.135149e-1	-3.057548e-2
184	8.240483e-1	-2.874771e-2	185	8.345712e-1	-2.686712e-2	186	8.450835e-1	-2.494426e-2
187	8.555852e-1	-2.297915e-2	188	8.660869e-1	-2.097178e-2	189	8.765781e-1	-1.893271e-2
190	8.870587e-1	-1.685138e-2	191	8.975393e-1	-1.472778e-2	192	9.080094e-1	-1.257250e-2
193	9.184689e-1	-1.038552e-2	194	9.289283e-1	-8.177409e-3	195	9.393772e-1	-5.927037e-3
196	9.498262e-1	-3.655534e-3	197	9.602645e-1	-1.373466e-3	198	9.707028e-1	9.402964e-4
199	9.811306e-1	3.264624e-3	200	9.915690e-1	5.599518e-3	201	9.961120e-1	6.624335e-3

Table 3.4.1: *Fourth standard configuration: Dimensionless airfoil coordinates [Bölcs and Fransson, 1986, p. 101]*

While the new profile definition (which corresponds to the one after which the experimental profiles where originally manufactured) is more detailed than the one originally given, it has been found that also the new coordinates show some oscillatory behavior when a very fine mesh is used [Hoyniak, 1991; Carstens, 1991b]. This can give some spurious steady-state and unsteady results, and can be avoided by performing a smoothing of the coordinates [Carstens, 1991b].

Another problem that was discussed is the treatment of the blunt trailing edge. Most prediction models use

a modified airfoil shape towards the trailing edge in order to close in towards a sharp edge.

It can generally be stated that the turbine geometry defined, with its corresponding 8 aeroelastic sample cases, is still of importance for the understanding of flutter-phenomena and further developments of numerical prediction models. The original cases are thus kept in the data-base. Much more work has to be done to find explanations for the differences between the data and the predictions.

3.5 Fifth standard configuration (compressor cascade in high subsonic flow).

Results on the fifth standard configuration (Fig. 3.5.1, Tables 3.5.1-2) are included by the courtesy of Dr. E. Széchényi at the "Office Nationale d'Etudes et de Recherche Aerospatiale" (ONERA) [Széchényi, 1984; Széchényi et at, 1981a,b]. The original experiments treated a large domain of incidence angles, ranging from attached to stalled flow conditions. In the 1986 report on the standard configurations only the small

incidence angles (i_6^o) cases were included, as at that time no models for prediction of the stalled cases were proposed. In the meantime a few viscous solvers have become available, and some researchers have asked for more information on the partially and fully stalled flow conditions. An updating of the aeroelastic sample cases of the fifth standard configuration is thus of interest. These updated cases are given in Table

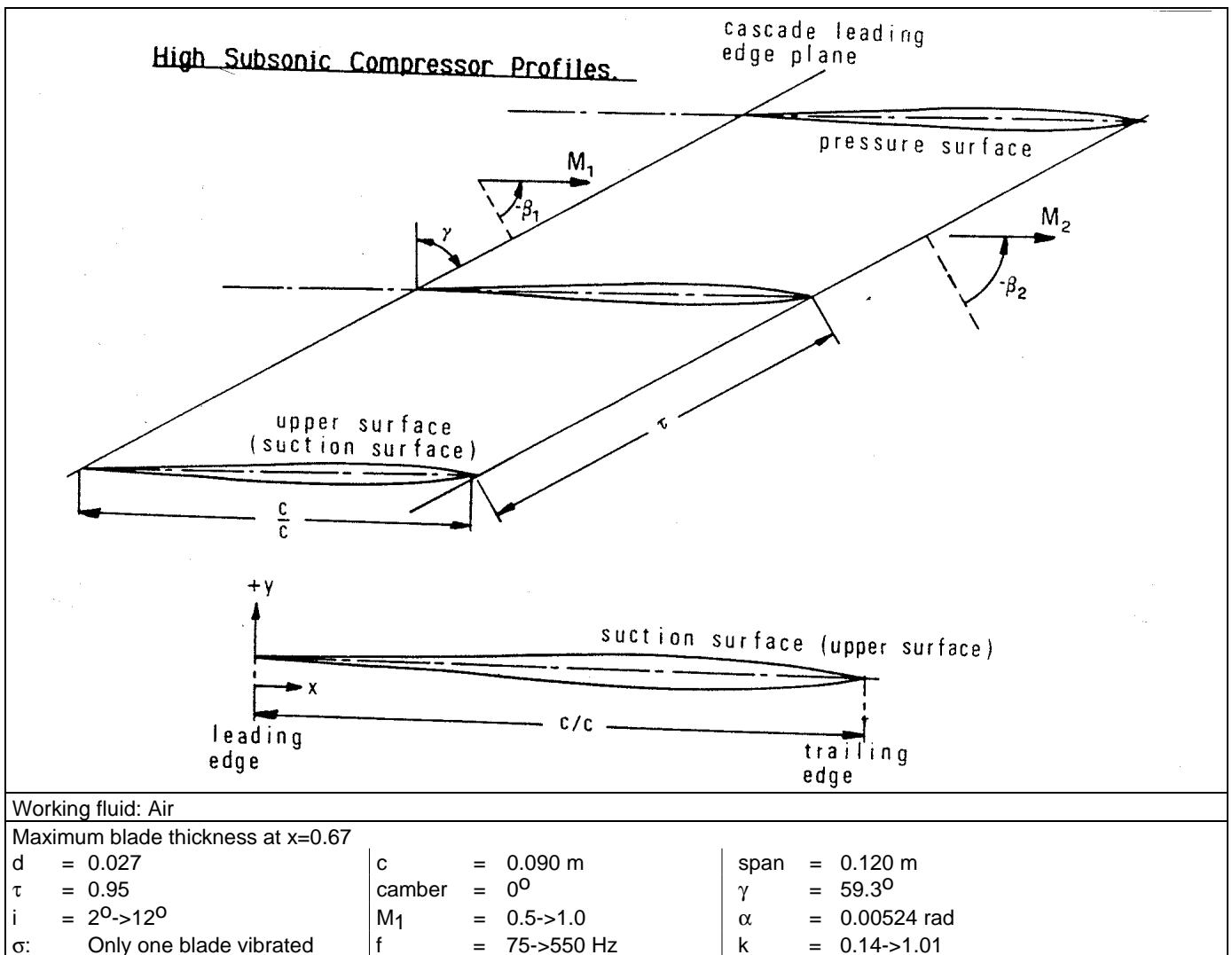| Working fluid: Air				
Maximum blade thickness at x=0.67				
d	= 0.027	c	= 0.090 m	span	= 0.120 m
τ	= 0.95	camber	= 0°	γ	= 59.3^o
i	= 2°->12°	M_1	= 0.5->1.0	α	= 0.00524 rad
σ:	Only one blade vibrated	f	= 75->550 Hz	k	= 0.14->1.01

Fig. 3.5.1: *Fifth standard configuration: Cascade geometry [Bölcs and Fransson, 1986, p. 124].*

3.5.2, and the experimental data are shown (in listings and plots) in appendices A3 and A4 (for previous experimental results, see also section 7.5 and appendix A5 in Bölcs and Fransson [1986]). In evaluating these data it should be kept in mind that the experimental results are obtained with **only one blade vibrating**. The data presented do thus not correspond to the time-dependent pressure coefficient in the traveling wave mode as for the other standard configurations, but instead to the eigen-influence of the reference blade on itself when all the other blades in the cascade are fixed.

Some researchers have pointed out that the original blade coordinates seem to have some "wiggles" in them when blown up for the numerical calculations. Unfortunately, it is presently not possible to give the profile definition with a better resolution. As with the fourth standard configuration, a smoothing of the data is necessary.

The question as how the pressure coefficients have been non-dimensionalized has been brought up. It has been pointed out that a better agreement between the data and one prediction model was found if the data would have been scaled with $\{2(\overline{p}_{w1} - \overline{p}_1)\}$. A verification of the original results presented has shown that the experimental data have all been non-dimensionalized with the measured upstream dynamic pressure $(\overline{p}_{w1} - \overline{p}_1)$, as originally proposed.

Again, as for Standard Configurations 1 and 4, an inconsistency exists between the inlet and outlet flow conditions. Some researchers have compensated this by modifying the inlet flow angle and some by an introduction of a stream tube contraction ratio. Others have left the original values given, and show therefore a less good correlation with the steady-state blade surface pressure distribution. How much these differences in the set-up of the theoretical steady-state flow conditions make out for the time-dependent flow is unclear.

Please note that cases 21 and 22 below are for the same flow conditions, with the only difference being the steady-state stagnation pressure. This can give some indications about stagnation pressure influence and the experimental accuracy and should be considered while analyzing the results.

Sidén [1991a,c] presents results from a Navier-Stokes solver on incidence angles 2°, 4° and 6° on this standard configuration. He shows a large unsteady pressure in the leading edge region where the experiments indicate a larger value than predictions with a linearized potential model. The viscous solver gives however a considerable overshoot compared to the data. Still, these results indicate the importance of considering viscous effects also at fairly low incidence angles on compressor blades with sharp leading edges. Széchényi [1991] points out that the viscous

separation bubble can be well trend wise predicted by a recently developed coupled inviscid/boundary layer code at ONERA [Soize, 1992]. Some of these results have been incorporated in the present data base (see appendix A4).

Point	x/c	Upper surface (Suction side) y/c	Lower surface (Pressure side) y/c
1	0.	0.	0.
2	0.0124	0.0016	-0.0016
3	0.0250	0.0018	-0.0018
4	0.0500	0.0026	-0.0026
5	0.0750	0.0033	-0.0033
6	0.1000	0.0041	-0.0041
7	0.1500	0.0053	-0.0053
8	0.2000	0.0062	-0.0062
9	0.2500	0.0079	-0.0079
10	0.3000	0.0101	-0.0101
11	0.3500	0.0103	-0.0103
12	0.4000	0.0111	-0.0111
13	0.4500	0.0119	-0.0119
14	0.5000	0.0124	-0.0124
15	0.5500	0.0128	-0.0128
16	0.6000	0.0133	-0.0133
17	0.6500	0.0135	-0.0135
18	0.7000	0.0135	-0.0135
19	0.7500	0.0128	-0.0128
20	0.8000	0.0116	-0.0116
21	0.8500	0.0098	-0.0098
22	0.9000	0.0076	-0.0076
23	0.9500	0.0048	-0.0048
24	1.0000	0.	0.
Chord: c = 0.090 m			
L.E. radius/c = T.E. radius/c =0.002			

Table 3.5.1: *Fifth standard configuration: Dimensionless airfoil coordinates [Bölcs and Fransson, 1986, p. 125]*

Aeroelastic sample case	Time averaged					Time dependent parameters				Flow
	M_1 (-)	i (^{o})	p_{w1} (bar)	p_2/p_{w1} (-)	Re_1 (-)	α or h (rad or -)	x_α/c (-)	f (Hz)	k (-)	
1	0.5	2	1.4	0.84	1.4×10^6	0.00524	0.5	200	0.37	Attached
2	"	4	"	0.86	"	"	"	"	"	"
3	"	6	"	0.87	"	"	"	"	"	Part. separated
4	"	4	"	0.86	"	"	"	75	0.14	Attached
5	"	"	"	"	"	"	"	125	0.22	"
6	"	"	"	"	"	"	"	300	0.54	"
7	"	"	"	"	"	"	"	550	1.02	"
8	"	6	"	0.87	"	"	"	75	0.14	Part. separated
9	"	"	"	"	"	"	"	125	0.22	"
10	"	"	"	"	"	"	"	300	0.56	"
11	"	"	"	"	"	"	"	550	1.02	"
12	"	8	"	0.87	"	"	"	200	0.37	"
13	"	10	"	0.88	"	"	"	"	"	Fully separated
14	"	12	"	0.89	"	"	"	"	"	"
15	"	10	"	0.88	"	"	"	75	0.14	"
16	"	"	"	"	"	"	"	125	0.22	"
17	"	"	"	"	"	"	"	300	0.56	"
18	"	"	"	"	"	"	"	550	1.01	"
19	0.6	"	"	0.84	1.6×10^6	"	"	200	0.31	"
20	0.7	"	"	0.80	1.7×10^6	"	"	"	0.27	"
21	0.8	"	"	0.77	1.8×10^6	"	"	"	0.24	"
22	"	"	2.0	"	"	"	"	"	0.23	"
23	0.9	"	"	0.72	2.0×10^6	"	"	"	0.21	"
24	1.0	"	"	0.69	2.1×10^6	"	"	"	0.19	"
25	0.5	6	1.4	0.88	1.4×10^6	"	0.0	125	0.22	Part. separated
26	"	"	"	0.87	"	"	0.92	"	"	"
27	"	10	"	0.87	"	"	0.0	"	"	Fully separated
28	"	"	"	0.88	"	"	0.92	"	"	"
29	"	6	"	0.87	"	0.001	heaving	200	0.37	Part. separated
30	"	10	"	0.88	"	"	"	"	"	Fully separated

- Sample cases 12-30 are new.
- Only the center blade is oscillated. The others are fixed.
- The y-position of the pitch axis is $y_\alpha=0$. for aeroelastic sample cases 1-28 above.
- Cases 29-30 are normal-to-chord heaving oscillations.
- The difference between cases 21 and 22 consists of a different inlet stagnation pressure.

Table 3.5.2: *Fifth standard configuration: Experimental values for 30 recommended aeroelastic sample cases [Bölcs and Fransson, 1986, p. 126].*

3.6   Sixth standard configuration

No modifications have been made to this standard configuration. All results, and a discussion thereof, are found in the 1986 report [Bölcs and Fransson, 1986]. A listing of all the results are found in appendix A3.

The compressible dynamic pressure has been used in the definition of the pressure coefficients by all participating researchers.

3.7   Seventh standard configuration (compressor cascade in supersonic flow).

The seventh standard configuration (Fig. 3.7.1 and Tables 3.7.1-2) was tested at Detroit Diesel Allison, and included in the workshop report by courtesy of the sponsoring agent, D. R. Boldman at NASA Lewis Research Center [Boldman, 1983; Riffel and Rothrock, 1980]. A question as regards to the validity of the profile coordinates did arise at the 1991 Aeroelasticity meeting. These have been verified

[Boldman, 1991], and it is confirmed that the originally presented blade coordinates were correct. The agreement between the data and the predictions is, at the present time, not satisfactory for any of the 12 aeroelastic sample cases. It is probable that some of the discrepancies comes from the viscous effects in the experiment, some from experimental accuracy and some from the prediction models, but not enough

predictions have been performed to analyze either the data or predictions for supersonic cascades with thickness. At the present time it is thus proposed to keep this standard configuration, and the corresponding aeroelastic sample cases, in its original form.

It should be pointed out that, as with the other experimental Standard Configurations, the pressure coefficients are scaled with the steady-state upstream dynamic pressure $(\overline{p}_{w1} - \overline{p}_1)$. As far as the authors are aware, all predicted results have been presented with this dynamic pressure in the pressure coefficient definitions.

The Reynolds number of the experiments were not given in the original report [Bölcs and Fransson, 1986], but are now included. They are situated in the range $1.1\text{-}1.6 \bullet 10^6$ [Riffel and Rothrock, 1980, p. 11] for the performed tests.

Gerolymos et al [1990] have presented calculations on this geometry. A stream sheet contraction of 0.85 was introduced for these computations in order to get a reasonable agreement with the steady-state outflow data. Trend wise agreement can be found in the unsteady pressures on the blade surfaces, and the experimental and numerical stability limits of the cascade agree fairly well.

| 31 | 1.0000 | -0.0029 | 1.0000 | -0.0029 |

Chord: c = 0.0762 m (=3.00 inches)
L.E. radius/c = 0.0027
T.E. radius/c = 0.0027

Table 3.7.1: *Seventh standard configuration: Dimensionless airfoil coordinates [Bölcs and Fransson, 1986, p. 155].*

Point No.	Upper surface (=Suction surface) x/c	y/c	Lower surface (=Pressure surface) x/c	y/c
1	0.	-0.0029	0.	-0.0029
2	0.0026	-0.0004	0.0027	-0.0056
3	0.0278	0.0015	0.0279	-0.0066
4	0.0655	0.0041	0.0657	-0.0079
5	0.1032	0.0065	0.1035	-0.0092
6	0.1410	0.0087	0.1412	-0.0103
7	0.1788	0.0107	0.1790	-0.0113
8	0.2165	0.0124	0.2168	-0.0123
9	0.2543	0.0139	0.2546	-0.0131
10	0.2921	0.0152	0.2923	-0.0138
11	0.3299	0.0162	0.3301	-0.0144
12	0.3551	0.0168	0.3552	-0.0148
13	0.3929	0.0175	0.3930	-0.0152
14	0.4307	0.0179	0.4308	-0.0155
15	0.4685	0.0181	0.4685	-0.0158
16	0.5063	0.0181	0.5063	-0.0159
17	0.5441	0.0179	0.5440	-0.0159
18	0.5820	0.0174	0.5818	-0.0158
19	0.6198	0.0167	0.6195	-0.0156
20	0.6576	0.0158	0.6573	-0.0153
21	0.6828	0.0150	0.6824	-0.0151
22	0.7205	0.0137	0.7202	-0.0146
23	0.7583	0.0122	0.7580	-0.0140
24	0.7961	0.0105	0.7958	-0.0133
25	0.8338	0.0087	0.8336	-0.0124
26	0.8716	0.0067	0.8714	-0.0112
27	0.9093	0.0047	0.9092	-0.0098
28	0.9471	0.0026	0.9470	-0.0082
29	0.9848	0.0003	0.9848	-0.0063
30	0.9974	-0.0005	0.9974	-0.0057

Table 3.7.2: *Seventh standard configuration: Experimental values for 12 recommended aeroelastic sample cases [Bölcs and Fransson, 1986, p. 156].*
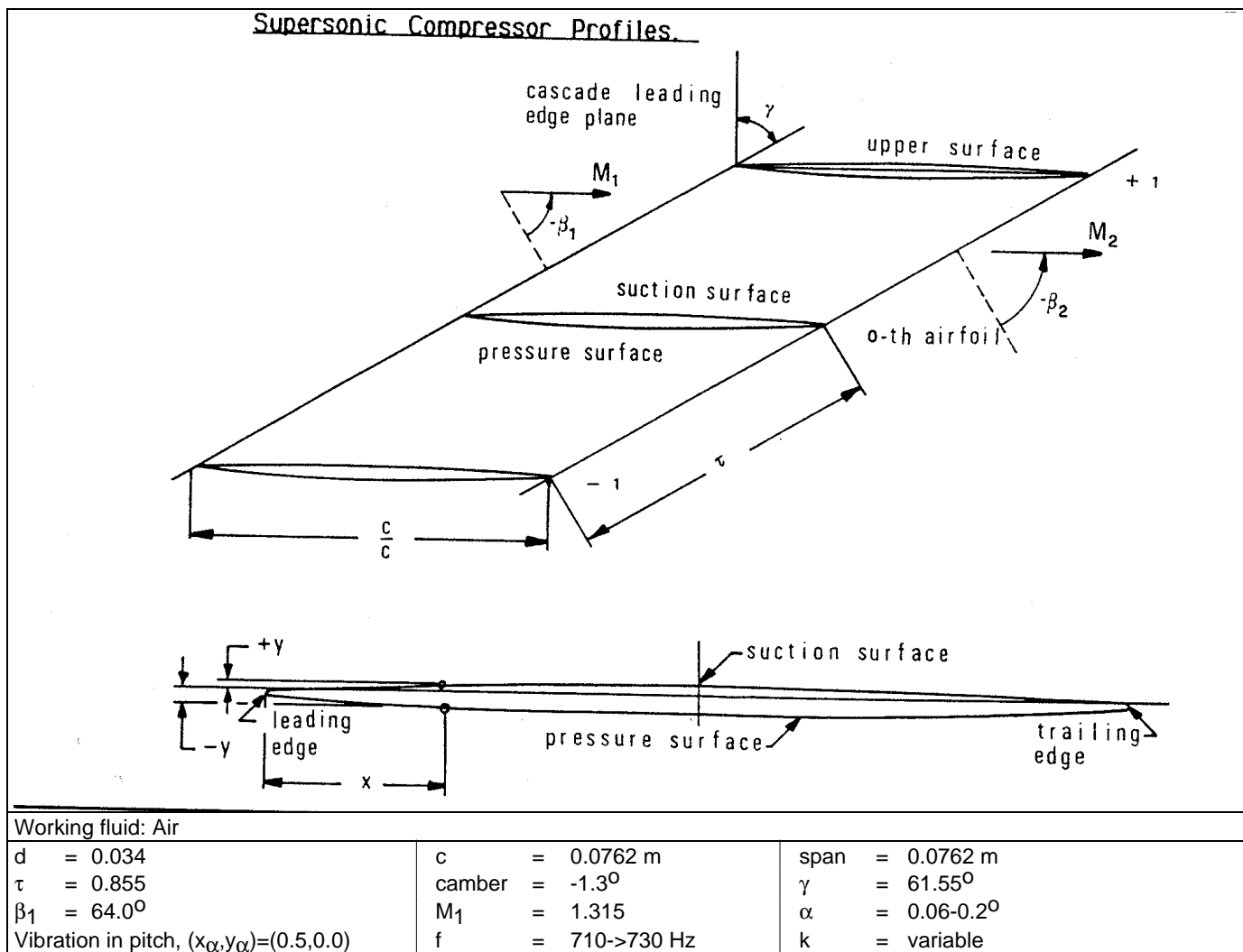
Time averaged parameters

Aeroelastic Test Case	M_1 (-)	β_1 (°)	p_{w2}/p_{w1} (-)	p_2/p_{w1} (-)	M_2 (-)	β_2 (°)
1-6	1.315	-64.0	0.958	1.04	1.25	-62.8
7-12	=	=	0.957	1.45	0.99	-63.6

a: Time-averaged values.

Time dependent parameters

Aeroelastic Test Case	$f_{nominal}$ (Hz)	f_{actual} (Hz)	k (-)	$\sigma_{nominal}$ (°)	$\sigma(-1)$ (°)	$\sigma(0)$ (°)	$\sigma(+1)$ (°)	$\sigma(+2)$ (°)	$\alpha_{nominal}$ (rad)	$\alpha(-2)/\alpha(0)$ (-)	$\alpha(-1)/\alpha(0)$ (-)	$\alpha(0)$ (rad)	$\alpha(+1)/\alpha(0)$ (-)	$\alpha(+2)/\alpha(0)$ (-)
1	725	725	0.44	180	-173	-187	-178	-180	.00349	0.76	0.52	.00122	1.27	0.0
2	=	714	0.43	-90	-91	-65	-81	-80	=	0.87	0.20	=	0.67	=
3	=	-	0.44	-45	-	-	-	-	-	-	-	-	-	-
4	=	724	=	0	+4	+6	-8	0	=	0.34	0.61	.00379	0.75	=
5	=	745	0.45	+45	+48	+53	+54	+50	=	0.71	0.78	.00206	0.32	=
6	=	724	0.44	+90	+91	+91	+84	+90	=	0.56	0.59	.00187	0.97	=
7	=	=	=	180	-172	-168	-163	-170	=	1.21	0.85	.00131	0.60	=
8	=	725	=	-45	-66	-69	-61	-66	=	0.54	0.44	.00178	0.34	=
9	=	724	=	0	-4	+8	-5	0	=	0.64	0.96	.00202	1.11	=
10	=	=	=	+45	+66	+59	+60	+60	=	0.36	0.65	.00386	0.50	=
11	=	725	=	+90	+92	+74	+86	+85	=	0.66	0.96	.00227	0.73	=
12	=	=	=	+120	+96	+115	+98	+100	=	0.35	0.40	.00129	0.25	=

b: Time-dependent values.

Working fluid: Air		
d = 0.034	c = 0.0762 m	span = 0.0762 m
τ = 0.855	camber = -1.3^o	γ = 61.55^o
β_1 = 64.0^o	M_1 = 1.315	α = 0.06-0.2^o
Vibration in pitch, $(x_\alpha,y_\alpha)=(0.5,0.0)$	f = 710->730 Hz	k = variable

Fig. 3.7.1:   *Seventh standard configuration: Cascade geometry [Bölcs and Fransson, 1986, p. 154].*

3.8   Eighth standard configuration (flat plate cascades at different flow conditions).

As flat plate configurations are the most important to compare against as regards to the numerical completeness and accuracy of non-analytical prediction models, it is important that such configurations cover as wide a scope as possible, especially as regards to Mach number variations. The number of aeroelastic sample cases will thus forcibly be large, but this is not a major problem as the analytical flat plate solutions used as baseline comparisons are usually fairly fast, and researchers who may want to compare a numerical result against an analysis will only choose the domain of current interest and perform a few calculations.

The 35 original aeroelastic sample cases will be kept (Fig. 3.8.1 and Table 3.8.1). The time-dependent cases 36 to 42, corresponding to some of the earlier cases but with a reduced frequency of k=0.5 instead of k=1.0, have been added. This lower reduced frequency (k=0.5) was recommended as the higher reduced frequency showed some differences, which may eventually be attributed to some numerical effects, between the different prediction models. To

these aeroelastic test cases are added two supplementary steady-state conditions (Figs. 3.8.2). These, denoted as aeroelastic test cases 43-54 and suggested by Dr. Verdon, are the well known "Cascades A and B" as defined by Verdon [1973] and Verdon and McCune [1975]. These cascade configurations were originally carefully selected to highlight wave reflections in supersonic flow and have been used frequently in the past as comparison for a number of analyses. They have provided useful insight into the physical phenomena of unsteady supersonic flow on vibrating flat plates and interesting, often positive, results from the comparisons. It is believed that they also in the future should be of special interest as baseline comparisons for numerical models for supersonic flow, also for supersonic leading edge locus configurations.

As far as the present authors are aware, all pressure coefficient results have been presented with the incompressible dynamic pressure, $(\rho_{-} \bullet v_{-}{}^2/2)$, as non-dimensionalized value.

Aeroel. Sample Case	Time-Averaged Conditions				Time-Dep.	
	M_1 (-)	Normal shock?	γ (°)	τ (-)	k (-)	σ (°)
1	Incomp.	-	60	0.75	1.0	90
2	"	-	45	"	"	"
3	"	-	30	"	"	"
4	"	-	0	"	"	"
5	0.5	-	60	"	"	"
6	0.6	-	"	"	"	"
7	0.7	-	"	"	"	"
8	0.8	-	"	"	"	"
9	0.9	-	"	"	"	"
10	0.95	-	"	"	"	"
11	0.8	-	45	"	"	"
12	"	-	30	"	"	"
13	"	-	0	"	"	"
14	"	-	60	0.5	"	"
15	"	-	"	1.0	"	"
16	1.1	-	"	0.75	"	"
17	"	at LE	"	"	"	"
18	"	at TE	"	"	"	"
19	1.2	-	"	"	"	"
20	"	at LE	"	"	"	"
21	"	at TE	"	"	"	"
22	1.3	-	"	"	"	"
23	"	at LE	"	"	"	"
24	"	at TE	"	"	"	"
25	1.4	-	"	"	"	"
26	"	at LE	"	"	"	"
27	"	at TE	"	"	"	"
28	1.5	-	"	"	"	"
29	"	at LE	"	"	"	"
30	"	at TE	"	"	"	"
31	1.3	-	"	0.5	"	"
32	"	-	"	1.0	"	"
33	"	at LE	"	0.5	"	"
34	"	"	"	1.0	"	"
35	"	"	45	0.75	"	"
36	Incomp.	-	60	0.75	0.5	"
37	0.5	-	"	"	"	"
38	0.7	-	"	"	"	"
39	0.8	-	"	"	"	"
40	1.3	-	"	"	"	"
41	1.4	-	"	"	"	"
42	1.5	-	"	"	"	"
43 ="A"	1.345	-	59.5	0.7886	0.5	0
44	"	-	"	"	"	60
45	"	-	"	"	"	120
46	"	-	"	"	"	180
47	"	-	"	"	"	240
48	"	-	"	"	"	300
49 ="B"	1.281	-	63.4	0.6711	0.5	0
50	"	-	"	"	"	60
51	"	-	"	"	"	120
52	"	-	"	"	"	180
53	"	-	"	"	"	240
54	"	-	"	"	"	300

Table 3.8.1: *Eighth standard configuration: 54 recommended aeroelastic sample cases [Bölcs and Fransson, 1986, p. 168; Verdon and McCune, 1975].*

Further information and interesting results on "Cascades A and B" have been presented by, among others, Gerolymos et al [1990b], Whitehead [1990], Fleeter and Hoyniak [1989], Topp and Fleeter [1986], Verdon [1977a,b]. More results on flat plates have been presented by several authors the last few years, among them Giles and Haimes [1991], Namba and Toshimitsu [1990], Huff [1989], Huff and Reddy [1989], Bakhle et al [1989], Verdon [1989a], and Schroeder and Fleeter [1989], to mention just a few.
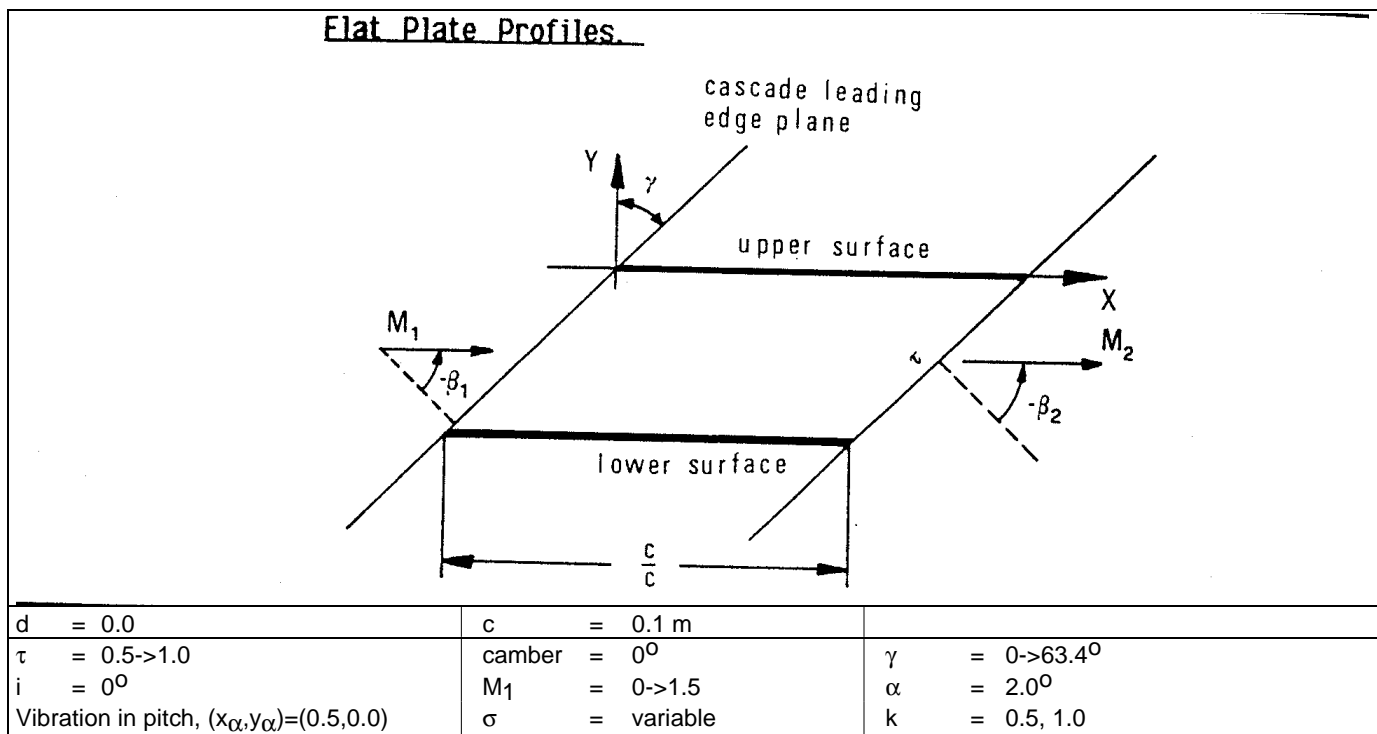
Flat Plate Profiles.

d	= 0.0	c	= 0.1 m		
τ = 0.5->1.0		camber = 0°		γ	= 0->63.4^o
i = 0°		M_1 = 0->1.5		α	= 2.0^o
Vibration in pitch, (x_α, y_α)=(0.5,0.0)		σ = variable		k	= 0.5, 1.0

Fig. 3.8.1:   *Eighth standard configuration: General cascade geometry [Bölcs and Fransson, 1986, p. 168].*

a: Verdon "Cascade A"	b: Verdon "Cascade B"
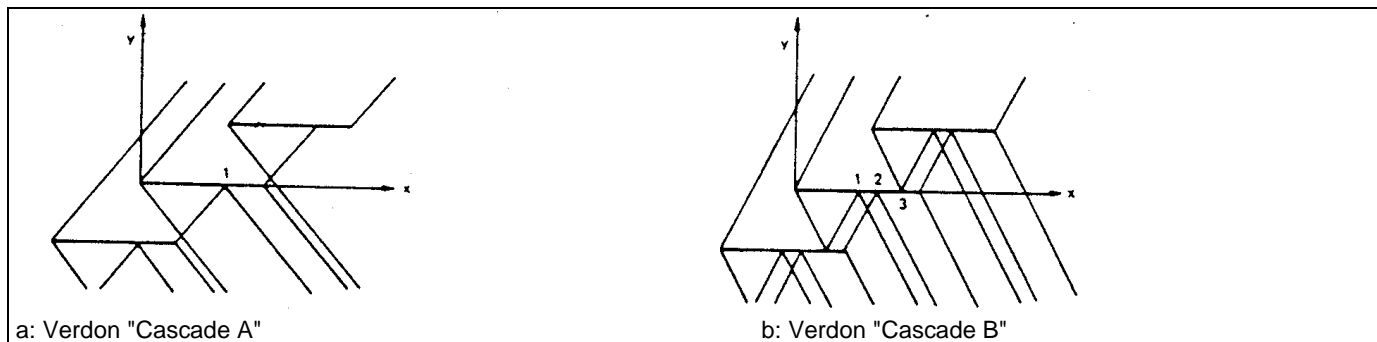
Fig. 3.8.2:   *Eighth standard configuration: Geometry of cascades "A" and "B" from Verdon and McCune [1975, p.2]. Included are also the leading and trailing edge wave configurations for aeroelastic sample cases 43-54.*

3.9   Ninth standard configuration (double circular arc cascades at different flow conditions).

The ninth standard configuration is a continuation of the eighth, but includes both thickness and camber effects. The geometry of the blades was proposed by Dr. J. M. Verdon from United Technologies Research Center (Fig. 3.9.1). At the present time it is proposed to keep the originally defined 21 aeroelastic sample cases for further studies (Table 3.9.1). However, it has been noted by the calculations done up to now that the high reduced frequency (k=1.0) gave some unexpected numerical problems which should not be the main purpose of the investigation. Furthermore, this high reduced frequency (based on half-chord) is not of extreme practical interest today. The same configurations are thus proposed, as sample cases 22-42, at the lower reduced frequency of k=0.5.

The results presented are, as far as the authors' are aware of, all presented with the incompressible

dynamic pressure, $(\rho_- \bullet v_-^2/2)$, as non-dimensionalized value.

Among others, Whitehead [1990], Li et al [1990], Huff [1989] and Verdon [1989a] have presented numerical results on unsteady flow through vibrating DCA cascades, and Buffum and Fleeter [1989a,b, 1988] and Giordano and Fleeter [1990] have presented experimental data.

The conclusions to be drawn are that promising results exist on this standard configuration, but that some unexplained effects still exist. The agreement between different prediction models is usually not as good as one would wish when the inlet flow Mach numbers are high or the blade thickness non negligible.

Symmetric/Flat-Bottomed Circular Arc Profiles.
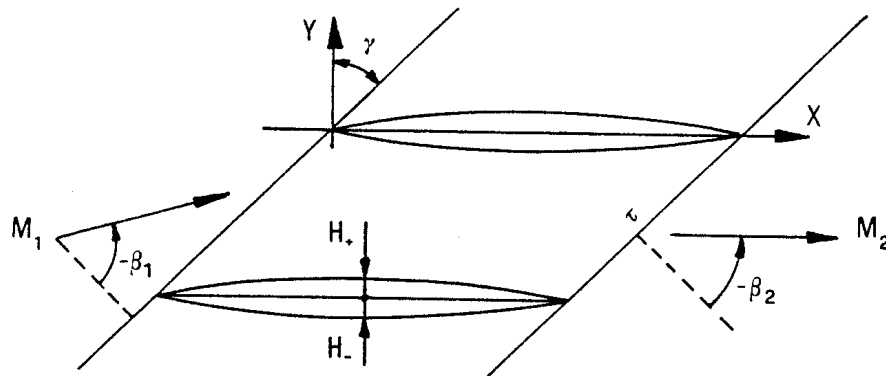
Symmetric/flat-bottomed circular arc profiles

Equation:

$$y_{\pm}(x) = \text{sgn}(H_{\pm}) \cdot \left\{ |H_{\pm}| - R_{\pm} + \left[R_{\pm}^2 - (x - 0.5)^2 \right]^{0.5} \right\} \text{ if } H_{\pm} \neq 0$$

$$y_{\pm}(x) = 0 \text{ if } H_{\pm} = 0$$

$$R = \frac{\left\{ H^2 + 0.5^2 \right\}}{2 \cdot |H|}$$

sgn (H) = ± 1 for H > 0 / H < 0;	( )$_+$ = upper surface;	( )$_-$	= lower surface
Maximum thickness at x = 0.5	d = 0.01 - 0.1	c	= 0.1 m
τ = 0.75	γ = 45°, 60°	camber	= 0° (for symmetric profiles)
i = 0° (for M_1 < 1.)	α = 2.0 °	M_1	= variable (0.0 -> 1.5)
k = 1.0	σ = 90°	Vibration in pitch around (x_α, y_α) = (0.5, camberline)	

Fig. 3.9.1:   Ninth standard configuration: Cascade geometry [Bölcs and Fransson, 1986, p. 180].

		Time-Averaged Conditions					Time-Dep.				Time-Averaged Conditions					Time-Dep.	
	M_1	γ (°)	β_1(°)	H_+ (-)	H_- (-)	d (-)	k (-)	σ (°)		M_1	γ (°)	β_1(°)	H_+ (-)	H_- (-)	d (-)	k (-)	σ (°)
1	0.0	60	-60	0.01	0.01	0.02	1.0	90	22	0.0	60	-60	0.01	0.01	0.02	0.5	90
2	"	"	"	0.02	0.02	0.04	"	"	23	"	"	"	0.02	0.02	0.04	"	"
3	"	"	"	0.03	0.03	0.06	"	"	24	"	"	"	0.03	0.03	0.06	"	"
4	"	"	"	0.05	0.05	0.10	"	"	25	"	"	"	0.05	0.05	0.10	"	"
5	0.5	"	"	0.01	0.01	0.02	"	"	26	0.5	"	"	0.01	0.01	0.02	"	"
6	0.7	"	"	0.005	0.005	0.01	"	"	27	0.7	"	"	0.005	0.005	0.01	"	"
7	"	"	"	0.01	0.01	0.02	"	"	28	"	"	"	0.01	0.01	0.02	"	"
8	"	"	"	0.015	0.015	0.03	"	"	29	"	"	"	0.015	0.015	0.03	"	"
9	"	"	"	0.02	0.02	0.04	"	"	30	"	"	"	0.02	0.02	0.04	"	"
10	0.8	"	"	0.01	0.01	0.02	"	"	31	0.8	"	"	0.01	0.01	0.02	"	"
11	1.3	"	"	"	"	"	"	"	32	1.3	"	"	"	"	"	"	"
12	1.4	"	"	"	"	"	"	"	33	1.4	"	"	"	"	"	"	"
13	1.5	"	"	"	"	"	"	"	34	1.5	"	"	"	"	"	"	"
14	0.0	45	-45	"	"	"	"	"	35	0.0	45	-45	"	"	"	"	"
15	0.5	"	"	"	"	"	"	"	36	0.5	"	"	"	"	"	"	"
16	0.7	"	"	"	"	"	"	"	37	0.7	"	"	"	"	"	"	"
17	0.8	"	"	"	"	"	"	"	38	0.8	"	"	"	"	"	"	"
18	0.5	"	-45	0.05	0.0	0.05	"	"	39	0.5	"	-45	0.05	0.0	0.05	"	"
19	0.7	"	"	"	"	"	"	"	40	0.7	"	"	"	"	"	"	"
20	0.8	"	"	"	"	"	"	"	41	0.8	"	"	"	"	"	"	"
21	0.9	"	"	"	"	"	"	"	42	0.9	"	"	"	"	"	"	"

Table 3.9.1: Ninth standard configuration: 42 recommended aeroelastic sample cases [Bölcs and Fransson, 1986, p. 181].

3.10   Tenth standard configuration (Modified cambered NACA 0006 cascade at subsonic and transonic flow conditions).

The tenth Standard Configuration, included by proposal of Dr. J. M. Verdon at the United Technologies Research Center [1987a,c], is a two-dimensional compressor cascade of modified NACA 0006 profiles that operates at subsonic inlet and exit conditions. The geometry is given by Verdon [1987a] and is repeated here for convenience.

The cascade has a stagger angle, γ, of 45° and a gap/chord ratio, τ, of unity. The blades are constructed by superimposing the thickness distribution of a modified NACA four digit series airfoil on a circular arc camber line. The thickness distribution is given by:

$$T(x) = H_T \cdot$$
$$(2.969 \cdot x^{0.5} - 1.26 \cdot x - 3.516 \cdot x^2 \qquad (3.10.1)$$
$$+ 2.843 \cdot x^3 - 1.036 \cdot x^4), \quad 0 \le x \le 1$$

where H_T is the nominal blade thickness. The coefficient of the x^4 in eq. (3.10.1) differs from that used in the standard NACA airfoil definition (i.e., -1.015) so that the example blades will close in as wedge-shaped trailing edges.

The camber distribution is given by:

$$C(x) = H_C - R + \sqrt{\{R^2 - (x-0.5)^2\}} \qquad (3.10.2)$$
$$0 \le x \le 1$$

where H_C (>0) is the height of the camber-line at midchord and

$$R = \frac{\{H_C^2 + 0.25\}}{2 \cdot H_C}$$

is the radius of the circular arc camber line. The surface coordinates of the reference blade are therefore given by:

$$[X,Y]_{\pm} = [x \mp 0.5 \cdot T(x) \cdot \sin(\theta), C(x) \pm 0.5 \cdot T(x) \cdot \cos(\theta)]$$
$$0 \le x \le 1$$
$$(3.10.3)$$

where the signs + and - refer to the upper (suction) and lower (pressure) surfaces, respectively, and $\theta = \tan^{-1}(dC/dx)$. For the present example we set H_T=0.06 and H_C=0.05 to study the unsteady aerodynamic response of a vibrating cascade of cambered NACA 0006 airfoils.

We consider two different steady-state inlet operating conditions. In the aeroelastic cases 1-16 the inlet Mach number, M_1, and flow angle, β_1, are 0.7 and -55°, respectively; for cases 17-32, M_1=0.8 and β_1=-58° (see Table 3.10.1). The flow through the cascade is assumed to satisfy a Kutta condition at blade trailing edges and, therefore, only inlet flow information must be specified. For M_1=0.7 and β_1=-55°, the mean or steady flow through the cascade is entirely subsonic; for M_1=0.8 and β_1=-58° it is transonic with a normal shock occurring in each blade passage.

As aeroelastic test cases we consider single-degree-of-freedom blade heaving, normal to chord, and pitching motions at four different frequencies, k=0.25, 0.50, 0.75 and 1.0, and at interblade phase angles lying in the range -π_σ_π. The amplitude of the heaving motion, h, is 0.01; that of the pitching motion, α, is 2^O. The blade pitching axis lies at midchord, i.e. (x_α, y_α)=(0.5, 0.05).

We are interested in the following aerodynamic response information for each of the two inlet operating conditions given, at reduced frequencies of k=0.25, 0.50, 0.75 and 1.0 (see Table 3.10.1 for details):

1: The time-averaged blade surface pressure coefficient, $\bar{c}_p(x)$ and Mach number.

2: a: Amplitude, $\tilde{c}_p(x)$, and phase lead angle, $\Phi_p(x)$, of the unsteady blade surface pressure coefficient for heaving and pitching motions at σ=0° and σ=90°.

   b: Amplitude, $\Delta\tilde{c}_p(x)$, and phase lead angle, $\Phi_{\Delta p}(x)$, of the unsteady blade surface pressure difference coefficient for heaving and pitching motions at σ=0° and σ=90°.

3: a: The amplitude, $\tilde{c}_l$, and phase lead angle, Φ_l, of the unsteady lift coefficient per unit amplitude vs interblade phase angle for the heaving motions at $-\pi \le \sigma \le \pi$.

   b: The amplitude, $\tilde{c}_m$, and phase lead angle, Φ_m, of the unsteady moment coefficient per unit amplitude vs interblade phase angle for the pitching motions at $-\pi \le \sigma \le \pi$.

4: The aeroelastic damping coefficient, Ξ, vs interblade phase angle for the heaving and pitching motions at $-\pi \le \sigma \le \pi$.

Usab and Verdon [1990, 1989b, 1987a,c], and Whitehead [1990] have already presented results on this cascade. Results from other prediction models were also recently presented [Huff, 1991; Hall, 1991]. Some very promising results have been obtained (these will be included in the complete updated report presently in preparation).

When comparing these results with each other it must be considered that no analytical results exist. Only the mutual agreement between several similar theoretical methods can thus indicate the accuracy of the models.
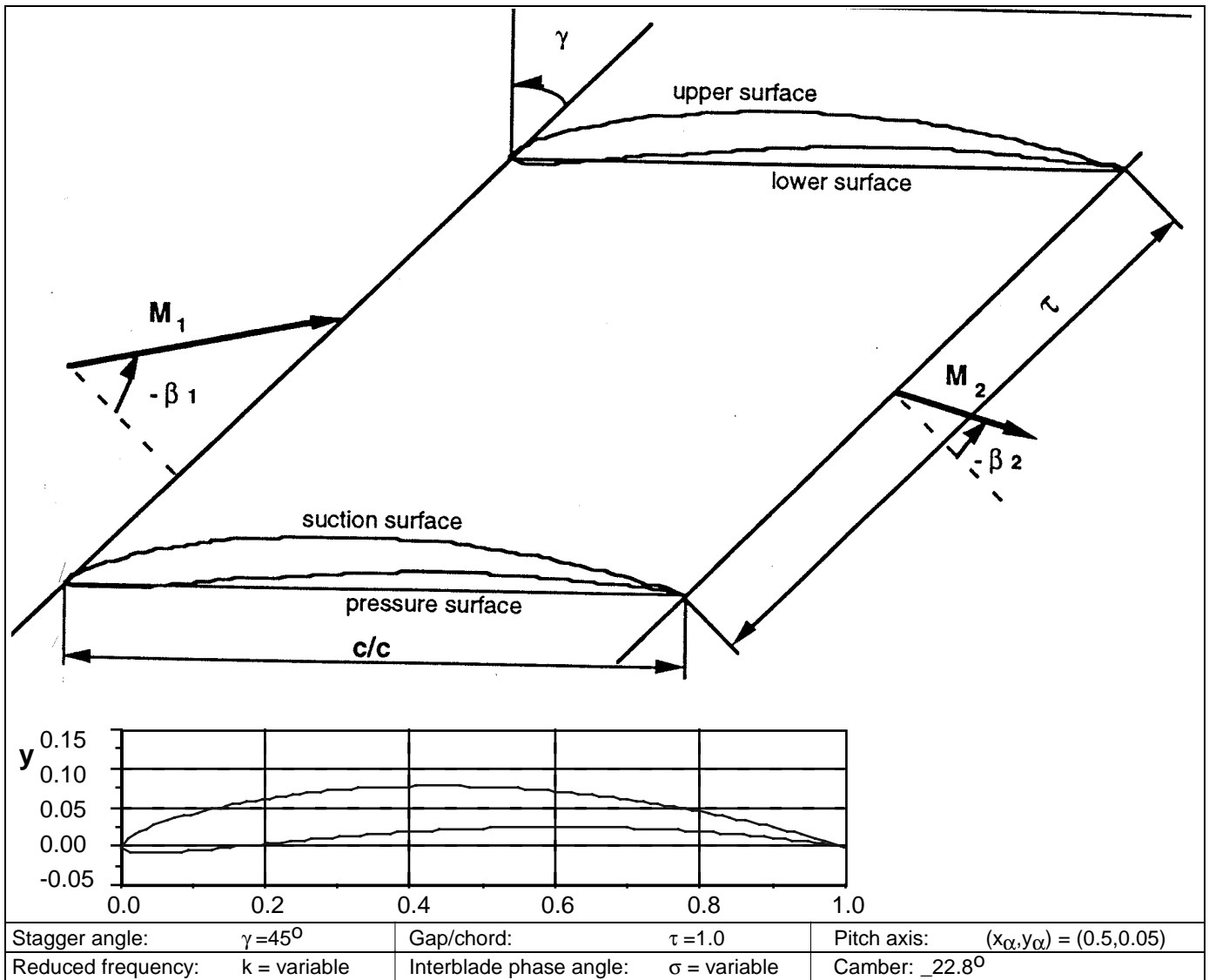
Stagger angle:	$\gamma = 45^O$	Gap/chord:	$\tau = 1.0$	Pitch axis: $(x_\alpha, y_\alpha) = (0.5, 0.05)$
Reduced frequency:	k = variable	Interblade phase angle:	σ = variable	Camber: $\_22.8^O$

Fig. 3.10.1:   *Tenth standard configuration: Modified cambered NACA 0006 cascade.*

Test case	Time averaged		Time dependent				Test case	Time averaged		Time dependent			
	M_1 (-)	β_1 (^{O})	α (^{O})	h (-)	σ (^{O})	k (-)		M_1 (-)	β_1 (^{O})	α (^{O})	h (-)	σ (^{O})	k (-)
1	0.7	-55	2	---	0	0.25	17	0.8	-58	2	---	0	0.25
2	"	"	"	---	90	"	18	"	"	"	---	90	"
3	"	"	"	---	0	0.50	19	"	"	"	---	0	0.50
4	"	"	"	---	90	"	20	"	"	"	---	90	"
5	"	"	"	---	0	0.75	21	"	"	"	---	0	0.75
6	"	"	"	---	90	"	22	"	"	"	---	90	"
7	"	"	"	---	0	1.0	23	"	"	"	---	0	1.0
8	"	"	"	---	90	"	24	"	"	"	---	90	"
9	"	"	---	0.01	0	0.25	25	"	"	---	0.01	0	0.25
10	"	"	---	"	90	"	26	"	"	---	"	90	"
11	"	"	---	"	0	0.50	27	"	"	---	"	0	0.50
12	"	"	---	"	90	"	28	"	"	---	"	90	"
13	"	"	---	"	0	0.75	29	"	"	---	"	0	0.75
14	"	"	---	"	90	"	30	"	"	---	"	90	"
15	"	"	---	"	0	1.0	31	"	"	---	"	0	1.0
16	"	"	---	"	90	"	32	"	"	---	"	90	"

Table 3.10.1:   *Tenth standard configuration: 32 recommended aeroelastic sample cases (the pitch axis is located at $(x_\alpha, y_\alpha) = (0.5, 0.05)$).*

Please note that, for this standard configuration, the compressible dynamic pressure, $(p_{w1}-p_1)$, as originally proposed, has been used in the definition of the pressure coefficients by Whitehead ("Method 2" in the plots in Appendices A3 and A4), Hall ("Method 22") and Carstens ("Method 25"), whereas Verdon ("Method 3") and Huff ("Methods 23 and 26") have employed the incompressible dynamic pressure as reference value.

4. CONCLUSIONS AND RECOMMENDATIONS

A large amount of work has been put into the field of unsteady flow through vibrating blade rows in the period between 1987 and 1991, both on the experimental and theoretical sides. The standard configurations for unsteady flow through vibrating axial flow turbomachine cascades, as originally defined, have been used by many researchers with the aim to compare prediction models against the data but also to analyze results for parametric studies. Unfortunately, due to the high computing costs involved in parametric studies with numerical time-dependent models, it is generally not possible to perform such investigations in order to better understand the physical reasons for aeroelastic effects on a special blade configuration.

Possibilities to predict aeroelastic phenomena have largely increased the last few years, to include aspects such as three-dimensionality and/or viscosity. In some cases these possibilities have overtaken the detailed experimental data available. As an example can be mentioned the prediction of time-dependent viscous flow (in most cases today still with steady-state turbulence models) on oscillating cascades, and the enormous difficulties to accurately measure enough details to be able to judge the quality of the viscous numerical predictions. As computers become more and more powerful, the computing cost will reduce simultaneously as the cost of an experimental investigation will increase. Comparisons between different predictions will thus probably increase in importance, at the expense of comparisons with experimental data. Comparisons between theoretical models, and with analytical solutions, are of large interest and necessity, as only through such efforts can the accuracy between the different models be assessed and the theoretical assumptions validated in detail. Only experimental test cases can, on the other hand, give information about the validity of all assumptions being made in the predictions. It is thus necessary to accurately measure, in detail, three-dimensional, transonic and viscous, flow effects in both linear and annular cascades, at realistic reduced frequencies, in the near future. This is an extremely difficult and expensive task and all contributions in this regard will be warmly welcomed. In this procedure it must however not be forgotten that two-dimensional aeroelastic problems are far from understood, and that basic comparisons, such as against different flat plate analyses, are of extreme importance to establish the fundamental validity of any model.

Although great improvements are presently made in the field of numerical computations of unsteady flow, it must be kept in mind that a general theory that can treat the subsonic through supersonic flow domain, on compressors, fans and turbines, including viscous effects is still very far away.

All the configurations discussed in the present study (and a large majority of all investigations performed on unsteady flow) consider rigid profiles, both in span- and chordwise directions. It is regularly shown by several authors that the strip theory assumption is of limited usefulness and that three-dimensional span wise effects can be of large importance. Furthermore, as it in the future will be important to also consider higher modes than pure bending and pitching, coupled and chord-wise non-rigid blade vibrations at high frequencies is a large challenge.

Prediction of aeroelastic phenomena of the new generation of swept fan blades will be necessary. The use of composite blades will open up new aeroelastic challenges and will probably couple the unsteady aerodynamics and the structural mechanics parts in turbomachinery closer together (as on aircraft structures) than what is presently the case.

From the above it can be concluded that the data collected as the "Standard Configurations" will be of use also in the next future, while new experiments must be initiated for the validation of the next generation of prediction models[7]. For these the exact treatment of unsteady shock waves and unsteady local separations seem to be the present most challenging theoretical parts before going into details about global separation.

Due to the success of the present comparative study, it has regularly been suggested that similar standard configurations should be defined also for gust response. This idea was concretely put forward during the panel discussion on the "Standard Configurations on Unsteady Flow Through Vibrating Axial-Flow Turbomachine Cascades" at the Aeroelasticity meeting in Notre Dame on September 15-19, 1991, through a suggestion that the same geometries as

---

[7] For this to be achieved, it has been proven useful to have all the existing experimental data and analyses in a common data base, often using the same format for the presentation of the results. It is suggested to continue to include new data and analyses into the data base as such results become available.

used for the cascades in the present study should be employed [Atassi, 1991]. This would help to avoid many problems, such as the previously mentioned difficulties in experimental blade coordinates, which by now to some extent are known on the present standard configurations.

5. ACKNOWLEDGMENTS

6. REFERENCES

Abdel-Rahim, A.; Sisto, F.; Thangam, S.; 1991
"Computational Study of Stall Flutter in Linear Cascades", *ASME Paper 91-GT-5, 1991.*

Adamczyk, J. J.; Goldstein, M. E.; 1978
"Unsteady Flow in a Supersonic Cascade with Subsonic Leading-Edge Locus." *AIAA Journal, Vol. 16, No. 12, pp. 1248-1254, 1978.*

AGARD; 1989
"Unsteady Aerodynamic Phenomena in Turbomachines", *AGARD Conference Proceedings No. 468, Luxembourg, August 28-30, 1989.*

Allmaras, S.; Giles, M. B.; 1989
"A Coupled Euler/Navier-Stokes Algorithm for 2-D Unsteady Transonic Flows", *AIAA Paper 89-0556, 1989.*

Allmaras S. R.; Giles M. B.; 1987
"A Second Order Flux Split Scheme for the Unsteady 2-D Euler Equations on Arbitrary Meshes", *AIAA paper No. 87-1119, pp. 198-209, 1987.*

Arkadyev, A. B.; Vanin, V. A.; Yershov, S. V.; 1989
"Numerical Simulation of Transonic Flow Through Oscillating and Multi-Row Two-Dimensional Airfoil Cascades", *Proceedings of the Fifth International Symposium on "Unsteady Aerodynamics and Aeroelasticity of Turbomachines and Propellers", pp. 93-107, Beijing, China, September 18-21, 1989.*

Atassi, H.; Editor; 1992
Proceedings of theSixth International Symposium on Unsteady Aerodynamics, Aeroacoustics and Aeroelasticity of Turbomachines and Propellers, September 15-19, University of Notre Dame, USA, 1991.

Atassi, H.; 1991
"Communication during the Panel Discussion", *Sixth International Symposium on Unsteady Aerodynamics, Aeroacoustics and Aeroelasticity of Turbomachines and Propellers, September 15-19, University of Notre Dame, USA, 1991.*

Atassi, H.; Akai, T. J.; 1980
"Aerodynamic and Aeroelastic Characteristics of Oscillating Loaded Cascades at Low Mach Number", *Trans. ASME, J. Eng. Power, no. 102, pp. 344-351, 1980.*

Atassi, H.; Akai, T. J.; 1978
"Aerodynamic Force and Moment on Oscillating Airfoils in Cascade", *ASME Paper 78-GT-181, 1978.*

Bakhle, M. A.; Mahajan, A. J.; Keith, T. G. Jr; Stefko, G. L.; 1991
"Cascade Flutter Analysis with Transient Response Aerodynamics", *AIAA Paper 91-0747, 1991.*

Bakhle, M. A.; Reddy, T. S. R.; Keith, T. G. K.; 1990
"Time Domain Flutter Analysis of Cascades Using a Full Potential Solver", *AIAA Paper 90-0984, 1990.*

Bakhle, M. A.; Keith, T. G. K.; Kaza, K. R. V.; 1989
"Application of a Full-Potential Solver to Bending-Torsion Flutter in Cascades", *AIAA Paper 89-1386-CP, 1989.*

Bassi, F.; Osnaghi, C.; Savini, M.; 1989
"High-Resolution Euler Computations of Unsteady Transonic Flows in Cascades", *AGARD Conference Proceedings No. 468, "Unsteady Aerodynamic Phenomena in Turbomachines", pp. 15.1-15.12, Luxembourg, August 28-30, 1989.*

Bendiksen, O. O.; 1990
"Aeroelastic Problems in Turbomachines", *AIAA Paper 90-1157-CP, 1990.*

Bland, S. R.; Editor; 1987
"Transonic Unsteady Aerodynamics and Aeroelasticity", *Proceedings of a symposium held at NASA Langley Research Center, May 20-22, 1987, NASA Conference Publication 3022.*

Bölcs, A; Fransson, T. H.; Schläfli, D.; 1989a
"Aerodynamic Superposition Principle in Vibrating Turbine Cascades" *AGARD, 74th Specialists' Meeting of the Propulsion and Energetics Panel on Unsteady Aerodynamic Phenomena in Turbomachines, Luxembourg, August 28 - September 1, 1989.*

Bölcs, A; Fransson, T. H.; Schläfli, D.; 1989b
"Time-Dependent Measurements on Vibrating Annular Turbine Cascades Under Various Steady State Conditions" *AGARD, 74th Specialists' Meeting of the Propulsion and Energetics Panel on Unsteady Aerodynamic Phenomena in Turbomachines, Luxembourg, August 28 - September 1, 1989.*

Bölcs, A; Fransson, T. H.; Platzer, M. F.; 1989c
"Numerical Simulation of Inviscid Transonic Flow Through Nozzles With Fluctuating Back Pressure", *Journal of Turbomachinery, Vol. 111, pp. 169-180, April 1989.*

Bölcs, A; Fransson, T. H.; 1986
"Aeroelasticity in Turbomachines: Comparison of Theoretical and Experimental Cascade Results",

Communication du Laboratoire de thermique appliquée et de turbomachines, EPF-Lausanne, Switzerland, No. 13, 1986.

Bölcs, A; Degen, M.; Schläfli, D.; 1985
"Flutter Investigations of a Highly Cambered Turbine Cascade in Sub- and Supersonic Flow", *Report LTT-2-85, Laboratoire de thermique appliquée et de turbomachines, EPF-Lausanne, Switzerland, 1985.*

Boldman, D. R.; 1991
"Private Communication"

Boldman, D. R.; 1983
"Private Communication"

Buffum, D. H.; Fleeter, S.; 1991
"Wind Tunnel Wall Effects in a Linear Oscillating Cascade", *ASME Paper 91-GT-133, 1991.*

Buffum, D. H.; 1990
"Aerodynamics of a linear oscillating cascade", *Ph. D. Thesis, Purdue University, West Lafayette, Indiana, USA, 1990.*

Buffum, D. H.; Fleeter, S.; 1990
"Oscillating Cascade Aerodynamics by an Experimental Influence Coefficient Technique." *Journal of Propulsion, Vol. 6, No. 5, pp. 612-620, 1990.*

Buffum, D. H.; Fleeter, S.; 1989a
"The Aerodynamics of an Oscillating Cascade in a Compressible Flow Field", *ASME Paper 89-GT-271, 1989.*

Buffum, D. H.; Fleeter, S.; 1989b
"Experimental Investigation of Transonic Oscillating Cascade Aerodynamics", *AIAA paper 89-0321, AIAA 27th Aerospace Sciences Meeting, January 9-12, Reno, Nevada, 1989.*

Buffum, D. H.; Fleeter, S.; 1989c
"Experimental Investigation of Oscillating Cascade Aerodynamics", *Proceedings of the Fifth International Symposium on "Unsteady Aerodynamics and Aeroelasticity of Turbomachines and Propellers", pp. 223-238, Beijing, China, September 18-21, 1989.*

Buffum, D. H.; Fleeter, S.; 1988
"Investigation of Oscillating Cascade Aerodynamics by an Experimental Influence Coefficient Technique." *AIAA paper 88-2815, AIAA 24th Joint Propulsion Conference, July 11-13, Boston, Massachusetts, 1988.*

Buffum, D. H.; Boldman, D. R.; Fleeter, S.; 1987
"The Unsteady Aerodynamics of an Oscillating Cascade in a Compressible Flow Field", *AIAA paper 89-0321, AIAA 27th Aerospace Sciences Meeting, January 9-12, Reno, Nevada, 1989.*

Butenko, K. K.; Osipov, A. A.; Reyent, K. S.; 1989
"Two- and Three- Dimensional Problems of Unsteady Aerodynamics of Low Loaded Turbomachinery Blade Row Stages", *Proceedings of the Fifth International Symposium on "Unsteady Aerodynamics and Aeroelasticity of Turbomachines and Propellers", pp. 3-20, Beijing, China, September 18-21, 1989.*

Carr, L.; Chandrasekhara, M.; Ahmed, S.; Brock, N.; 1991
"A Study of Dynamic Stall Using Real Time Interferometry", *AIAA Paper 91-0007, 1991.*

Carr, L. W.; Platzer, M. F.; Chandrasekhara, M. S.; Ekaterineras, J.; 1990
"Experimental and Computational Studies of Dynamic Stall", *Numerical and Physical Aspects of Aerodynamic Flows, Editor T. Cebeci, Springer Verlag, 1990.*

Carr, L. W.; Platzer, M. F.; Chandrasekhara, M. S.; Ekaterinaris, J.; 1989
"Experimental and Computational Studies of Dynamic Stall." *Paper presented at the 4th Symposium on Numerical and Physical Aspects of Aerodynamic Flows, Long Beach, California, USA, January 16-19, 1989.*

Carr, L.; Chandrasekhara, M. S.; 1989
"Design and Development of a Compressible Dynamic Stall Facility." *AIAA Paper 89-0647, 1989.*

Carstens, V.; 1991a
"Calculation of the Unsteady Transonic 2D Cascade Flow for Aeroelastic Applications", *International Forum on Aeroelasticity and Structural Dynamics, Aachen, Germany, June 3-6, 1991.*

Carstens, V.; 1991b
"Communication during the Panel Discussion", *Sixth International Symposium on Unsteady Aerodynamics, Aeroacoustics and Aeroelasticity of Turbomachines and Propellers, September 15-19, University of Notre Dame, USA, 1991.*

Carta F. O.; 1984
"Private Communication"

Carta F. O.; 1982a
"Unsteady gapwise periodicity of oscillating cascaded airfoils", *ASME paper 82-GT-286, 1982.*

Carta F. O.; 1982b
"An experimental investigation of gapwise periodicity and unsteady aerodynamic response in an oscillating cascade (3 Volumes)", *NASA-CR 3513, 1982.*

Cedar, R. D.; Stow, P.; 1985a
"The addition of quasi three-dimensional terms into a finite element method for transonic turbomachinery blade-to-blade flows", *International Journal for Numerical Methods in Fluids, Vol. 5, pp. 101-114, 1985.*

Cedar, R. D.; Stow, P.; 1985b
"A compatible mixed design and analysis finite element method for the design of turbomachinery blades", *International Journal for Numerical Methods in Fluids, Vol. 5, pp. 331-345, 1985.*

Chandrasekhara, M. S.; Platzer, M. F.; 1991
"Compressibiltity effects on dynamic stall of oscillating airfoils: Final Report" *, NASA-CR-187870, 1991.*

Chandrasekhara, M. S.; Brydges, B. E.; 1990
"Amplitude Effects on Dynamic Stall of an Oscillating Airfoil." *AIAA Paper 90-0575, 1990.*

Chandrasekhara, M. S.; Carr, L.; 1989
"Flow Visualization Studies of the Mach Number Effects on the Dynamic Stall of an Oscillating Airfoil." *AIAA Paper 89-0023, 1989.*

Chen, Q.; Chen, J.; Fan, F.; 1989
Effect of Blade Mistuning and Coupled Disk-Blade on Cascade Flutter Boundaries", *Proceedings of the Fifth International Symposium on "Unsteady Aerodynamics*

and Aeroelasticity of Turbomachines and Propellers",
pp. 339-350, Beijing, China, September 18-21, 1989.

Chen, R.; Wei, X.; Zhou, S.; 1989
"Some Explorations on the Mechanism of Blade
Flutter Suppression by Porous Wall Casing",
*Proceedings of the Fifth International Symposium on
"Unsteady Aerodynamics and Aeroelasticity of
Turbomachines and Propellers", pp. 213-220, Beijing,
China, September 18-21, 1989.*

Chen, S.; 1989
"The Non.Synchronous Vibrations of the Shrouded
Blade Row Operating under Steam Condensation",
*Proceedings of the Fifth International Symposium on
"Unsteady Aerodynamics and Aeroelasticity of
Turbomachines and Propellers", pp. 441-458, Beijing,
China, September 18-21, 1989.*

Chi, R. M.; 1991
"An Unsteady Lifting Surface Theory for Ducted Fan
Blades",*ASME Paper 91-GT-131, 1991.*

Chiang, H.; Fleeter, S.; 1989a
"Oscillating Aerodynamics and Flutter of an
Aerodynamically Detuned Cascade in an
Incompressible Flow." *AIAA paper 89-0289, AIAA
27th Aerospace Sciences Meeting, January 9-12,
Reno, Nevada, 1989.*

Chiang, H.; Fleeter, S.; 1989b
"Oscillating Incompressible Aerodynamics of a Loaded
Airfoil Cascade", *AIAA Journal, Vol. 27, No. 4, pp.
446-454, 1989.*

Christiansen, J. P.; 1973
*Journal of Computational Physics, Vol. 13, pp. 363ff,
1973.*

Crawley, E. F.; Ducharme, E. H.; 1989
"Parametric Trends in the Flutter of Advanced
Turboprops." *ASME Paper 89-GT-280, 1989.*

Crawley, E. F.; 1984
"Aeroelastic Formulations for Turbomachines and
Propellers.", *Proceedings of the Third International
Symposium on Unsteady Aerodynamics of
Turbomachines and Propellers, Cambridge, UK,
September 1984, pp. 13-28.*

Currier, J.; Fung, K.-Y.; 1991
"An Analysis of the Onset of Dynamic Stall", *AIAA
Paper 91-0003, 1990.*

De Ruyck, J.; Hazarika, B.; Hirsch, C.; 1989
"Measurement of Velocity Profiles and Reynolds
Stresses on an Oscillating Airfoil", *AGARD
Conference Proceedings No. 468, "Unsteady
Aerodynamic Phenomena in Turbomachines", pp.
23.1-23.15, Luxembourg, August 28-30, 1989.*

Duan, S.; Zhou, S.; 1989
A Model of Small-Disturbance Wave in Large-Scale
Separation Zone Associated with Stall Flutter",
*Proceedings of the Fifth International Symposium on
"Unsteady Aerodynamics and Aeroelasticity of
Turbomachines and Propellers", pp. 206-212, Beijing,
China, September 18-21, 1989.*

Ezzat, A.; Fransson, T. H.; Jolles, F.; 1989a
"Steady-State and Time Dependent Aerodynamics in
an Annular Turbine Cascade Operating at High
Subsonic Mach Numbers." *AIAA paper 89-2941,*

*AIAA-ASME-SAE-ASEE 25th Joint Propulsion
Conference, July 10-12, Monterey, California, 1989.*

Ezzat, A.; Fransson, T. H.; Jolles, F.; 1989b
"Self-Started Blade Vibrations in an Annular Turbine
Cascade Operating at Transonic and Supersonic
Mach Numbers." *1989 ASME COGEN-TURBO
Symposium, IGTI Vol. 4, Nice, France, August 30-
September 1, 1989.*

Fleeter, S.; Hoyniak, D.; 1989
"Aeroelastic Detuning for Stability Enhancement of
Unstalled Supersonic Flutter", *International Journal of
Turbo and Jet-Engines, No. 6; pp. 17-26, 1989.*

Fransson, T. H.; 1990
"Analysis of Experimental Time-Dependent Blade
Surface Pressures from an Oscillating Turbine
Cascade with the Influence-Coefficient Technique",
ASME Paper 90-GT-225, 1990.

Fransson, T. H.; Pandolfi, M; 1986
"Numerical Investigation of Unsteady Compressible
Flow Through an Oscillating Cascade", *ASME Paper
86-GT-304, 1986.*

**Fujimoto, I.; Nagai, H.; Tanaka, H.; Hirano, T.; Ishii,
S.; 1989**
"Mistuning Effects on Fully Stalled Cascade Flutter",
*Proceedings of the Fifth International Symposium on
"Unsteady Aerodynamics and Aeroelasticity of
Turbomachines and Propellers", pp. 363-374, Beijing,
China, September 18-21, 1989.*

Gallus, H. E.; Kau, H.-P.; 1989
"Blade Loads Due to Unsteady Flow in
Turbomachinery Cascades", *Proceedings of the Fifth
International Symposium on "Unsteady Aerodynamics
and Aeroelasticity of Turbomachines and Propellers",
pp. 53-68, Beijing, China, September 18-21, 1989.*

Gallus, H. E.; Servaty, S.; 1987
*Proceedings of the Fourth International Symposium
on "Unsteady Aerodynamics and Aeroelasticity of
Turbomachines and Propellers", Aachen, Germany,
September, 1987.*

Gerolymos, G. A.; 1990a
"Implicit Euler Computations of Unsteady Flow in
Vibrating Cascades", *Submitted for publication, 1990.*

Gerolymos, G. A.; Blin, E.; Quinio, H.; 1990b
"Comparison of Inviscid Computations with Theory
and Experiment in Vibrating Transonic Compressor
Cascades", *ASME Paper 90-GT-??, 1990.*

Gerolymos, G. A.; 1988a
"Periodicity, Superposition and 3D Effects in
Supersonic Flutter Aerodynamics." *ASME Paper 88-
GT-136, 1988.*

Gerolymos, G. A.; 1988b
"Numerical Investigation of the 3D Unsteady Euler
Equations for Flutter Analysis of Axial Flow
Compressors." *ASME Paper 88-GT-255, 1988.*

Gerolymos, G. A.; 1988c
"Numerical Integration of the Blade-to-Blade Surface
Euler Equations in Vibrating Cascades", *AIAA Journal,
Vol. 26, No. 12, pp. 1483-1492, 1988.*

Giles, M.; Haimes, R.; 1991
"Validation of a Numerical Method for Unsteady Flow
Calculations",*ASME Paper 91-GT-271, 1991.*

Giles, M. B.; 1989
"Non-Reflecting Boundary Conditions For Euler Equation Calculations", *AIAA Paper 89-1942-CP, 1989.*

Giles, M. B.; 1987
"Calculations of Unsteady Wake/Rotor Interactions", *AIAA Paper 87-0006*

Giordano, D. D.; Fleeter, S.; 1990
"Investigation of Oscillating Airfoil Shock Phenomena", *AIAA Paper 90-0695, 1990.*

Goldstein M. F.; Braun W.; Adamczyk J. J.; 1977
"Unsteady flow in a supersonic cascade with strong in-passage shocks" *J. Fluid Mechanics, Vol. 83, No. 3, pp. 569-604, 1977.*

Hall, K. C.; Clark, W. S.; 1991
"Prediction of Unsteady Aerodynamic Loads in Cascades Using the Linearized Euler Equations on Deforming Grids", *AIAA Paper 91-3378.*

Hall, K. C.; Crawley, E. F.; 1989
"Calculation of Unsteady Flows in Turbomachinery Using the Linearized Euler Equations." *AIAA Journal, Vol. 27, No. 6, pp. 777-787, 1989.*

Hanamura, Y.; Yamaguchi, K.; 1988
"An Experimental Investigation on the Flutter of the Cascade of Turbomachinery in the Transonic Flow." *Journal of the Faculty of Engineering, The University of Tokyo (B), Vol. XXXIX, No. 3, pp. 311-338, 1988.*

Hanamura, Y.; Tanaka, H.; Yamaguchi, Y.; 1980
"A Simplified Method to Measure Unsteady Forces Acting on the Vibrating Blades in a Cascade", *Bulletin of the JSME, Vol. 23, No. 180, 1980.*

He, L.; 1989
"An Euler Solution for Unsteady Flows Around Oscillating Blades." *ASME Paper 89-GT-279, 1989.*

He, L.; Denton, J. D.; 1991a
"An Experiment on Unsteady Flow Over an Oscillating Airfoil", *ASME Paper 91-GT-181, 1991.*

He, L.; Denton, J. D.; 1991b
"Inviscid-Viscous Coupled Solution for Unsteady Flows Through Vibrating Blades - Part 1: Description of the Method", *ASME Paper 91-GT-125, 1991.*

He, L.; Denton, J. D.; 1991c
"Inviscid-Viscous Coupled Solution for Unsteady Flows Through Vibrating Blades - Part 2: Computational Results", *ASME Paper 91-GT-126, 1991.*

Hoyniak, D.; 1991
"Communication during the Panel Discussion", *Sixth International Symposium on Unsteady Aerodynamics, Aeroacoustics and Aeroelasticity of Turbomachines and Propellers, September 15-19, University of Notre Dame, USA, 1991.*

Huff, D. L.; 1991
"Communication during the Panel Discussion", *Sixth International Symposium on Unsteady Aerodynamics, Aeroacoustics and Aeroelasticity of Turbomachines and Propellers, September 15-19, University of Notre Dame, USA, 1991.*

Huff, D. L.; Swafford, T. W.; Reddy, T. S. R.; 1991
"Euler Flow Predictions for an Oscillating Cascade Using a High Resolution Wave-Split Scheme", *ASME Paper 91-GT-198, 1991.*

Huff, D. L.; Reddy, T. S. R.; 1989
"Numerical Analysis of Supersonic Flow Through Oscillating Cascade Sections by Using a Deforming Grid", *AIAA paper 89-2805, AIAA/ASME/SAE/ASEE 25th Joint Propulsion Conference, Monterey, California, July 10-13, 1989.*

Huff, D. L.; 1989
"Numerical Analysis of Flow Through Oscillating Cascade Sections", *AAA paper 89-0437, AIAA 27th Aerospace Sciences Meeting, January 9-12, Reno, Nevada, 1989.*

Imanari, K.; Kaji, S.; 1989
"Unsteady Aerodynamic Forces Acting on Vibrating Cascade Blades in a Three-Dimensional Flow Field", *JSME International Journal, Series II, Vol. 32, No. 1, pp. 57-62, 1989.*

Jacquet-Richardet, G.; 1990
"Flottement aeroélastique des aubes a faible élancement: application a une grille annulaire.", *Thèse No. 90 ISAL 0025, INSA Lyon, France, 30 mars 1990.*

Jacquet-Richardet, G.; Henry, R.; 1990
"Flutter Analysis of Plate-Like Rotating Blades", *3ème Congès International sur La Dynamique Des Rotors, Editeurs M. Lalanne, R. Henry, pp. 171-176, September 10-12, Lyon, France, 1990*

Jang, H. M.; Ekaterinaris, J. A.; Platzer, M. F.; Cebeci, T.; 1990
"Essential Ingredients for the Computation of Steady and Unsteady Boundary Layers", *ASME Paper 90-GT-160, 1990.*

Jennions, I. K.; Stow, P.; 1984
"A quasi three-dimensional turbomachinery blade design system. Part 1: Through-flow analysis; Part 2: Computerized system", *ASME Papers 84-GT-26 and 84-GT-27, 1984.*

Joubert, H.; 1984
"Supersonic Flutter in Axial Flow Compressors", *Proceedings of the Symposium on Unsteady Aerodynamics in Turbomachines and Propellers, pp. 231-254, Cambridge, United Kingdom, September 24-27, 1984.*

Kaminer, A. A.; Chervonenko, A. G.; 1989
"Interaction between Vibrating Cascade Blades and Shear Flow", *Proceedings of the Fifth International Symposium on "Unsteady Aerodynamics and Aeroelasticity of Turbomachines and Propellers", pp. 254-266, Beijing, China, September 18-21, 1989.*

Kau, H. P.; Gallus, H. E.; 1989
"Numerical Investigation of Unsteady Flow in Oscillating Turbine and Compressor Cascades", *AGARD Conference Proceedings No. 468, "Unsteady Aerodynamic Phenomena in Turbomachines", pp. 2.1-2.11, Luxembourg, August 28-30, 1989.*

Kennedy, J. L., Marsden, D. M.; 1976
Canadian Aeronautical and Space Journal, Vol. 22, pp. 243ff, 1976.

Kielb R. E.; Ramsey J. K.; 1988

"Flutter of a Fan Blade in Supersonic Axial Flow", *ASME paper No. 88-GT-78, 1988.*

Kiessling, F.; Hennings, M.; 1991
"New Test Facility at DFVLR-Göttingen", *Private Communication, 1991.*

Klose, A.; Heinig, K.; 1989
"A Comparison of Flutter Calculations Based on Eigenvalue and Energy Method", *AGARD Conference Proceedings No. 468, "Unsteady Aerodynamic Phenomena in Turbomachines", pp. 1.1-1.9, Luxembourg, August 28-30, 1989.*

Kobayakawa, M.; Ogushi, M.; 1989
"Flow Field Around an Oscillating Cascade", *Proceedings of the Fifth International Symposium on "Unsteady Aerodynamics and Aeroelasticity of Turbomachines and Propellers", pp. 86-92, Beijing, China, September 18-21, 1989.*

Kobayashi, H.; 1989
"Annular Cascade Study of Low Back-Pressure Supersonic Fan Blade Flutter." *ASME Paper 89-GT-297, 1989.*

Kobayashi H.; 1988
"Effect of Shock Wave Movement on Aerodynamic Instability of Annular Cascade Oscillating in Transonic Flow."*ASME paper No. 88-GT-187, 1988.*

Kodama, H.; Namba, M.; 1991
"Unsteady Lifting Surface Theory for a Rotating Transonic Cascade of Swept Blades",*ASME Paper 91-GT-178, 1991.*

Kodama, H.; Namba, M.; 1990
"Unsteady Lifting Surface Theory for a Rotating Cascade of Swept Blades", *Journal of Turbomachinery, Vol. 112, July, pp. 411-417, 1991.*

Koller, F.; Kluwick, A.; 1989
"Asymptotic Analysisi of Transonic Flow Through Oscillating Cascades", *AGARD Conference Proceedings No. 468, "Unsteady Aerodynamic Phenomena in Turbomachines", pp. 16.1-16.10, Luxembourg, August 28-30, 1989.*

Kovats, S.; 1990
"Predicting aerodynamic damping and stability of low-pressure turbine blades using the influence coefficient technique", *Proceedings of ASME COGEN-TURBO V, Budapest, September 3-6, 1991.*

Krainer, A.; 1988
"A Numerical Method for Computing Unsteady 2-D Boundary Layer Flows." *Report, Naval Postgraduate School, Monterey, California, February 1988.*

Ku, C. C.; Williams, M. H.; 1990
"Three Dimensional Full Potential Method for the Aeroelastic Modeling of Propfans", *AIAA Paper 90-1120-CP.*

Kurkov, A. P.; Mehmed, O.; 1991
"Optical Measurements of Unducted Fan Flutter", *ASME Paper 91-GT-19, 1991.*

Lane F.; 1957
"Supersonic Flow Past an Oscillating Cascade with Supersonic Leading-Edge Locus" *Journal of the Aeronautical Sciences, Vol. 24, pp. 65-66, 1957.*

Lee, Y-T.; Bein, T. W.; Feng, J. Z.; Merkle, C. L.; 1991

"Unsteady Rotor Dynamics in Cascade", *ASME Paper 91-GT-147, 1991.*

Li, C.-C.; Messiter, A. F.; van Leer, B.; 1990
"Unsteady Transonic Cascade Flow with In-Passage Shock Wave", *AIAA Journal, Vol. 28, No. 6, pp. 1135-1138, 1990.*

Liang, S.-M.; Tsai, C.-J.; Ho, C.-K.; 1991
"Numerical Investigation of Unsteady Transonic Nozzle Flows", *Submitted for publication in AIAA Journal, 1991.*

Liou, M. S.; Adamson, T. C. Jr.; 1977
"Unsteady Transonic Flow in Two-Dimensional Channels.", *Report UM 014534-F, University of Michigan, USA, June 1977.*

Liu, G.-L.; 1989
"Variational Formulation of 2-D Unsteady Transonic Aerodynamics of Oscillating Cascades", *Proceedings of the Fifth International Symposium on "Unsteady Aerodynamics and Aeroelasticity of Turbomachines and Propellers", pp. 76-85, Beijing, China, September 18-21, 1989.*

Liu, Q.; Shen, M.; Zhang, Q.; 1989
"A New Method for High Speed Propeller Flutter Prediction", *Proceedings of the Fifth International Symposium on "Unsteady Aerodynamics and Aeroelasticity of Turbomachines and Propellers", pp. 32-42, Beijing, China, September 18-21, 1989.*

Mehmed, O.; Murthy, D. V.; 1991
"Experimental Investigation of Propfan Aeroelastic Response in Off-Axis Flow with Mistuning", *Journal of Propulsion, Vol. 7, No. 1, pp. 90-98, 1991.*

Molls, F.; 1985
NASA Contractor Report 3925, September 1985.

Namba, M.; Li, P.; 1990
"Double linearization theory for a rotating supersonic annular cascade of oscillating blades", *Memoirs of Kyushu University, Japan, Vol. 50, September, pp. 309-340, 1990.*

Namba, M.; Toshimitsu, K.; 1990
"Effects of Chordwise Displacement and Nonrigid Section Deformation on Unsteady Aerodynamic Response of Subsonic and Supersonic Oscillating Cascades", *ASME Paper 90-GT-246, 1990.*

Namba, M.; Toshimitsu, K.; Li, P.; 1989
"Mean Loading Effects on Flutter of Subsonic Rotating Annular Cascade", *Proceedings of the Fifth International Symposium on "Unsteady Aerodynamics and Aeroelasticity of Turbomachines and Propellers", pp. 21-31, Beijing, China, September 18-21, 1989.*

Namba, M.; Toshimitsu, K.; 1988
"Double Linearization Theory Applied to Unsteady Analysis of Three-Dimensional Subsonic Cascade Vibrating with Spanwise Nonuniform Mean Loading" (In Japanese), *Trans. Japan Soc. Mech. Eng. Ser. B, Vol. 54, pp. 1073-1080, 1988.*

Newman, S. P.; Stow, P.; 1985
"Semi-inverse mode boundary layer coupling", *Proceedings of the conference on Numerical Methods ifor Fluid Dynamicss, Reading, United Kingdom, 1985.*

Newton, S., Whitehead, D. S.; 1985

"A finite element method for the solution of two-dimensional transonic and supersonic flows", *International Journal for Numerical Methods in Fluids, Vol. 5, pp. 115-132, 1985.*

Pan, T.; Lu, Y.; Yan, W.; Wu, X.; Editors; 1989
"Unsteady Aerodynamics and Aeroelasticity of Turbomachines and Propellers", *Proceedings of the Symposium held in Beijing, China, on September 18-21, 1989.*

Perumal, P. V. K.; Sisto, F.; 1974
"Lift and Moment Prediction for an Oscillating Airfoil with a Moving Separation Point", *Journal of Engineering for Power, Transactions of the ASME, Vol. 96, pp. 372-382, 1974*

Platzer, M. F.; Carta, F. O.; Editors; 1987
"AGARD Manual on Aeroelasticity in Axial-Flow Turbomachines. Volume 1: Unsteady Turbomachinery Aerodynamics", *AGARD-AG-298, Vol. 1, 1987.*

Platzer, M. F.; Carta, F. O.; Editors; 1988
"AGARD Manual on Aeroelasticity in Axial-Flow Turbomachines. Volume 2: Structural Dynamics and Aeroelasticity", *AGARD-AG-298, Vol. 2, 1988.*

Quiniou, H.; 1989
"Etudes théoriques d'aéroélasticité dans les compresseurs aéronautiques", *Revue Française de Mécanique No. 1, pp. 61-71, 1989.*

Ramsey, J. K.; 1991
"Influence of Thickness and Camber on the Aeroelastic Stability of Supersonic Throughflow Fans", *Journal of Propulsion and Power, Vo. 7, No. 3, pp. 404-411, May-June, 1991*

Ramsey, J. K.; 1989
"Influence of Thickness and Camber on the Aeroelastic Stability of Supersonic Throughflow Fans: An Engineering Approach", *NASA TM 101949, 1989.*

Ramsey, J. K.; Kielb, R. E.; 1987
"A Computer Program for Calculating Unsteady Aerodynamic Coefficients for Cascades in Supersonic Axial Flow", *NASA TM 100204, 1987.*

Rao, B. M.; Jones, W. F.; 1976
"Unsteady Airloads for a Cascade of Staggered Blades in Subsonic Flow" *Unsteady Phenomena in Turbomachinery, AGARD-CP-177, 1976.*

Reddy, T. S. R.; Bakhle, M. A.; Huff, D. L.; Swafford, T. W.; 1991
"Flutter Analysis of Cascades Using a Two Dimensional Euler Solver", *AIAA Paper 91-1681, 1991.*

Riffel R. E.; Rohtrock M. D.; 1980
"Experimental determination of unsteady blade element aerodynamics in torsion mode cascade, final report", *NASA CR-159831, Vol. 1, 1980.*

Saren, V. E.; 1989
"Asymptotic Theory for High-Solidity Cascade of Unsteady Incompressible Fluid", *Proceedings of the Fifth International Symposium on "Unsteady Aerodynamics and Aeroelasticity of Turbomachines and Propellers", pp. 178-196, Beijing, China, September 18-21, 1989.*

Schläfli, D.; 1989
"Experimentelle Untersuchung der instationären Strömung in Oszillierenden Ringgittern" *PH. D. Thesis No. 800, EPF-Lausanne, 1989.*

Schroeder, L. M.; Fleeter, S.; 1989
"Viscous Aerodynamic Analysis of an Oscillating Flat-Plate Airfoil" *AIAA Journal, Vol. 27, No. 8, August, pp. 1021-1022, 1989.*

Servaty, S. Gallus, H. E.; Kau, H.-P.; 1987
"Computation of Aerodynamic Blade Loads Due to Wake Influence and Aerodynamic Damping of Turbine and Compressor Cascades", *Proceedings of the Fourth International Symposium on "Unsteady Aerodynamics and Aeroelasticity of Turbomachines and Propellers", Aachen, West Germany, September 6-10, 1987.*

Shaw, L.M., Boldman, D.R., Buggele, A.E., Buffum, D.H. ; 1985
"Unsteady Pressure Measurements on a Biconvex Airfoil in a Transonic Oscillating Cascade", *ASME paper 85-GT-212, 1985.*

Sidén, L. D. G.; 1991a
"Numerical Simulation of Unsteady Viscous Compressible Flows Applied to Blade Flutter Analysis", *ASME Paper 91-GT-203, 1991.*

Sidén, L. D. G.; Albråten, P. J; 1991b
"A Flutter Study of a Two-Dimensional Transonic Fan Blade Configuration", *10th International Symposium on Air Breathing Engines, September 1-6, Nothingham, England, 1991.*

Sidén, L. D. G.; 1991c
"Numerical Simulation of Viscous Compressible Flows Applied to Turbomachinery Blade Flutter", *Ph. D. Thesis, Chalmers University of Technology, Gothenbourg, Sweden, 1991.*

Sidén, L. D. G.; 1990
"Unsteady Navier Stokes Solver For The Simulation Of Compressor Flutter In Turbomachines", *Department of Turbomachinery, Chalmers University of Technology, Gothenbourg, Sweden, 1990.*

Sidén, L. D. G.; Dawes, W. N.; Albråten, P. J.; 1989a
"Numerical Simulation of the Two-Dimensional Viscous Compressible Flow in Blade Cascades Using a Solution-Adaptive Unstructured Mesh", *ASME Paper 89-GT-211, 1989, and Journal of Turbomachinery, Vol. 112, July, pp. 311-319, 1990.*

Sidén, L. D. G.; Dawes, W. N.; Albråten, P. J.; 1989b
"A Solution Adaptive Finite Element Method Applied to Two-Dimensional Unsteady Viscous Compressible Cascade Flow", *9th International Symposium on Air Breathing Engines, pp. 1169-1177, September 3-8, Athens, Greece, 1989.*

Sisto, F.; Thangam, S.; Abdel-Rahim, A.; 1990
"Computational Prediction of Stall Flutter in Cascaded Airfoils", *AIAA Paper 90-1116-CP, 1990.*

Sisto, F.; Wu, W.; Thangam, S.; Jonnavithula, S.; 1989
"Computational Aerodynamics of Oscillating Cascades with the Evolution of Stall", *AIAA Journal, Vol. 27, No. 4, pp. 462-471, 1989.*

Smith, T. E.; Kadambi, J. R.; 1991
"The Effect of Steady Aerodynamic Loading on the Flutter Stability of Turbomachinery Blading",*ASME Paper 91-GT-130, 1991.*

Smith, T. E.; 1990
"Aeroelastic Stability Analysis of a High-Energy Turbine Blade", *AIAA Paper 90-2351, 1990.*

Smith S. N.; 1972
"Discrete frequency sound generation in axial flow turbomachines", *Reports & Memoranda , No. 3709, March 1972.*

Soize, C.; 1992
"Couplage fort fluide parfait couche limite pour des profils à bord d'attaque aigu. II: Cas 2D instationnaire pour les profils isolés et les grilles rectilignes", *Recherche Aérospatiale, printemps (?) 1992.*

Song, Z.-H.; Feng, Y.-C.; Wang, Y.-W.; 1989
"The Experimental Research in the Flutter Characteristics of the BF-1 Series of Rotors", *Proceedings of the Fifth International Symposium on "Unsteady Aerodynamics and Aeroelasticity of Turbomachines and Propellers", pp. 301-311, Beijing, China, September 18-21, 1989.*

Spara, K.; Fleeter, S.; 1990
"Aerodynamic Detuning for Control of Supersonic Rotor Forced Response", *AIAA Paper 90-2018, 1990.*

Spara, K. M.; Fleeter, S.; 1989
"Supersonic Turbomachine Rotor Flutter Control by Aerodynamic Detuning", *AIAA paper 89-2685, AIAA/ASME/SAE/ASEE 25th Joint Propulsion Conference, Monterey, California, July 10-13, 1989.*

Stecco, S. S.; Marchi, L.; 1989
"A Linear Computer Code to Determine Aeroelastic Stability in Airfoil Cascades at Unsteady Flow Conditions.", *1989 ASME COGEN-TURBO, 3rd International Symposium, IGTI-ASME Vol. 4, pp. 497-502, 1989.*

Stecco, S. S.; Marchi, L.; 1988
"A Linear Computer Code to Determine Aeroelastic Stability in Airfoil Cascades at Unsteady Flow Conditions.", *ASME FED-Vol. 66, G00466, Advances and Application in Computational Fluid Dynamics, Proceedings of the Winter Annual Meeting of the ASME, Chicago, Illinois, Nov. 27-Dec. 2, 1988.*

Stecco, S. S.; Marchi, L.; Lazzati, P.; Michelotti, P. Solari, A.; Ursino, G.; Rebizzo, A; 1988
"Commenti e confronti su alcuni risultati sperimentale relative all'instabilità delle palettature", *Proceedings, Genoa Meeting on Turbomachinery, Genoa, Italy, pp. 359-376, 1988.*

Széchényi, E.; 1991
"Communication during the Panel Discussion", *Sixth International Symposium on Unsteady Aerodynamics, Aeroacoustics and Aeroelasticity of Turbomachines and Propellers, September 15-19, University of Notre Dame, USA, 1991.*

Széchényi, E.; Cafarelli, I.; 1989
"Le flottement des aubes de compresseur: Une certaine compréhension grâce à des essais en soufflerie."

Revue Française de Mécanique No. 1, pp. 73-87, 1989.

Széchényi E.; 1984
"Private Communication"

Széchényi E.; Finas R.; 1981a
"Aeroelastic testing in a straight cascade wind tunnel", *Communication de L'ITA/ EPFL, No. 10, pp. 143-149,1981.*

Széchényi E.; Girault J.-Ph.; 1981b
"A study of compressor blade stall flutter in a straight cascade wind-tunnel", *Communication de L'ITA/ EPFL, No. 10, pp. 163-169,1981.*

Toshimitsu, K.; Namba, M.; Li, P.; 1990
"Double linearization theory for a rotating subsonic annular cascade of oscillating blades; Part 1: Mathematical expressions of disturbance flow field; Part II: Numerical study of unsteady aerodynamic forces", *Memoirs of Kyushu University, Japan, Vol. 50, June, pp. 161-199, 1990.*

Toshimitsu, K.; Namba, M.; 1989
"Application of the double linearization theory to three-dimensional subsonic and supersonic cascade flutter", *9th International Symposium on Air Breathing Engines, pp. 1169-1177, September 3-8, Athens, Greece, 1989.*

Topp, D. A.; Fleeter, S.; 1986
"Splitter Blades as an Aeroelastic Detuning Mechanism for Unstalled Supersonic Flutter of Turbomachine Rotors." *ASME Paper 86-GT-99, 1986.*

Usab, W. J.; Verdon, J. M.; 1990
"Advances in the Numerical Analysis of Linearized Unsteady Cascade Flows", *ASME Paper 90-GT-11, 1990.*

Verdon, J. M.; 1990
"Linearized Unsteady Aerodynamics for Turbomachinery Aeroelastic Applications", *AIAA Paper 90-2355, 1990.*

Verdon, J. M.; 1989a
"The Unsteady Flow in the Far Field of an Isolated Blade Row", *Journal of Fluids and Structures, No. 3, pp. 123-149, 1989.*

Verdon, J. M.; 1989b
"The Unsteady Aerodynamic Response to Arbitrary Modes of Blade Motion", *Journal of Fluids and Structures, No. 3, pp. 255-274, 1989.*

Verdon, J. M.; 1987a
"Linearized Unsteady Aerodynamic Theory"", *AGARD Manual on Aeroelasticity in Axial-Flow Turbomachines, Vol. 1, Eds. M. F. Platzer and F. O. Carta, AGARD-AG-298, chapter 2, March 1987.*

Verdon, J. M.; 1987b
"Unsteady Aerodynamics of Blade Rows", *In "Transonic Unsteady Aerodynamics and Aeroelasticity", Proceedings of a symposium held at NASA Langley Research Center, May 20-22, 1987, NASA Conference Publication 3022, Editor: S. R. Bland.*

Verdon, J. M.; 1987c
"Private communication, December 8, 1987"

Verdon, J. M.; 1986

"Unsteady Aerodynamics of Blade Rows", *Tenth U.S. National Congress of Applied Mechanics, June 16-20, 1986.*

Verdon J. M.; Usab, W. J.; 1985
"Application of a Linearized Unsteady Aerodynamic Analysis to Standard Cascade Configurations", *NASA contracter report, prepared for NASA Lewis research center, 1985.*

Verdon J. M.; Caspar J. R.; 1984
"A linear aerodynamic analysis for unsteady transonic cascades", *NASA contracter report, prepared for NASA Lewis research center, under contract NAS3-23696,1984.*

Verdon J. M.; Caspar J. R.; 1982
"Development of a linear unsteady aerodynamic analysis for finite-deflection subsonic cascades", *AIAA journal, Vol. 20, No. 9, pp. 1259-1267, 1982.*

Verdon J. M.; 1977a
"Further developments in the aerodynamic analysis of unsteady supersonic cascades (Part I of 2)", *ASME paper 77-GT-44, 1977.*

Verdon J. M.; 1977b
"Further developments in the aerodynamic analysis of unsteady supersonic cascades (Part II of 2)", *ASME paper 77-GT-45, 1977.*

Verdon J. M.; McCune J. E.; 1975
"Unsteady supersonic cascade in subsonic axial flow", *AIAA journal, Vol. 13, No. 2, pp. 193-201, 1975.*

Verdon J. M.; 1973
"The unsteady aerodynamics of a finite supersonic cascade with subsonic axial flow.", *J. of applied mechanics, Vol. 40, No. 3, pp. 667-671, 1973.*

Watanabe, T.; Kaji, S.; 1989
"Theoretical Study on the Unsteady Aerodynamic Characteristics of an Oscillating Cascade with Tip Clearance (In the Case of a Nonloaded Cascade)", *JSME International Journal, Series II, Vol. 32, No. 3, 1989.*

Watanabe, T.; Kaji, S.; 1988
"Experimental Study on Unsteady Aerodynamic Characteristics of an Oscillating Cascade with Tip Clearance", *JSME International Journal, Series II, Vol. 31, No. 4, pp. 660-667, 1988*

Whitehead, D. S.; 1990
"A Finite-Element Solution of Unsteady Two-Dimensional Flow in Cascades", *International Journal for Numerical Methods in Fluids, Vol. 10, pp. 13-34, 1990.*

Whitehead, D. S.; 1987
"Flutter of Turbine Blades", *Proceedings of the Fourth Symposium on Unsteady Aerodynamics and Aeroelasticity of Turbomachines and Propellers, pp. 437-452, Aachen, West Germany, September 6-10, 1987.*

Whitehead D. S.; 1962
"Force and moment coefficients for vibrating aerofoils in cascade." *R&M London, No. 3254, 1962.*

Wu, J.-C.; 1988
"A Study of Unsteady Turbulent Flow Past Airfoils", *Ph. D. Thesis, Georgia Institute of Technology, 1988.*

Yamamoto, K.; Tanida, Y.; 1989
"Self-Excited Oscillation of Transonic Flow Around an Airfoil in Two-Dimensional Channel." *ASME Paper 89-GT-58, 1989.*

Yamane, T.; Friedmann, P. P.; 1989
"Aeroelastic Tailoring Analysisi for Preliminary Design of Advanced Turbo Propellers with Composite Blades", *Proceedings of the Fifth International Symposium on "Unsteady Aerodynamics and Aeroelasticity of Turbomachines and Propellers", pp. 323-338, Beijing, China, September 18-21, 1989.*

Yang, X. D.; Feng, Y. C.; 1989
"The Interaction Between Distortion of Inlet Flow and Blade Stall in Axial-Flow Compressor", *Proceedings of the Fifth International Symposium on "Unsteady Aerodynamics and Aeroelasticity of Turbomachines and Propellers", pp. 167-177, Beijing, China, September 18-21, 1989.*

Yang. X. D.; Tao, D. P.; Zhou, S.; 1989
"A Method for Predicting Stall Flutter under Variable Interblade Phase Angle Along Rotating Direction", *Proceedings of the Fifth International Symposium on "Unsteady Aerodynamics and Aeroelasticity of Turbomachines and Propellers", pp. 43-52, Beijing, China, September 18-21, 1989.*

Yang, K.-C.; Yamasaki, N.; Namba, M.; 1989
"Finite Element Method for Unsteady Three-Dimensional Subsonic Flows through a Cascade Oscillating with Steady Loading", *Trans. Japan Soc. Aeros. Space Sci., Vol. 32, No. 96, August, pp. 51-66, 1989.*

Yue, J.; Kong, R.-L.; Song, Z.-H.; 1989
"The Research of Blade Flutter Characteristics under Quasi-Three Dimensional Unsteady Aerodynamics Load", *Proceedings of the Fifth International Symposium on "Unsteady Aerodynamics and Aeroelasticity of Turbomachines and Propellers", pp. 351-362, Beijing, China, September 18-21, 1989.*

Updated report on
"Standard Configurations for Unsteady Flow Through Vibrating Axial-Flow Turbomachine-Cascades"

Status as of July 1991

Compiled by

T. H. Fransson and J. M. Verdon

Appendices:

A1: Introduction to the Prediction Models Used

A2: Key to read the input files for the plot program "AEROEL"

A3: Listing of all values used on the plots
(these can be obtained on a floppy disk upon request)

A4: Computer plots of the results in the study

Updated report on
"Standard Configurations for Unsteady Flow Through Vibrating Axial-Flow Turbomachine-Cascades"

Status as of July 1991

Compiled by

T. H. Fransson and J. M. Verdon

Appendix A1: Introduction to the Prediction Models Used

INTRODUCTION

Several prediction models have been applied to the standard configurations during the years. The ones that are included in the present report are identified in Table A1.1. A brief introduction to each of the models are given below, whereas the reader is referred to the different articles mentioned in the text for details.

Method	Name/Affiliation	Stand. Config. Computed
1	Smith+Whitehead/ Cambridge University	1, 2, 5, 8,10
2	D. S. Whitehead/ Cambridge University	5, 8, 9, 10
3	J. M. Verdon/ United Technologies Research Center	1, 5, 8, 9, 10
4	M. Atassi/ University of Notre Dame	1
5	P. Salaün ONERA	1, 7, 8
6	S. Zhou/ Beijing Institute of Aeronautics and Astronautics	1, 2, 5
7	S. Newton Rolls Royce, plc	1, 4, 7, 8
8	V. Carstens DFVLR-AVA	1
9	F. Molls/ NASA Lewis Research Center	8
10	S. Kaji University of Tokyo	6
14	J. M. R. Graham Imperial College	1
18	H. Joubert SNECMA	7
19	M. Namba Kushuy University	6, 8
20	L. He University of Cambridge	4
21	L. He University of Cambridge	5, 7
22	K. Hall Duke University	10
23	D. Huff NASA Lewis	5, 10
24	H. E. Gallus Technical University, Aachen	4
25	V. Carstens DLR-Göttingen	4, 10
26	D. Huff NASA Lewis	10
27	E. Széchényi ONERA	5

Table A1.1: *Aeroelastic Prediction Models*

METHOD 1:
LINSUB (Courtesy of D. S. Whitehead, 1985)

The program calculates the unsteady two-dimensional linearized subsonic flow in cascades in traveling wave formulation, using the theory published by Smith [1972]. The blades are assumed to be flat plates operating at zero incidence.

Both the pressure jump and lift and moment coefficients are computed for different options:
- Translational vibration of the blades normal to their chord
- Torsional vibration of the blades about the origin at the leading edge.
- Sinusoidal wakes shed from some obstructions upstream, which move relative to the cascade in question.
- Incoming acoustic waves, coming from downstream
- Incoming acoustic waves, coming from upstream.

Furthermore, the condition of acoustic resonance is calculated.

METHOD 2:
Finite Element Method (FINSUP) (Courtesy of D. S. Whitehead, 1985)

The numerical field method program has three sections: mesh generation, analysis of steady flow, and analysis of unsteady flow. The mesh generation and analysis of steady flow have been described by Whitehead and Newton [1985]. The analysis of unsteady flow has been described by Whitehead [1990].

A typical mesh is composed of triangular finite elements covering a strip, one blade spacing high, with the blade in the middle. The fluid is assumed to be a perfect gas with no viscosity or thermal conductivity, and the flow is assumed to be adiabatic, reversible and irrotational, so the equations are those for a velocity potential. The potential is continuous, except for a jump across the wake. In order to calculate in regions of supersonic flow it is necessary to use "upwind" densities; that means that instead of taking the density at the element under consideration, the density is taken from the neighboring element in the most nearly upwind direction. This device stabilizes the computation in supersonic flow, but is unnecessary in subsonic flow. Weak shock waves are well simulated, but are "potential" since there is no entropy increase across the shock, and they are smeared over a few elements. The flow is matched to a linearized solution at the inlet and outlet faces of the computational domain, and is arranged to repeat between corresponding points on the top and bottom faces. The conditions specified to the program are effectively the inlet circumferential velocity and the jump in potential between the bottom left and the

bottom right corners of the domain. This choice of input conditions uniquely specifies the location of a shock in a cascade of flat plates at zero incidence, which no specification of flow conditions at either inlet or outlet can achieve. The non-linear equations are then solved by the Newton-Raphson technique. Convergence is usually achieved in three or four iterations, although up to about twelve may be necessary in difficult cases with supersonic inlet velocities. The nodes are numbered in such a way as to minimize the bandwidth of the dividing matrix at each iteration, so the method is fast. Good agreement with other methods of calculating steady transonic cascade flow in cascades has been demonstrated.

The program then goes on to the third stage in which small unsteady perturbations of the steady flow due to vibration of the blades is analyzed.

Solid body motion of the blades is assumed, either in bending or torsion. The unsteady calculation is therefore similar to one more iteration of the steady calculation, except that the potential perturbation is complex, and the boundary conditions are different. Again the flow at the inlet and exit faces is matched to a linearized solution, which includes propagating or decaying acoustic waves and in the downstream flow the effect of the unsteady wake shed from the trailing edge. The repeat condition between corresponding points on the top and bottom surfaces is arranged to give the required phase difference between neighboring blades. It is again necessary to use upwind densities in regions of supersonic flow in order to stabilize the calculation. A difficulty arises due to the term

$$(\vec{r} \cdot \Delta \vec{v}) \cdot \vec{n} \qquad \qquad (A1.1)$$

for the boundary condition at the blade surface. A modified perturbation potential is defined by

$$\qquad \qquad (A1.2)$$

where r is given by

$$\vec{r} = \vec{h} + \vec{\alpha} \times \vec{R} \qquad \qquad (A1.3)$$

and this equation is now extended over the whole domain of calculation, and not just at the blade surface. This device gets rid of the awkward term in the boundary condition at the blade surface, and also eliminates a similar awkward term in the calculation of the pressure perturbation at the surface. The unsteady pressure perturbations at the surface are then integrated to give the axial and circumferential blade forces and the moment.

METHOD 3:
Linearized Unsteady Aerodynamic Analyses (LINFLO) (Courtesy of J. M. Verdon, 1985)

The isentropic and irrotational flow of a perfect gas through a two-dimensional cascade of vibrating airfoils is considered. The blades are undergoing identical harmonic motions at frequency ω, but with a constant phase angle σ between the motions of adjacent blades. It is assumed that the flow remains attached to the blade surfaces and that the blade motion is the only source of unsteady excitation.

The flow through the cascade is thus governed by the field equations, written in form of the time-dependent velocity potential [Verdon and Usab, 1985]. In addition to the field equations, the flow must be tangential to the moving blade surfaces and acoustic waves must either attenuate or propagate away from or parallel to the blade row in the far field. Finally, we also require that the mass and tangential momentum be conserved across shocks and that pressure and the normal component of the fluid velocity be continuous across the vortex-sheet unsteady wakes which depart from the blade trailing edges and extend downstream.

In order to limit the computing resources required to solve the equation system, a small-unsteady-disturbance assumption is involved. Thus, the blades are assumed to undergo small-amplitude unsteady motions around an otherwise steady flow. The resulting first-order or linearized unsteady flow equation is solved subject to both boundary conditions at the mean positions of the blade, shock and wake surfaces and requirements on the behavior of the unsteady disturbances far upstream and downstream from the blade row.

Moreover, because of the cascade geometry and the assumed form of the blade motion, the steady and linearized unsteady flows must exhibit blade-to-blade periodicity. Thus, the numerical resolution of the steady and the linearized unsteady flow equations can be restricted to a single extended blade-passage region of the cascade.

METHOD 4:
Aerodynamic Theory for Two-Dimensional Unsteady Cascades of Oscillating Airfoils in Incompressible Flows (Courtesy of H. Atassi, 1985)

A complete first order theory is developed for the analysis of oscillating airfoils in cascade in a uniform upstream flow. The flow is assumed to be incompressible and irrotational. The geometry of the airfoil is arbitrary. The angle of attack of the mean flow and the stagger and solidity of the cascade can assume any prescribed set of values. The airfoils have a small harmonic oscillation about their mean position with a constant interblade phase angle. Both translational and rotational oscillations are considered.

The boundary-value problem for the unsteady component of the velocity is formulated in terms of

sectional analytic functions which must satisfy the impermeability condition along the airfoils surfaces, the Kutta condition at the trailing edges of the airfoils, and the jump condition along the airfoils wakes. The expression for the velocity jump in the wakes is derived to a multiplicative constant from the condition of pressure continuity across the wakes. The velocity field is split into two components: one satisfying the oscillating motion along the airfoils surfaces and the other accounts for a normalized jump condition along the wakes. This leads to two singular integral equations in the complex plane. The two equations are coupled by Kelvin's theorem of conservation of the circulation around the airfoils and their wakes. The integral equations are solved by a collocation technique.

The results obtained from this theory show that the airfoil geometry and loading and the cascade stagger and solidity strongly affect the aerodynamic forces and moments acting upon oscillating cascades. As a result stability and flutter boundaries are significantly modified for highly loaded cascades.

METHOD 5:
(Courtesy of P. Salaün, 1985)

The two-dimensional cascade is an infinite array of thin blades, the fluid is an inviscid perfect gas and the flow is assumed to be irrotational and isentropic. The blades are performing harmonic motions of so small amplitude that the theory can be linearized about the undisturbed, uniform flow, and the supersonic theory is restricted to the case of subsonic leading edge locus.

The pressure difference between the two sides of the blades are taken into account when they are replaced by sheets of pressure dipoles in both subsonic and supersonic flow. Then, the perturbation velocity potential is expressed and the boundary conditions on the blades give an integral equation where the unknown is the pressure difference on the reference blade, and the right hard side the angle of attack. This integral equation is solved numerically.

METHOD 6:
Zhou Sheng (1985)

A finite difference method is used to solve the unsteady velocity potential equation. The velocity potential is split into one steady and one unsteady part, and the unsteady small perturbation is solved with a relaxation procedure.

METHOD 7:
Extended FINSUP (Courtesy of R. D. Cedar, 1985)

The flutter calculation used at Rolls Royce is an extension of the finite element method developed by D.S. Whitehead (Method 2 above). Since the programs introduction to Rolls Royce in 1981 it has been continually developed and evaluated [see for example Newton and Whitehead, 1985]. The finite element mesh generator has been fully automated to the extent that it now contains "rules" about how good a mesh is. Using these "rules" the mesh construction parameters are automatically changed until a satisfactory mesh is obtained.

The steady flow calculation has been extended from being purely two-dimensional to include the quasi-three-dimensional effects of blade rotation and variations of streamtube height and streamline radius [Cedar and Stow, 1985a]. This has allowed the program to be included in the quasi-three-dimensional design system used at Rolls Royce [Jennions and Stow, 1984]. Improvements to the upwinding scheme has been made that produce sharp shocks. A coupled boundary layer calculation (using both direct and semi-inverse coupling) has been developed [Newman and Stow, 1985] as well as a design or inverse calculation [Cedar and Stow, 1985b]. This allows transonic blades to be designed, including the removal of shocks, to give a controlled diffusion.

The unsteady flow calculation has been extended to include the quasi-three-dimensional effects. It has been found that it is essential to include the effect of variation in streamtube height if test data is to be predicted correctly.

METHOD 8:
Theoretical Flutter Investigation on a Cascade in Incompressible Flow (Courtesy of V. Carstens, 1985)

I: Calculation of unsteady aerodynamic coefficients
The calculation of the unsteady aerodynamic coefficients due to harmonic bending and torsion of the cascade's blades is to replace each blade's surface and its wake by a distribution of vorticity. The kinematic boundary condition and the law of vorticity transport allow the formulation of the flow problem as an integral equation, the solution of which yields the correct value of the unknown unsteady blade vorticity. Two important items in the formulation of the problem should be mentioned:
- The prescribed harmonic motion of the entire cascade unit is a fundamental mode, in which all blades perform oscillations with the same amplitude but with a constant phase lag from blade to blade (interblade phase angle).
- The influence of the steady flow on the unsteady quantities is obtained by a special linearizing procedure.

The unsteady pressure distribution and the aerodynamic lift and moment coefficients are

calculated as a function of the blade vorticity by means of Bernouilli's equation.

II: Flutter analysis

The flutter analysis is done on the basis of two-degree-of freedom model, which allows for bending perpendicular to the chord and torsion around a given elastic axis. The rearrangement of the two linearized equations of motion for a blade section in non dimensional matrix form yields the formulation of the flutter problem as a non linear eigenvalue problem. Stability boundaries are found by determining the real eigenvalues of the matrix equation in an iterative procedure if a set of elasto-mechanical and aerodynamic parameters is prescribed. The result of each flutter calculation is a stability curve in a reduced frequency - interblade phase angle diagram, the maximum of which yields the absolute stability boundary and hence the non dimensional flutter speed for the given configuration.

METHOD 9:
(Courtesy of F. Molls, 1985)

The model allows for two shock waves to occur in a tip blade passage in which the inlet Mach number is supersonic. A weak oblique shock from the leading edge lies off the pressure surface of the upper blade and its angle is great enough that the shock intersects the lower blade. Off the suction surface of the lower blade there is a normal wave at the trailing edge which intersects the upper blade. The oblique shock angle corresponds to the pressure ratio but not to the metal angle at the leading edge. The model blade, however, has a wedge angle in agreement with the pressure ratio and inlet Mach number. Where the oblique shock strikes the adjacent blade, the flow turns from the inlet direction through the wedge angle to become parallel to the pressure surface; thus, as observed in actual flow, there is no reflection.

There are two options in the model. Either the pressure and suction surfaces continue uniformly to a blunt trailing edge, or the trailing surfaces are tapered to a specified thickness at the trailing edge. In the former case the differential equations for the unsteady component of the flow have constant coefficients and may be solved analytically. In the latter option, the mean flow in one portion of the blade passage is a slowly varying flow and numerical integration of the disturbance equations is required. A more detailed description with a diagram and references to experimental examples of the modeled flow is given by Molls [1985].

METHOD 10:
Semi-Actuator Disk Method (Courtesy of S. Kaji, 1985)

The semi-actuator disk model converts an actual blade row to a continuous cascade by inserting many fictious blades in between and parallel to the original blades. Aerodynamic loading and inter-blade phase change are all shared by inserted blades. Thus the change of physical quantity in the cascade direction is given by crossing each blade stepwise, and we can treat the flow inside a blade channel one-dimensionally.

Method of Analysis:

Solve first linearized governing equations of mass, momentum and energy for the upstream, inside and downstream field of the cascade separately. We have a pressure wave in the upstream field, two pressure waves going back and forth (and an entropy wave if the total pressure loss is present) inside the cascade and also we have a pressure wave, (an entropy wave) and a vorticity wave due to blade oscillation in the downstream field. The unknown amplitude of each wave is related to the known amplitude of blade oscillation through boundary conditions at the leading edge plane and the trailing edge plane of the cascade. They are as follows: At the leading edge plane we use mass flow continuation, relative total enthalpy continuation, and the condition of total pressure loss change in accordance with flow incidence. At the trailing edge plane we can assume a smooth continuation of all physical quantities, i.e., two components of velocity, pressure and density.

The aerodynamic forces acting on blades can be evaluated by use of the momentum principle applied to the control volume taken for a blade channel.

Merit and Demerit:
Aerodynamic loading
Total-pressure-loss
Arbitrary direction of oscillation
Not large inter-blade phase angle

Method of Analysis
Solve equations for upstream field, cascade channel and downstream field separately combine 3 fields by proper boundary conditions on leading edge and trailing edge planes use momentum principle to evaluate aerodynamic forces acting on blades

METHOD 14:
Discrete Vortex (Cloud-in-Cell) Method for Unsteady Cascade Flows (Courtesy of J. M. R. Graham and J. Basuki, 1985)

This method represents shed vortex wakes in two-dimensional incompressible flow by large numbers of discrete point vortices which are convected by the local velocity field. In the cloud-in-cell method the vorticity associated with the moving point vortices is transferred to a fixed Eulerian mesh [Christiansen, 1973]. The streamfunction and hence velocity

distribution is calculated from the vorticity on this mesh using a standard fast Poisson solver.

The presented version of this method used to calculate unsteady flow through a cascade represents the individual aerofoils in the cascade by a boundary integral method [Kennedy and Marsden, 1976] which uses piecewise constant vorticity panels. The appropriate streamfunction boundary condition is satisfied on the surface of each aerofoil by summing the contributions of the surface vorticity panels (including implied periodicity) and the mesh streamfunction. The boundary condition on the mesh also assumes periodicity along the cascade with the interblade phase angle limited to a small integral number of aerofoils within the mesh flow field. The computation follows the evolution of an unsteady flow by forward time marching, tracking the positions of the vortices.

The program has been used to compute cases with superimposed unsteady flow, upstream wakes, and blade vibration. In the latter case when the interblade phase angle is non-zero, exact application of the boundary integral method requires the influence functions to be recalculated at each time-step to account for changes in the relative blade to blade displacement. This has not been done in the present program for reasons of computational cost. The present boundary condition includes the relative motion but is evaluated on the mean surface of each blade and is therefore limited to small displacement amplitudes compared to the blade spacing.

The program evaluates time histories of surface pressures and forces induced on the aerofoils by the unsteady flows. Since the method involves time marching from an impulsive start fairly long computations are required to reach a final state free of initial transients.

METHOD 18:
(Courtesy of H. Joubert, 1985)

A model was developed at SNECMA for calculating the unsteady aerodynamic flow through vibrating cascades in view of studying supersonic flutter in axial flow compressors. The calculation deals with an ideal fluid, in unsteady transonic flow, including shocks, through a quasi three-dimensional cascade. The explicit MacCormack scheme was used to numerically solve the unsteady Euler's equations on a blade surface. An 80x15 grid points mesh was used which was displaced to follow the blade motion [Joubert, 1984].

This model has been applied to the seventh standard configuration of the workshop on aeroelasticity in turbomachine-cascades. Two cases were studied, the first one corresponding to an exit Mach number of 1.25 and the second one to an exit Mach number of

0.99. The unsteady aerodynamic damping coefficients for both cases are represented and the magnitude and phase lead of blade surface pressure coefficient for two interblade angles are plotted.

METHOD 19:
Method of Calculating Unsteady Aerodynamic Forces on Two-Dimensional Cascades (Courtesy of M. Namba, 1985)

The basic assumptions of the method are that the flow should be inviscid and isentropic. The gas should be perfect and the blade oscillations small. The blades are represented by pressure dipoles of fluctuating strength.

$$\boxed{} \tag{A.1.4}$$

and the problem is reduced to an integral equation for $\Delta p(x_o)$:

$$\int_0^c \Delta p(x_0) \, K(x-x_0) \, dx_0 = i\omega \, \alpha(x) + U\alpha'(x) \tag{A.1.5}$$

The Kernel function $K(x-x_o)$ is resolved into:
- a singular part $K(S)(x-x_o)$ in a closed form
- a regular part $K(R)(x-x_o)$ in an infinite series form of uniform convergence. (A sufficient convergence with truncation at the 30th term is confirmed).

The dipole distribution function $\Delta p(x_o)$ is then expanded into a mode function series.

The flow can be either sub- or supersonic:
- Subsonic cascade

$$\Delta p(x_0) = \sum_{k=0}^{K-1} P_k Y_k(\varphi) \tag{A1.6}$$

where
- $\quad x_0 = 0.5c(1-\cos\varphi)$
- $\quad Y_0(\varphi) = \cot(0.5\varphi)$
- $\quad Y_k(\varphi) = \sin(k\varphi) \quad (k\_1) \quad$ (Glauert series)

- Supersonic cascade

$$\tag{A1.7}$$

where
- r=reflection number (this technique corresponds to the Nagashima & Whitehead technique)

- $$g(x_0) = \sum_{k=0}^{K-1} P_k Y_k(\varphi) \quad , \text{with} x_0 = 0.5 c(1-\cos\varphi)$$
$$\tag{A1.8}$$
- $\boxed{}$ (equivalent to shifted Chebyshev polynomials)

The integral equation is converted into algebraic equation for Pk (k=0, 1, 2,...K-1)

$$\sum_{k=0}^{K-1} P_k \ YK_k \ (x_j) K(\ x - x_0\ ) d x_0 = i\omega \ \alpha \ (\ x_j) + U x' \ (\ x_j\ )$$

$$; j = 1, 2, \dots , K$$

(A1. 9)

where

$$YK_k (\ x_j) = \int Y_k ($$

(A1.10)

with the first term calculated analytically and the second numerically integrated with about 240 integration points from $x_0 = 0$ to c). In the present cases, calculations were conducted with six control points (K=6).

METHOD 20:
Euler solution for unsteady flows around oscillating blades (From He [1989])

The time-marching method is based on the two- and quasi three-dimensional unsteady Euler equations. The numerical integration follows with a finite volume scheme with a cell-vertex discretization in space and a two-step Runge-Kutta integration in time. Extra fluxes due to the deformation of the moving finite volumes are directly included in the conservation equations in the physical coordinate system. A zonal moving grid technique is used, in which only sub-regions near oscillating blades are moved to fit both the moving (blade) coordinates and fixed regions. See He [1989] for details.

METHOD 21:
Inviscid-viscous coupled solution for unsteady flows through vibrating blades (From He and Denton [1991])

A coupled approach between an inviscid Euler and a integral boundary layer solution is used for quasi three-dimensional unsteady flows induced by vibrating blades. For unsteady laminar and turbulent boundary layers, steady corrections are adopted in a quasi-steady way to close the integral boundary layer model. To conduct the coupling between the inviscid and viscous solutions for strongly interactive flows, the unsteady Euler and integral boundary layer equations are simultaneously time-marched using a multi-step Runge-Kutta scheme, and the boundary layer displacement effect is accounted for by a first order transpiration model. The time-resolved coupling method converges at conditions with considerable boundary layer separation. For further details, see He and Denton [1991a,b].

METHOD 22:
A deforming grid variational principle and finite element method for computing unsteady small disturbance flows in cascades (Courtesy of K. Hall, 1991)

The method describes a variational principle with the harmonic small disturbance behavior of the full two-dimensional potential equations around a nonlinear mean flow. Included is the effect of a deforming computational grid. A finite element technique is used to discretize the variational principle and the resulting discretized equations are solved using the LU decomposition. Exact far-field non reflecting boundary conditions are employed. The method is described in detail by Hall [1991].

METHOD 23:
Flutter analysis of cascades using a two-dimensional Euler solver (Courtesy of D. Huff, 1991)

The aerodynamic forces are obtained from an unsteady, two-dimensional cascade solver based on the Euler equations. The solver uses a time marching flux-differencing scheme and the flutter stability is analyzed in both frequency and time domains. In the frequency domain method the blades are oscillated harmonically for a given flow condition, oscillation frequency and interblade phase angle. In the time domain approach the aerodynamic and the structural equations are simultaneously integrated. The method is described in detail by Huff [1989] and Huff et al [1989, 1991].

METHOD 24:
Two-dimensional Euler solver (H. E. Gallus, 1989)

The non-linear two-dimensional Euler equations in conservative law form are solved by a combined method consisting of MacCormack's explicit predictor-corrector scheme at the interior points and a characteristic method for the time-dependent boundary conditions. The flow is considered subsonic and the method can handle unsteadinesses due to oscillating cascades and incoming wakes. See Kau and Gallus [1989] for details.

METHOD 25:
(V. Carstens, 1991)

The method computes the unsteady transonic two-dimensional inviscid flow through cascades with harmonically oscillating blades. The calculation of the flow field is based on a non-linear Euler solver using flux vector splitting on a modified H-grid. The implementation of the inlet and outlet boundary conditions is closely related to the theory of characteristics, and implemented in a non-reflective way. The method is described in detail by Carstens [1991].

METHOD 26:
Flutter analysis of cascades using a two-dimensional Euler solver (Courtesy of D. Huff, 1991)

Identical to Method 23 above, but with the blades as flat plates.

METHOD 27:
Strong coupling between a perfect fluid and a boundary layer (C. Soize, ONERA. Obtained from E. Széchényi, ONERA, 1991)

The method treats cascaded blades (sharp-leading edges) in two dimensions at positive incidence, where the flow on the suction surface is separated at the leading edge and reattached on the profile. The perfect gas equations are based on the small perturbation Euler equations, with the use of a non-structured finite element mesh. See Soize [1992] for details.

Updated report on
"Standard Configurations for Unsteady Flow Through Vibrating Axial-Flow Turbomachine-Cascades"

Status as of July 1991

Compiled by

T. H. Fransson and J. M. Verdon

Appendix A2: Key to read the input files for the plot program "AEROEL"

CONTENTS:

1:   DIFFERENT REPRESENTATION POSSIBILITIES

The plot program used for the Standard Configurations can give 10 different representations for each standard configuration, namely:

- **Type 1:**   Steady-state pressure distribution along blade chord ($\overline{c}_P = f(x)$.
- **Type 2:**   Time-dependent pressure coefficient amplitude and phase angle distribution along blade chord ($\tilde{c}_P = f(x))\Phi_P = f(x)$.
- **Type 3:**   Time-dependent pressure difference coefficient amplitude and phase angle distribution along blade chord ($\Delta \tilde{c}_P = f(x))\Phi_{\Delta P} = f(x)$.
- **Type 4:**   Time-dependent lift coefficient amplitude and phase angle distribution along any chosen parameter ($\tilde{c}_L = f(\text{parameter}))\Phi_L = f(\text{parameter})$.
- **Type 5:**   Time-dependent force coefficient amplitude and phase angle distribution along any chosen parameter (⎽⎽⎽⎽⎽⎽⎽⎽⎽⎽⎽⎽⎽⎽⎽⎽⎽).
- **Type 6:**   Time-dependent moment coefficient amplitude and phase angle distribution along any chosen parameter ($\tilde{c}_M = f(\text{parameter}))\Phi_M = f(\text{parameter})$.
- **Type 7:**   Time-dependent aerodynamic damping coefficient along any chosen parameter ($\Xi = f(\text{parameter})$.
- **Type 8:**   Time-dependent local aerodynamic damping coefficient amplitude and phase angle distribution along blade chord ($\Xi_{local} = f(x)$.
- **Type 9:**   Steady-state isentropic Mach number distribution along blade chord ($\overline{M}_{is} = f(x)$.
- **Type 10:**   Time-dependent drag coefficient amplitude and phase angle distribution along any chosen parameter ($\tilde{c}_D = f(\text{parameter}))\Phi_D = f(\text{parameter})$.

2:INPUT VALUES FOR THE PLOT PROGRAM "AEROEL"

2.1:   Information in the beginning of all files

It should be pointed out that the file is formatted, so the exact position of all the information is important. Integers must thus be positioned as justified to the right.

Line 1:   **General information**
- Columns 1-5:   ISTCON   = Standard Configuration number
- Columns 6-10:   NEWOLD   = 0 for old nomenclature (< 1.1. 1985)
                                                      = 1 for new nomenclature (>1.1. 1986)

Line 2:   **Types and quantity of plots desired.**
- Columns 1-5:   N1   = Number of plots of type 1 ($\overline{c}_P = f(x)$.
- Columns 6-10:   N2   = Number of plots of type 2 (⎽⎽⎽⎽⎽⎽⎽⎽⎽⎽⎽⎽⎽).
- Columns 11-15:   N3   = Number of plots of type 3 ($\Delta \tilde{c}_P = f(x))\Phi_{\Delta P} = f(x)$.
- Columns 16-20:   N4   = Number of plots of type 4 ($\tilde{c}_L = f(\text{parameter}))\Phi_L = f(\text{parameter})$.
- Columns 21-25:   N5   = Number of plots of type 5 ($\tilde{c}_F = f(\text{parameter}))\Phi_F = f(\text{parameter})$.
- Columns 26-30:   N6   = Number of plots of type 6 ($\tilde{c}_M = f(\text{parameter}))\Phi_M = f(\text{parameter})$.
- Columns 31-35:   N7   = Number of plots of type 7 (⎽⎽⎽⎽⎽⎽⎽⎽⎽⎽).
- Columns 36-40:   N8   = Number of plots of type 8 ($\Xi_{local} = f(x)$.
- Columns 41-45:   N9   = Number of plots of type 9 ($\overline{M}_{is} = f(x)$.
- Columns 46-50:   N10   = Number of plots of type 10 ($\tilde{c}_D = f(\text{parameter}))\Phi_D = f(\text{parameter})$.

Note that in the following all plots of a certain type must follow each other, and that it is not possible to mix plots of different types.

- o - o - o - o - o -

2.2: Plot-types 1, 8 and 9:

Lines 3-5:   **General information**
- Columns 1-60:   Text to identify the plot.
- Columns 61-65 on line 3:   HUS   =   Upper blade surface thickness. Only for standard configuration 9 and plot type 1.
- Columns 66-70 on line 3:   HLS   =   Lower blade surface thickness. Only for standard configuration 9 and plot type 1.

Line 6:   **Scales on y-axis**
- Columns 1-5:   ORDSYM(1)   =   Lowest value
- Columns 6-10:   ORDSYM(2)   =   Value at 1/4 of scale
- Columns 11-15:   ORDSYM(3)   =   Middle value
- Columns 16-20:   ORDSYM(4)   =   Value at 3/4 of scale
- Columns 21-25:   ORDSYM(5)   =   Highest value

Line 7:
- Columns 1-5:   NPLOT   =   Number of experimental c_p data on the upper blade surface. NPLOT_20.

Lines 8-8a: **Experimental data on the blade upper surface**
- Columns 1-10:   x(1)   =   x-value of first experimental data
- Columns 11-20: c_p(1)   =   Experimental data in first point
- Columns 21-30:   x(2)   =   x-value of 2nd experimental data
- Columns 31-40: c_p(2)   =   Experimental data in second point
- Columns 41-50:   x(3)   =   x-value of 3rd experimental data
- Columns 51-60: c_p(3)   =   Experimental data in third point
- Columns 61-70:   x(4)   =   x-value of 4th experimental data
- Columns 71-80: c_p(4)   =   Experimental data in fourth point
-> This line is repeated until all NPLOT values are given.

Line 9:
- Columns 1-5:   NPLOT   =   Number of experimental c_p data on the lower blade surface. NPLOT_20.

Lines 10-10a: **Idem lines 8-8a, but on the blade lower surface.**

Line 11:   **Indication about prediction model or end of results.**
- Columns 1-5:   ->   "0" if no more results are to be plotted
                               ->   Number of prediction model used (for definition, see Bölcs and Fransson [1986, pp. 41-42])
- Columns 6-10:   LTYPE =   Identification of the line type to be plotted for this prediction model.
- Columns 11-15:   NPLOT =   Number of calculated data that follows.

Lines 12-12a: **Results from prediction model in the same format as the data apart from the fact that it is assumed that the prediction models use the same number of points on each blade surface. The upper surface results are first given, and thereafter the lower surface results.**
- Columns 1-80:   Identical to lines 8-8a.

-> RETURN TO LINE 11!

Line 13:   **Indication about parameters to be written on the plot.**
- Columns 1-5:   NVAL   =   Number of parameters to be written in the list to the right on the plots. NVAL must be _40.

Lines 14-14a: **Indication about values of the parameters on the plot.**

- Columns 1-5: K = Number of first parameter (see below).
- Columns 6-10: VAL(K) = Value and dimension of first parameter.
- Columns 11-15: K = Number of 2nd parameter.
- Columns 16-20: VAL(K) = Value and dimension of 2nd parameter.
- Columns 21-25: K = Number of 3rd parameter (see below).
- Columns 26-30: VAL(K) = Value and dimension of 3rd parameter.
- Columns 31-35: K = Number of 4th parameter.
- Columns 36-40: VAL(K) = Value and dimension of 4th parameter.
- Columns 41-45: K = Number of 5th parameter (see below).
- Columns 46-50: VAL(K) = Value and dimension of 5th parameter.
- Columns 51-55: K = Number of 6th parameter.
- Columns 56-60: VAL(K) = Value and dimension of 6th parameter.
- Columns 1-60 on following lines: Continuation of the rest of the NVAL parameters.

1: c	2: τ	3: γ	4: x_α	5: y_α	6: M_1	7: β_1	8: i
9: M_2	10: β_2	11: h_x	12: h_y	13: α	14: ω	15: k	16: δ
17: σ	18: $\overline{c}_p$	19: $\Phi_p^{(us)}$	20: $\Phi_p^{(ls)}$	21: $\tilde{c}_p$	22: $\square$	23: $\Delta\tilde{c}_p$	24: Φ_L
25: $\tilde{c}_L$	26: Φ_M	27: $\tilde{c}_M$	28: σ	29: $\Xi\downarrow$	30: $c_w\uparrow$	31: x	32: Φ_F
33: $\tilde{c}_F$	34: d						

Table A2.1: *Key to list of parameters on each plot.*

Return to line 3 and repeat the information for a total of N1, N8 or N9 times.

- o - o - o - o - o - o -

2.3: Plot-type 2:

Lines 3-5:   General information
- Columns 1-60:   Text to identify the plot.

Line 6:
- Columns 1-5:   NPLOT   =   Number of experimental c_p data on the upper blade surface. NPLOT_20.

Lines 7-7a: Experimental data on the blade upper surface

For all standard configurations apart from number 4:
- Columns 1-10:   x(1)   =   x-value of first experimental data
- Columns 11-20: $c_p(1)$ =   Amplitude of experimental data in first point
- Columns 21-30: $\phi_p(1)$ =   Phase angle of experimental data in first point
- Columns 31-40:   x(2)   =   x-value of experimental data in second point
- Columns 41-50: $c_p(2)$ =   Amplitude of experimental data in 2nd point
- Columns 51-60: $\phi_p(2)$ =   Phase angle of experimental data in 2nd point
-> This line is repeated until all NPLOT values are given.

For standard configuration 4:
- Columns 1-10:   x(1)   =   x-value of first experimental data
- Columns 11-20: $c_p(1)$ =   Amplitude of experimental data in first point
- Columns 21-30: $\phi_p(1)$ =   Phase angle of experimental data in first point
- Columns 31-40: $c_p(1)$-conf.int   =   95% confidence interval of $c_p(1)$
- Columns 41-50: $\phi_p(1)$-conf.int   =   95% confidence interval of $\phi_p(1)$
-> This line is repeated until all NPLOT values are given.

Line 8:
- Columns 1-5:   NPLOT   =   Number of experimental c_p data on the lower blade surface. NPLOT_20.

Lines 9-9a: Idem lines 7-7a, but on the blade lower surface.

Line 10:   Scales on y-axis
- Columns 1-5:   ORDSYM(1)   =   Lowest value
- Columns 6-10:   ORDSYM(2)   =   Value at 1/4 of scale
- Columns 11-15:   ORDSYM(3)   =   Middle value
- Columns 16-20:   ORDSYM(4)   =   Value at 3/4 of scale
- Columns 21-25:   ORDSYM(5)   =   Highest value

Line 11:   Indication about prediction model or end of results.
- Columns 1-5:   ->   "0" if no more results are to be plotted
          ->   Number of prediction model used (for definition, see Bölcs and Fransson [1986, pp. 41-42])
- Columns 6-10:   LTYPE =   Identification of the line type to be plotted for this prediction model.
- Columns 11-15:   NPLOT =   Number of calculated data that follows.

Lines 12-12a: Results from prediction model in the same format as the data apart from the fact that it is assumed that the prediction models use the same number of points on each blade surface. The upper surface results are first given, and thereafter the lower surface results.
- Columns 1-80:   Identical to lines 7-7a.

-> RETURN TO LINE 11!

Line 13:   Indication about parameters to be written on the plot.
- Columns 1-5:   NVAL   =   Number of parameters to be written in the list to the right on the plots. NVAL must be _40.

Lines 14-14a: **Indication about values of the parameters on the plot.**
- Columns 1-5:   K   =   Number of first parameter (see below).
- Columns 6-10:   VAL(K)   =   Value and dimension of first parameter.
- Columns 11-15:   K   =   Number of 2nd parameter.
- Columns 16-20:   VAL(K)   =   Value and dimension of 2nd parameter.
- Columns 21-25:   K   =   Number of 3rd parameter (see below).
- Columns 26-30:   VAL(K)   =   Value and dimension of 3rd parameter.
- Columns 31-35:   K   =   Number of 4th parameter.
- Columns 36-40:   VAL(K)   =   Value and dimension of 4th parameter.
- Columns 41-45:   K   =   Number of 5th parameter (see below).
- Columns 46-50:   VAL(K)   =   Value and dimension of 5th parameter.
- Columns 51-55:   K   =   Number of 6th parameter.
- Columns 56-60:   VAL(K)   =   Value and dimension of 6th parameter.
- Columns 1-60 on following lines: Continuation of the rest of the NVAL parameters.
- For key to list of parameters on each plot, see table A2.1:

Return to line 3 and repeat the information for a total of N2 times.

- o - o - o - o - o - o -

2.4: Plot-type 3:

Lines 3-5:   General information
- Columns 1-60:   Text to identify the plot.

Line 6:
- Columns 1-5:   NPLOT   =   Number of experimental Δc_p data on the blade surface. NPLOT_20.

Lines 7-7a: Experimental data on the blade surface
- Columns 1-10:   x(1)   =   x-value of first experimental data
- Columns 11-20: $\Delta c_p(1)$ =   Amplitude of experimental data in first point
- Columns 21-30: $\phi_{\Delta p}(1)$ =   Phase angle of experimental data in first point
- Columns 31-40:   x(2)   =   x-value of experimental data in second point
- Columns 41-50: $\Delta c_p(2)$ =   Amplitude of experimental data in 2nd point
- Columns 51-60: $\phi_{\Delta p}(1)$ =   Phase angle of experimental data in 2nd point

-> This line is repeated until all NPLOT values are given.

Line 8:   Scales on y-axis
- Columns 1-5:   ORDSYM(1)   =   Lowest value
- Columns 6-10:   ORDSYM(2)   =   Value at 1/4 of scale
- Columns 11-15:   ORDSYM(3)   =   Middle value
- Columns 16-20:   ORDSYM(4)   =   Value at 3/4 of scale
- Columns 21-25:   ORDSYM(5)   =   Highest value

Line 9:   Indication about prediction model or end of results.
- Columns 1-5:   ->   "0" if no more results are to be plotted
        ->   Number of prediction model used (for definition, see Bölcs and Fransson [1986, pp. 41-42])
- Columns 6-10:   LTYPE =   Identification of the line type to be plotted for this prediction model.
- Columns 11-15:   NPLOT =   Number of calculated data that follows.

Lines 10-10a: Results from prediction model in the same format as the data.
- Columns 1-80:   Identical to lines 7-7a.

-> RETURN TO LINE 9!

Line 13:   Indication about parameters to be written on the plot.
- Columns 1-5:   NVAL   =   Number of parameters to be written in the list to the right on the plots. NVAL must be _40.

Lines 14-14a: Indication about values of the parameters on the plot.
- Columns 1-5:   K   =   Number of first parameter (see below).
- Columns 6-10:   VAL(K) =   Value and dimension of first parameter.
- Columns 11-15:   K   =   Number of 2nd parameter.
- Columns 16-20:   VAL(K) =   Value and dimension of 2nd parameter.
- Columns 21-25:   K   =   Number of 3rd parameter (see below).
- Columns 26-30:   VAL(K) =   Value and dimension of 3rd parameter.
- Columns 31-35:   K   =   Number of 4th parameter.
- Columns 36-40:   VAL(K) =   Value and dimension of 4th parameter.
- Columns 41-45:   K   =   Number of 5th parameter (see below).
- Columns 46-50:   VAL(K) =   Value and dimension of 5th parameter.
- Columns 51-55:   K   =   Number of 6th parameter.
- Columns 56-60:   VAL(K) =   Value and dimension of 6th parameter.
- Columns 1-60 on following lines: Continuation of the rest of the NVAL parameters.

- For key to list of parameters on each plot, see table A2.1:

Return to line 3 and repeat the information for a total of N3 times.

- o - o - - o - o - o - o -

2.5: Plot-types 4, 5, 6 and 10:

Lines 3-5:   General information
- Columns 1-60:   Text to identify the plot.

Line 6:   Symbol and scale on horizontal axis
- Columns 1-5 (integer):   ISYMB   =   Symbol, according to Table A2.1, to be represented and written on horizontal axis.
- Columns 6-10 (real):   ABSSYM(1)   =   Lowest value of scale on horizontal axis.
- Columns 11-15 (real): ABSSYM(2)   =   Middle value of scale on horizontal axis.
- Columns 16-20 (real): ABSSYM(3)   =   Highest value of scale on horizontal axis.

Line 7:
- Column 1 (I1):   NSYM   =   Number for identification of symbol to be plotted. NSYM should only take the values 3, 4, 5, 7, 1 or 2 in order not to charge the figure too much.
                                    =   0 for end of information.
- Columns 2-5 (I4):   NPLOT   =   Number of experimental data on the blade surface. NPLOT_20.
- Columns 6-10 (I5):   NVAR   =   Number of variables.
- Columns 11-16 (A5):   VAL   =   Value of the variables.

Lines 8-8a: Experimental data as function of the parameter chosen
- Columns 1-10:   Par(1)   =   Parameter-value of first experimental data
- Columns 11-20:   A (1)   =   Amplitude of experimental data in first point
- Columns 21-30: ϕ(1)   =   Phase angle of experimental data in first point
- Columns 31-40:   Par(2)   =   Parameter-value of experimental data in 2nd point
- Columns 41-50:   A (2)   =   Amplitude of experimental data in 2nd point
- Columns 51-60: ϕ(2)   =   Phase angle of experimental data in 2nd point
- -> This line is repeated until all NPLOT values are given.

-> Lines 7+8 are repeated until NSYM = 0

Line 9:   Scale on vertical axis
- Columns 1-5:   ORDSYM(1)   =   Lowest value
- Columns 6-10:   ORDSYM(2)   =   Value at 1/4 of scale
- Columns 11-15:   ORDSYM(3)   =   Middle value
- Columns 16-20:   ORDSYM(4)   =   Value at 3/4 of scale
- Columns 21-25:   ORDSYM(5)   =   Highest value

Line 10:   Indication about prediction model or end of results.
- Columns 1-5:   ->   "0" if no more results are to be plotted
                       ->   Number of prediction model used (for definition, see Bölcs and Fransson [1986, pp. 41-42])
- Columns 6-10:   LTYPE =   Identification of the line type to be plotted for this prediction model.
- Columns 11-15:   NPLOT =   Number of calculated data that follows.

Lines 11-11a: Results from prediction model in the same format as the data.
- Columns 1-80:   Identical to lines 8-8a.

-> RETURN TO LINE 10!

Line 12:   Indication about parameters to be written on the plot.
- Columns 1-5:   NVAL   =   Number of parameters to be written in the list to the right on the plots. NVAL must be _40.

Lines 13-13a: Indication about values of the parameters on the plot.
- Columns 1-5:   K   =   Number of first parameter (see below).
- Columns 6-10:   VAL(K) =   Value and dimension of first parameter.
- Columns 11-15:   K   =   Number of 2nd parameter.
- Columns 16-20:   VAL(K) =   Value and dimension of 2nd parameter.
- Columns 21-25:   K   =   Number of 3rd parameter (see below).
- Columns 26-30:   VAL(K) =   Value and dimension of 3rd parameter.
- Columns 31-35:   K   =   Number of 4th parameter.
- Columns 36-40:   VAL(K) =   Value and dimension of 4th parameter.
- Columns 41-45:   K   =   Number of 5th parameter (see below).
- Columns 46-50:   VAL(K) =   Value and dimension of 5th parameter.
- Columns 51-55:   K   =   Number of 6th parameter.
- Columns 56-60:   VAL(K) =   Value and dimension of 6th parameter.
- Columns 1-60 on following lines: Continuation of the rest of the NVAL parameters.
- For key to list of parameters on each plot, see table A2.1:

Return to line 3 and repeat the information for a total of N4, N5, N6 or N10 times.

- o - o - o - o - o - o -

2.6: Plot-type 7:

Lines 3-5:   General information
- Columns 1-60:   Text to identify the plot.

Line 6:   Symbol and scale on horizontal axis
- Columns 1-5 (integer):   ISYMB   =   Symbol, according to Table A2.1, to be represented and written on horizontal axis.
- Columns 6-10 (real):   ABSSYM(1)   =   Lowest value of scale on horizontal axis.
- Columns 11-15 (real): ABSSYM(2)   =   Middle value of scale on horizontal axis.
- Columns 16-20 (real): ABSSYM(3)   =   Highest value of scale on horizontal axis.

Line 7:   Scale to the left of vertical axis (c_W)
- Columns 1-5:   ORDSYM(1)   =   Lowest value
- Columns 6-10:   ORDSYM(2)   =   Value at 1/4 of scale
- Columns 11-15:   ORDSYM(3)   =   Middle value
- Columns 16-20:   ORDSYM(4)   =   Value at 3/4 of scale
- Columns 21-25:   ORDSYM(5)   =   Highest value

Line 8:
- Column 1 (I1):   NSYM   =   Number for identification of symbol to be plotted. NSYM should only take the values 3, 4, 5, 7, 1 or 2 in order not to charge the figure too much.
-   =   0 for end of information.
- Columns 2-5 (I4):   NPLOT   =   Number of experimental data on the blade surface. NPLOT_20.
- Columns 6-10 (I5):   NVAR   =   Number of variables.
- Columns 11-16 (A5):   VAL   =   Value of the variables.

Lines 9-9a: Experimental data as function of the parameter chosen

For all standard configurations apart from number 4:
- Columns 1-10:   Par(1)   =   Parameter-value of first experimental data.
- Columns 11-20: Ξ(1)   =   Experimental aerodynamic coefficient data in first point.
- Columns 21-30:   Par(2)   =   Parameter-value of experimental data in 2nd point
- Columns 31-40: Ξ(2)   =   Experimental aerodynamic coefficient data in 2nd point.
- Columns 41-50:   Par(3)   =   Parameter-value of experimental data in 3rd point
- Columns 51-60: Ξ(3)   =   Experimental aerodynamic coefficient data in 3rd point.
   -> This line is repeated until all NPLOT values are given.

For standard configuration 4:
- Columns 1-10:   Par(1)   =   Parameter-value of first experimental data.
- Columns 11-20: Ξ(1)   =   Experimental aerodynamic coefficient data in first point.
- Columns 21-30: Ξ(1)-conf.int   =   95% confidence interval of Ξ(1)
   -> This line is repeated until all NPLOT values are given.

-> Lines 8+9 are repeated until NSYM = 0

Line 10:   Scale to the right of vertical axis (Ξ)
- Columns 1-5:   ORDSYM(1)   =   Lowest value
- Columns 6-10:   ORDSYM(2)   =   Value at 1/4 of scale
- Columns 11-15:   ORDSYM(3)   =   Middle value
- Columns 16-20:   ORDSYM(4)   =   Value at 3/4 of scale
- Columns 21-25:   ORDSYM(5)   =   Highest value

Line 11:   Indication about prediction model or end of results.
- Columns 1-5:   ->   "0" if no more results are to be plotted
-                         ->   Number of prediction model used (for definition, see Bölcs and Fransson [1986, pp. 41-42])
- Columns 6-10:   LTYPE =   Identification of the line type to be plotted for this prediction model.
- Columns 11-15:   NPLOT =   Number of calculated data that follows.

Lines 12-12a: Results from prediction model in the same format as the data.
- Columns 1-80:   Identical to lines 8-8a.

-> RETURN TO LINE 11!

Line 13:   Indication about parameters to be written on the plot.
- Columns 1-5:   NVAL =   Number of parameters to be written in the list to the right on the plots. NVAL must be _40.

Lines 14-14a: **Indication about values of the parameters on the plot.**

- Columns 1-5:   K   =   Number of first parameter (see below).
- Columns 6-10:   VAL(K)   =   Value and dimension of first parameter.
- Columns 11-15:   K   =   Number of 2nd parameter.
- Columns 16-20:   VAL(K)   =   Value and dimension of 2nd parameter.
- Columns 21-25:   K   =   Number of 3rd parameter (see below).
- Columns 26-30:   VAL(K)   =   Value and dimension of 3rd parameter.
- Columns 31-35:   K   =   Number of 4th parameter.
- Columns 36-40:   VAL(K)   =   Value and dimension of 4th parameter.
- Columns 41-45:   K   =   Number of 5th parameter (see below).
- Columns 46-50:   VAL(K)   =   Value and dimension of 5th parameter.
- Columns 51-55:   K   =   Number of 6th parameter.
- Columns 56-60:   VAL(K)   =   Value and dimension of 6th parameter.
- Columns 1-60 on following lines: Continuation of the rest of the NVAL parameters.
- For key to list of parameters on each plot, see table A2.1:

Return to line 3 and repeat the information for a total of N7 times.

<div align="center">

- o - o - o - o - o - o -

</div>

Updated report on
"Standard Configurations for Unsteady Flow Through Vibrating Axial-Flow Turbomachine-Cascades"

Status as of July 1991

Compiled by

T. H. Fransson and J. M. Verdon

Appendix A3: Listing of all values used on the plots
(these can be obtained on a floppy disk upon request)

Updated report on
"Standard Configurations for Unsteady Flow Through Vibrating Axial-Flow Turbomachine-Cascades"

Status as of July 1991

Compiled by

T. H. Fransson and J. M. Verdon

Appendix A4: Computer Plots of Results in the Study

The results presented in the following appendix follows exactly the scheme laid out for the presentation of previous results in the workshop. The plot numbers shown correspond to the numbers of the plots in Appendix A5 of the original workshop report [Bölcs and Fransson, 1986]. The figures in the present appendix can thus be put together with the old appendix A5, with no loss of information. If the present plot numbers correspond to a number existing in the old appendix A5, some new results (experimental or theoretical) have been added to the plot.

To facilitate the task for anyone who would like to compare the numerical values of the results (experimental or theoretical) given in the workshop, the input files for all the plots are also given (Appendix A3). The key to read these files is given (Appendix A2), and a floppy disk with all the numerical values can be obtained upon request.

Fifth Standard Configuration

1: Case 1
2: Cases 2, 4-7
3: Cases 3, 8-11, 25-26, 29.
4: Case 12.
5: Cases 13, 15-18, 27-28, 30.
6: Case 14.
7: Case 19.
8: Case 20.
9: Case 21, p_{w1}=1.4 bar.
10: Case 22, p_{w1}=2.0 bar.
11: Case 23.
12: Case 24.
13: Cases 27-28,30.

Plots 7.5-1.1 to 7.5-1.13: *Fifth standard configuration: Steady-state blade surface pressure distribution for aeroelastic sample cases 1-30.*

12: Case 12
13: Case 13
...
...
...
30: Case 30.

Plots 7.5-2.12 to 7.5-2.30: *Fifth standard configuration: Magnitude and phase lead of the unsteady blade surface pressure coefficient for aeroelastic sample cases 12-30.*

12: Case 12
13: Case 13
...
...
...
30: Case 30.

Plots 7.5-3.12 to 7.5-3.30: *Fifth standard configuration: Magnitude and phase lead of the unsteady blade surface pressure difference coefficient for aeroelastic sample cases 12-30.*

1: Function of i, M_1=0.5, k= 0.37, cases 1-3, 12-14
2: Function of k, M_1=0.5, i= 4, cases 2, 4-7
3: Function of k, M_1=0.5, i= 6, cases 3, 8-11
4: Function of k, M_1=0.5, i= 10, cases 13, 15-18
5: Function of k, M_1=0.5, i= 4, cases 13, 19-24

Plots 7.5-5.12 to 7.5-5.30: *Fifth standard configuration: Aerodynamic moment coefficient for aeroelastic sample cases 1-30.*

1: Function of i, M_1=0.5, k= 0.37, cases 1-3, 12-14
2: Function of k, M_1=0.5, i= 4, cases 2, 4-7
3: Function of k, M_1=0.5, i= 6, cases 3, 8-11
4: Function of k, M_1=0.5, i= 10, cases 13, 15-18
5: Function of k, M_1=0.5, i= 4, cases 13, 19-24

Plots 7.5-6.12 to 7.5-6.30: *Fifth standard configuration: Aerodynamic damping coefficient for aeroelastic sample cases 1-30.*

Eighth Standard Configuration

36: Case 36
37: Case 37
...
...
...
54: Case 54.
Plots 7.8-2.36 to 7.5-2.54: *Eighth standard configuration: Magnitude and phase lead of the unsteady blade surface pressure coefficient for aeroelastic sample cases 26-54.*

36: Case 36
37: Case 37
...
...
...
54: Case 54.
Plots 7.8-3.36 to 7.5-3.54: *Eighth standard configuration: Magnitude and phase lead of the unsteady blade surface pressure difference coefficient for aeroelastic sample cases 26-54.*

8: Function of M, k= 0.5, cases 36-42
9: Function of σ, cases 43-48
10: Function of σ, cases 49-54
Plots 7.8-5.8 to 7.5-5.10:   *Eighth standard configuration: Aerodynamic moment coefficient for aeroelastic sample cases 36-54.*

8: Function of M, k= 0.5, cases 36-42
9: Function of σ, cases 43-48
10: Function of σ, cases 49-54
Plots 7.8-6.8 to 7.5-6.10:   *Eighth standard configuration: Aerodynamic damping coefficient for aeroelastic sample cases 36-54.*

Ninth Standard Configuration

1: Cases 1-4, 22-25
2: Cases 5, 26
3: Cases 6-9, 27-30.
4: Cases 10, 31.
5: Cases 11, 32.
6: Cases 12, 33.
7: Cases 13, 34.
8: Cases 14, 35.
9: Cases 15, 36.
10: Cases 16, 37.
11: Cases 17, 38.
12: Case18, 39.
13: Cases 19, 40.
14: Cases 20, 41
15: Cases 21, 42.

Plots 7.9-1.1 to 7.9-1.15: *Ninth standard configuration: Steady-state blade surface pressure distribution for aeroelastic sample cases 1-42.*

22: Case 22
23: Case 23
...
...
...
42: Case 42.

Plots 7.9-2.22 to 7.9-2.42: *Ninth standard configuration: Magnitude and phase lead of the unsteady blade surface pressure coefficient for aeroelastic sample cases 22-42.*

22: Case 22
23: Case 23
...
...
...
42: Case 42.

Plots 7.9-3.22 to 7.9-3.42: *Ninth standard configuration: Magnitude and phase lead of the unsteady blade surface pressure difference coefficient for aeroelastic sample cases 22-42.*

6: Function of M_1, k= 0.5, cases 22, 26, 28, 31-34
7: Function of M_1, k= 0.5, cases 35-38
8: Function of M_1, k= 0.5, cases 39-42
9: Function of d, cases 22-25
10: Function of d, cases 27-30

Plots 7.9-5.6 to 7.9-5.10: *Ninth standard configuration: Aerodynamic moment coefficient for aeroelastic sample cases 22-42.*

6: Function of M_1, k= 0.5, cases 22, 26, 28, 31-34
7: Function of M_1, k= 0.5, cases 35-38
8: Function of M_1, k= 0.5, cases 39-42
9: Function of d, cases 22-25
10: Function of d, cases 27-30

Plots 7.9-6.6 to 7.9-6.10: *Ninth standard configuration: Aerodynamic damping coefficient for aeroelastic sample cases 22-42.*

Tenth Standard Configuration

1: Cases 1-16
2: Cases 17-32
Plots 7.10-1.1 to 7.10-1.2: *Tenth standard configuration: Steady-state blade surface pressure distribution for aeroelastic sample cases 1-32.*

1: Case 1
2: Case 2
...
...
...
32: Case 32.
Plots 7.10-2.1 to 7.10-2.32: *Tenth standard configuration: Magnitude and phase lead of the unsteady blade surface pressure coefficient for aeroelastic sample cases 1-32.*

1: Case 1
2: Case 2
...
...
...
32: Case 32.
Plots 7.10-3.1 to 7.10-3.32: *Tenth standard configuration: Magnitude and phase lead of the unsteady blade surface pressure difference coefficient for aeroelastic sample cases 1-32.*

1: Heaving motion, M1=0.7, Function of σ, k=0.25, cases 9-10 +extra
2: Heaving motion, M1=0.7, Function of σ, k=0.5, cases 11-12 +extra
3: Heaving motion, M1=0.7, Function of σ, k=0.75, cases 13-14 +extra
4: Heaving motion, M1=0.7, Function of σ, k=1.0, cases 15-16 +extra
5: Heaving motion, M1=0.8, Function of σ, k=0.25, cases 25-26 +extra
6: Heaving motion, M1=0.8, Function of σ, k=0.5, cases 27-28 +extra
7: Heaving motion, M1=0.8, Function of σ, k=0.75, cases 29-30 +extra
8: Heaving motion, M1=0.8, Function of σ, k=1.0, cases 31-32+ extra
Plots 7.10-4.1 to 7.10-4.8: *Tenth standard configuration: Aerodynamic lift coefficient for aeroelastic sample cases 9-16, 25-32.*

1: Pitching motion, M1=0.7, Function of σ, k=0.25, cases 1-2+extra
2: Pitching motion, M1=0.7, Function of σ, k=0.5, cases 3-4+extra
3: Pitching motion, M1=0.7, Function of σ, k=0.75, cases 5-6+extra
4: Pitching motion, M1=0.7, Function of σ, k=1.0, cases 7-8+extra
5: Pitching motion, M1=0.8, Function of σ, k=0.25, cases 17-18+extra
6: Pitching motion, M1=0.8, Function of σ, k=0.5, cases 19-20+extra
7: Pitching motion, M1=0.8, Function of σ, k=0.75, cases 21-22+extra
8: Pitching motion, M1=0.8, Function of σ, k=1.0, cases 23-24+extra
Plots 7.10-5.1 to 7.10-5.8: *Tenth standard configuration: Aerodynamic moment coefficient for aeroelastic sample cases 1-8, 17-24.*

1: Heaving motion, M1=0.7, Function of σ, k=0.25, cases 9-10 +extra
2: Heaving motion, M1=0.7, Function of σ, k=0.5, cases 11-12 +extra
3: Heaving motion, M1=0.7, Function of σ, k=0.75, cases 13-14 +extra
4: Heaving motion, M1=0.7, Function of σ, k=1.0, cases 15-16 +extra
5: Heaving motion, M1=0.8, Function of σ, k=0.25, cases 25-26 +extra
6: Heaving motion, M1=0.8, Function of σ, k=0.5, cases 27-28 +extra
7: Heaving motion, M1=0.8, Function of σ, k=0.75, cases 29-30 +extra
8: Heaving motion, M1=0.8, Function of σ, k=1.0, cases 31-32+ extra
9: Pitching motion, M1=0.7, Function of σ, k=0.25, cases 1-2+extra
10: Pitching motion, M1=0.7, Function of σ, k=0.5, cases 3-4+extra
11: Pitching motion, M1=0.7, Function of σ, k=0.75, cases 5-6+extra
12: Pitching motion, M1=0.7, Function of σ, k=1.0, cases 7-8+extra
13: Pitching motion, M1=0.8, Function of σ, k=0.25, cases 17-18+extra
14: Pitching motion, M1=0.8, Function of σ, k=0.5, cases 19-20+extra
15: Pitching motion, M1=0.8, Function of σ, k=0.75, cases 21-22+extra
16: Pitching motion, M1=0.8, Function of σ, k=1.0, cases 23-24+extra
Plots 7.10-6.1 to 7.10-6.16: *Tenth standard configuration: Aerodynamic damping coefficient for aeroelastic sample cases 1-32.*